uOttawa

L'Université canadienne
Canada's university

Towards the identification of candidate gene(s) for fusarium head blight resistance on the 7EL chromosome of *Thinopyrum elongatum*: design and use of genetic markers

by

Farideh Tekieh

Thesis Submitted to the Faculty of Graduate and Postdoctoral Studies
in partial fulfillment of the requirements for the degree of

Master of Science in Biology

Thesis directed by:

Dr. Thérèse Ouellet

Department of Biology
Faculty of Science
University of Ottawa

December 2016

In the name of God,

the compassionate, the merciful

ABSTRACT

Triticum aestivum (bread wheat), one of the most globally important cereal crops, is vulnerable to fusarium head blight (FHB). The disease is mainly associated with the pathogen *Fusarium graminearum* and generates yield losses and mycotoxin contaminated grains with low quality. One possible solution to overcome this problem is the production of FHB resistant wheat varieties by crossing with strongly resistant germplasm from either wheat or closely related species. *Thinopyrum elongatum* is a wild grass that carries genetic resistance to FHB on the long arm of its chromosome 7E (7EL). In the first part of this research project, five *Th. elongatum* accessions were characterized for their response to *F. graminearum* infection. In the second part, BC_1F_4 progeny derived from the cross CS-*ph1b* × CS-7E(7D) were characterized to better define the 7E fragments introgressed into the 7D chromosome. Progeny were screened with a series of known 7E-specific genetic markers and for their FHB resistance. Among the 43 wheat plants tested, twelve FHB resistant progeny were shown to carry a similar, smaller 7EL introgressed fragment based on genetic marker screening. To characterize further the introgressed 7EL fragments, additional 7EL-specific markers as well as 7DL-specific markers for homoeologous wheat sequences were designed. As neither wheat nor *Th. elongatum* genomes were fully sequenced at the time, this made the designing procedure challenging; a cross-walking strategy between wheat and *Th. elongatum* draft genomic sequences was used. Twelve pairs of markers for homoeologous sequence regions of 7EL and 7DL chromosomes plus six individual 7EL- and four 7DL-specific markers were successfully designed. Nine novel 7EL-specific markers were associated with the smallest 7EL fragment carrying FHB resistance. That smallest introgressed 7EL fragment replaced approximately half of the 7DL chromosome, based on the absence of 7DL markers in some progeny. The novel

7EL- and 7DL-specific markers as well as the proposed genetic order for novel and previously designed markers contributed greatly to the characterization of the introgressed 7EL fragments in the 7DL chromosome. Further analysis of progeny from the next generations of these plants and from other families will be required to confirm the results and possibly obtain much smaller 7EL fragments.

ACKNOWLEDGEMENT

Two years after commencing my Master's study, now I'm grateful to write the final note in my thesis. This research study increased my knowledge on a very interesting aspect of science dealing with plants as one of the most lively and beautiful creatures in the world. Additionally, studying on the molecular level provides very precise insight into life. I would like to reflect on the people who have continuously supported and directed me all the way through this time period.

My special thanks go to my supervisor, Dr. Thérèse Ouellet, for providing me with this great opportunity to work in her lab. I am sincerely thankful for all of her support, attention, kindness and encouraging spirit. This research would not be possible to conduct without her precious help. I would also like to thank our lab technicians, Margaret Balcerzak and Hélène Rocheleau, for their kindness and patient attitudes plus their ongoing technical assistance and advice. I am so happy that I had the experience of working in such a friendly lab environment.

I am also grateful to my committee members: Dr. Sylvie Cloutier, Dr. Doug Johnson and Dr. Laurian Robert for their time and invaluable feedback on my research reports. Besides, many thanks to University of Ottawa and Agriculture and Agri-Food Canada for providing and facilitating this great study and research chance for me.

Moreover, I take this opportunity to highly thank my parents for all of their support and encouragements through my life. Last but not the least, I wish to sincerely thank my husband, Mohammad Hossein, for being with me all the time and his endless efforts in backing me and give me confidence and motivation to face challenges.

TABLE OF CONTENTS

LIST OF FIGURES

LIST OF TABLES

LIST OF ABBREVIATIONS

Abbreviation	**Explanation**
7ABD contigs	Wheat contigs from 7A, 7B and 7D chromosomes
7EL	Long arm of 7E chromosome
AAFC	Agriculture and Agri-Food Canada
ANOVA	Analysis of variance
$BC_1F_{(1\text{-}4)}$	First Back-Cross, (First-Forth) Family
BLAST	Basic Local Alignment Search Tool
CS	*Triticum aestivum* cv. Chinese Spring
CS-7E	CS addition line (full wheat genome & a full 7E chromosome)
CS-7E(7D)	Substitution line (7E chromosome has replaced wheat 7D chromosome)
CS-7EL	CS addition line (full wheat genome & long arm of 7E chromosome)
CS-7ES	CS addition line (full wheat genome & short arm of 7E chromosome)
CS-ph1b	Chinese Spring carrying an inactive *Ph1* locus
DNA	Deoxyribonucleic acid
DNA-Seq	Deoxyribonucleic acid-Sequencing
DON	Deoxynivalenol
DPI	Days Post Inoculation
EcoRI	*Escherichia coli* restriction endonuclease R1
ESTs	Expressed Sequence Tags
FHB	Fusarium Head Blight
H_2O_2	hydrogen peroxide
IDT	Integrated DNA Technologies

JA	Jasmonic Acid
KASP	Kompetitve Allele-Specific PCR
LB	Luria Broth
n.d.	no date specified for the reference
NRC	National Research Council of Canada
ORDC	Ottawa Research and Development Centre
PCR	Polymerase Chain Reaction
Ph1	Pairing Homoeologous Locus
PLUG	PCR-based Landmark Unique Gene
PR proteins	Pathogenesis-related proteins
QTL	Quantitative Trait Loci
RNA-Seq	Ribonucleic acid-Sequencing
ROS	Reactive Oxygen Species
SA	Salicylic Acid
SAR	Systemic Acquired Resistance
SLAF-seq	Specific Length Amplified Fragment sequencing
SNP	Single Nucleotide Polymorphism
SSR	Simple Sequence Repeat
TAE	Tris-acetate-EDTA
URGI	Unité de Recherche Génomique Info (research unit in genomics and bioinformatics)
UV	Ultraviolet

Chapter One

1 INTRODUCTION

As the global population is still growing at the rate of 1.13% in 2016 ("Worldometers," 2016), enhancing the crops' yield remains a pressing need. It is expected that global food demand will double by 2050 (Green, Cornell, Scharlemann, & Balmford, 2005). Humans have tried to manage these demands by increasing the superficies of farmlands under cultivation and by utilizing environmentally unfriendly chemical pesticides. Cereal grains play an important role in humans' dietary requirements due to their rich source of vitamins, minerals, carbohydrates and proteins. According to statistics from the Food and Agriculture Organization of the United Nations, wheat was the fourth most-produced cereal in 2013, after sugar cane, maize and rice, which shows the significance of the wheat nourishment for humans all around the world ("FAOSTAT," 2015). While the European Union has the largest wheat production, Canada has achieved the fifth ranking stage globally with major production (more than 90%) in its western provinces (Market Analysis Group, Grains and Oilseeds Division, Food Value Chain Bureau, 2010).

Similar to other agricultural products, wheat is also subjected to various pests and diseases. Fusarium head blight (FHB) is one of the most threatening fungal diseases in temperate regions around the world. The economic loss resulting from FHB in Canada was estimated at over a billion dollar from 1993 to 2000 (Gilbert & Tekauz, 2000). One valuable way to enhance the efficiency of crop production in order to satisfy the needs for food in the near future is producing genetically improved crop varieties with a greater amount of resistance to diseases.

This can be accomplished by crossing with resistant germplasm of the same species or from closely related species.

Fusarium head blight impacts on wheat crops, fungus virulence tactics and transferring FHB resistance from the tall wheatgrass *Thinopyrum elongatum* are the main themes of this literature review and, more specifically, the following questions are addressed:

1. How does fusarium head blight cause DON contamination in cereals?
2. Why has FHB outbreak increased in recent decades?
3. What are the sources of FHB resistance and what are their applications in wheat breeding programs?
4. How can we protect wheat crops from FHB?
5. Why is the wheat genome considered to be complex?
6. How can FHB resistance gene(s) be transferred into wheat?

1.1 Structure of the thesis

The thesis is divided into four chapters. The most relevant literature and related research are reviewed in the first chapter. In Chapter 2, the material and methods that were used in all four objectives of this study are described in details. The results and analysis of each objective are presented in Chapter 3. A broader discussion of the results, conclusion and future work are provided in the fourth chapter.

1.2 Wheat – Genetic overview

Wheat has been considered a main dietary staple for most of the people living around the world during the last 8000 years; therefore, more agricultural lands globally are allocated to grow this essential plant comparing to the other crops (Curtis, 2002). Hexaploid common wheat

(*Triticum aestivum* ssp. *aestivum*; AABBDD genomes; 2n=6×=42) and tetraploid durum wheat (*Triticum turgidum* ssp. *durum*; AABB genomes; 2n=4x=28) are two main types of wheat. Different bread and biscuit types are commonly produced from *T. aestivum* species, while *T. turgidum* species are mostly used in pasta manufacturing. Regardless of polyploidy, both types are derived from the same two closely related ancestors with AA and BB genomes that grew thousands of years ago. Sometime after the tetraploid wheat (AABB genomes) became established, another hybridization with a diploid plant (*Aegilops tauschii*; DD genome) occurred which produced the hexaploid *Triticum aestivum* species (Figure 1.1).

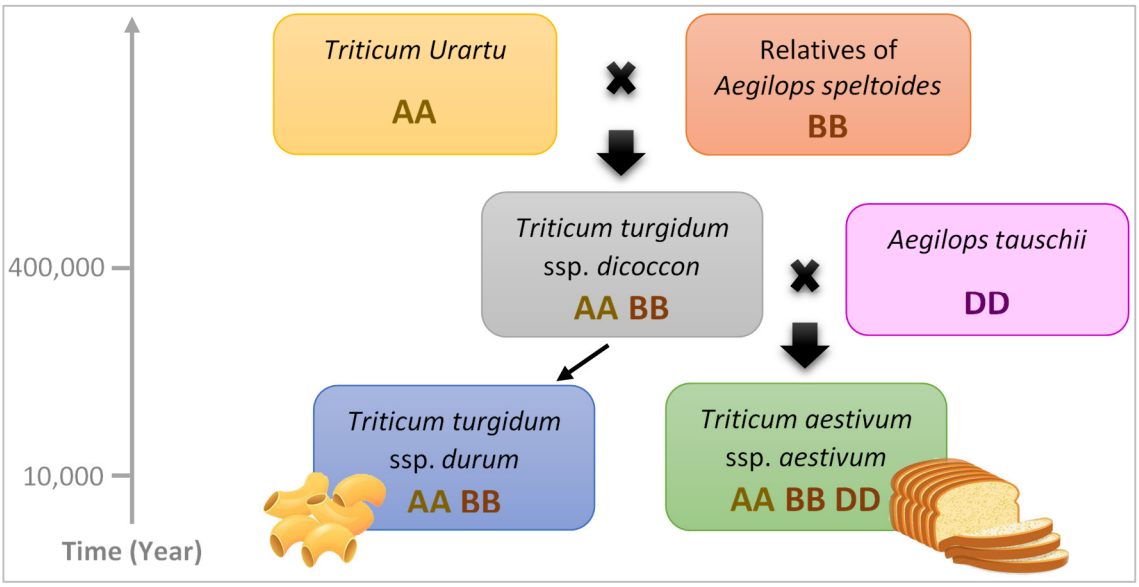

Figure 1.1: Wheat hybridization and polyploidization over time. Modified from (Borrill, Adamski, & Uauy, 2015).

Each of the A, B and D diploid genomes contains seven sets of homologous chromosomes. In general, the homologous chromosomes (both members of a given pair in a given genome) (Figure 1.2), have the same genes in the same order, but with possibly different alleles. On the other hand, chromosomes with the same number (1:7) but from different ancestors (A, B, or D) are called homoeologous (Figure 1.2). The homoeologous chromosomes can have a similar gene content and order but they most often have different repetitive DNA contents. It has been

confirmed that there are two or three copies of each gene present in the hexaploid wheat genome as 95 % of the coding regions in A, B and D genomes comprise the same sequences (Borrill et al., 2015).

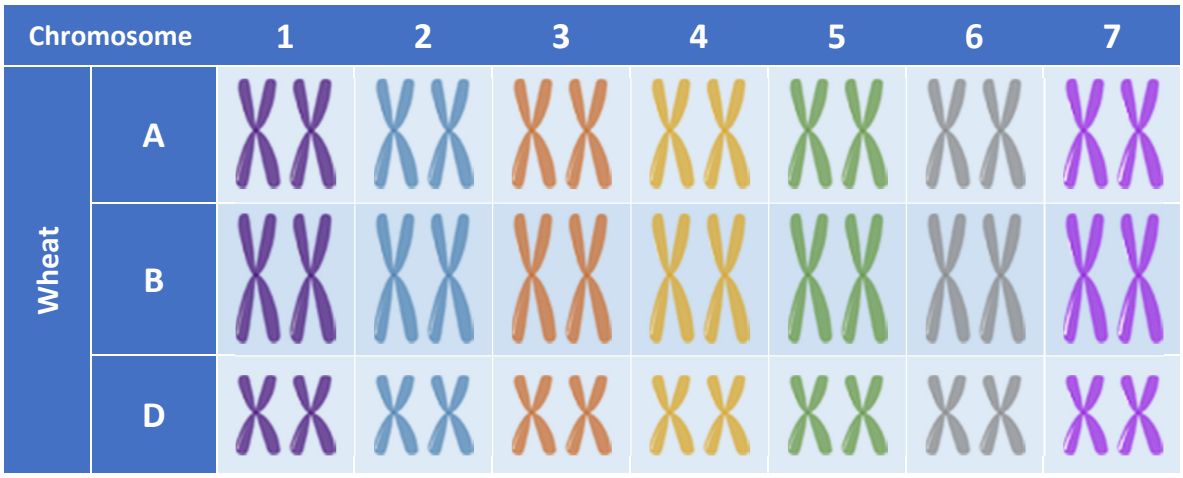

Figure 1.2: Triticum aestivum genome.
Chromosomes are not to scale. Modified from (Moore, 2014).

The size of the wheat genome is very big (six copies of each of the seven chromosomes = total of 42, 17 giga-base pairs) and it contains approximately 94-96,000 genes (Brenchley et al., 2012). In addition, many complex repetitive DNA sequences are present among wheat genomes (80% of the wheat genome is composed of DNA repeats). Both mentioned features together have made sequencing of the wheat genome a big challenge (Brenchley et al., 2012). The International Wheat Genome Sequencing Consortium, including participants from fifteen countries, started a project to generate a high-quality genome sequence for *T. aestivum* in 2005. Although a draft wheat genome sequence has been established and is publicly available, assembly of the thousands of sequenced-DNA fragments is not ordered. However, with a recently developed NRGene's DeNovoMAGICTM2.0 assembler technology a promising assembly for 14.6 Gb of wheat genome has been accomplished (Pozniak et al., 2016).

Meanwhile, researchers try to use the available sequencing information accumulated as contigs and scaffolds in their fields of study. During the sequencing procedure of an organism, many short overlapping DNA sequences (sequence reads) are produced in the first step. The contiguous assembly of adjacent components generates sequences referred to as contigs. The term scaffold is used when a genome sequence segment is composed of a series of oriented contigs interspersed with roughly estimated gap length (Figure 1.3).

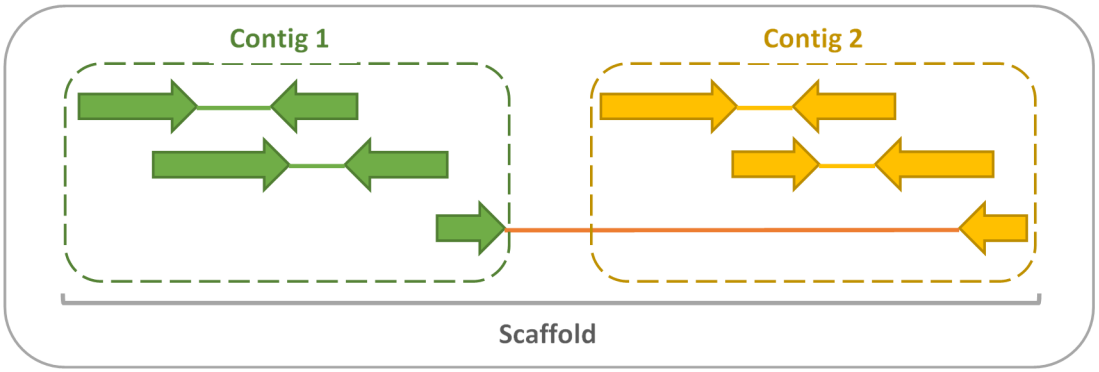

Figure 1.3: Graphical representation of contig and scaffold terminology applied in genome sequence assembly. Arrows illustrate components with known sequence and lines representing regions with unknown sequence but roughly estimated length. Modified from ("JGI Genome Portal Help: What is a Scaffold," n.d.).

1.3 Fusarium head blight (FHB)

FHB is one of the threatening diseases in cereals worldwide that affects more seriously wheat and barley. It was recognized for the first time in North America around 1880; however, FHB outbreaks have significantly increased in Canada in the last 30 years. It can be tracked from the extensive growing of highly vulnerable FHB wheat varieties specifically when grown with no or short crop rotations and when the weather is conducive to the fungus activity; these combined conditions lead to the accumulation of infected residues (Alberta Fusarium Action Committee, 2012).

The disease, associated with closely related *Fusarium* species, negatively impacts kernel development and results in yield losses and mycotoxin contaminated grains with low quality. Although at least 17 causal *Fusarium* species have been recorded (Parry, Jenkinson, & McLeod, 1995), the principal pathogen of FHB in North America is *Fusarium graminearum* (sexual stage: *Gibberella zeae*), which causes disease on wheat, barley and corn (Gale, 2003; Shaner, 2003). *F. graminearum* infection, particularly in wheat, leads to reduced grain yield as a considerable portion of the infected heads becomes bleached. FHB can prevent the normal development of grain or produce shriveled seeds with low weight (McMullen et al., 2012). Deoxynivalenol (DON), a major trichothecene mycotoxin produced by some *Fusarium* species and correlated to FHB, has significant negative effects on the health of cereal consumers - both humans and animals (Figure 1.4). Immune system disorders and embryo abnormalities are negative effects of DON on humans, while weight loss can be observed in herbivorous animals due to this mycotoxin (Desjardins, 2006). The negative impacts of *F. graminearum* and FHB have compelled scientists to find prevention remedies against this disease.

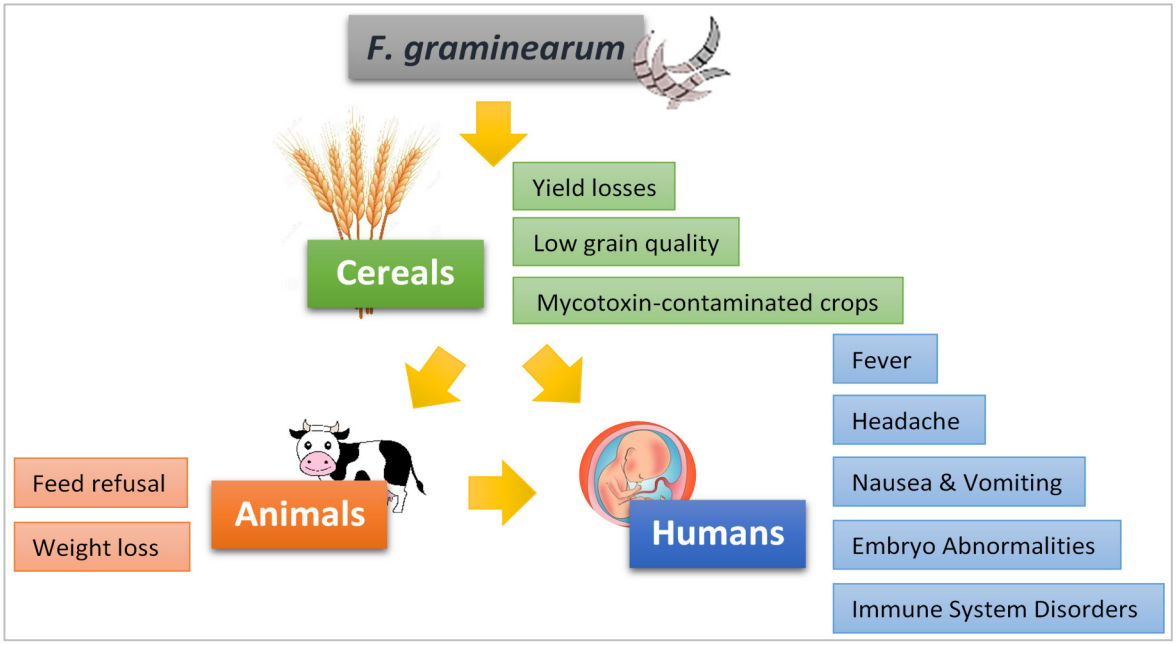

Figure 1.4: The negative impacts of FHB on cereals, animals and humans.

1.3.1 *F. graminearum* virulence tactics

In North America, *F. graminearum* is the main FHB pathogen infecting wheat. At the beginning, *F. graminearum* spores (either ascospores or macroconidia) get deposited onto wheat spikelets by air movement, water droplets or insects; the spores germinate and the growing mycelia enter into the wheat spikelets. Wheat is particularly susceptible during its flowering stage. The infected spikelets become bleached because of loss of their chlorophyll. Extended warm and humid weather conditions accelerate disease progression to the secondary stage, which causes the fungus to spread within the spike (Gilchrist & Dubin, n.d.). The fungus is utilizing DON and several hydrolytic enzymes, such as subtilisin-like and trypsin-like proteases, through most of the disease progression (Pekkarinen & Jones, 2003; Walter, Nicholson, & Doohan, 2010). DON secretion is occurring in both initial and secondary disease phases (Boenisch & Schäfer, 2011; Seong et al., 2009). However, as the initial infection is hardly detectable, the purpose of this preliminary secretion has not been identified yet (Brown et al., 2011). In the second phase, increased DON secretion facilitates the spread of hyphae from both infected spikelets to the rachis and rachis to uninfected spikelets up and down the spike (Bai, Desjardins, & Plattner, 2002; Proctor, Holm, & McCormick, 1995). It has been proposed that DON might suppress the cell wall defense strategies against the vertical movement of fungal hyphae up and down the rachis (Jansen et al., 2005). It has also been shown that a *Fusarium eumartii* hydrolytic enzyme, serine subtilisin protease, can degrade the pathogenesis-related (PR) proteins chitinase and β-1,3-glucanase in potato, which reduces the efficiency of the defense response (Olivieri, Zanetti, Oliva, Covarrubias, & Casalongué, 2002). *F. graminearum* might be categorized as a hemibiotrophic pathogen (Brown, Urban, van de Meene, & Hammond-Kosack, 2010). During the initial phase of infection, the fungal hyphae

spread in the intercellular space of the rachis without producing cell death (biotrophy). However, in the secondary phase, there is intracellular spread, the fungus causes cell necrosis and its lifestyle is converted from biotrophy to necrotrophy. In this stage, it is proposed that DON and protease enzyme activity cooperate to cause cell death in the host (Agrios, 1997; Pekkarinen & Jones, 2002; Y. Wang et al., 2005).

1.3.2 Wheat strategies to reduce FHB

The response of wheat and the mechanisms of resistance to FHB in certain wheat varieties remain largely unknown. However many studies have led to an understanding of some aspects of the interaction between wheat and *Fusarium* species. Scientists have shown a significantly higher amount of DON biosynthesis in infected plants when comparing to *in vitro* fungal cultures, indicating that wheat might have some stimulator signals which increase DON biosynthesis by *Fusarium* species (Mudge et al., 2006; Voigt, Schäfer, & Salomon, 2005). These inducers may include:

1. Polyamine compounds: nitrogen sources such as ornithine, agmatine and putrescine play a role in the stress response pathway in wheat (Gardiner, Kazan, & Manners, 2009). It was previously confirmed that polyamine gene expression is up-regulated by *F. graminearum* infection (Gardiner et al., 2010).
2. pH: DON biosynthesis is triggered by extracellular acidic environments (Gardiner, Osborne, Kazan, & Manners, 2009). In *in vitro* culture, acidification of the medium has been observed when *F. graminearum* and other fungi use ammonium as the sole source of nitrogen. It is suspected that some amines can also trigger acidification. It has been shown that amines alone -without the presence of acidic conditions- are not able to induce DON production (Gardiner, Osborne, et al., 2009). Although it has not

been proven that extracellular acidification happens in wheat when attacked by *F. graminearum*, it commonly occurs in other diseases caused by fungi such as *Penicillium expansum*, *Sclerotinia sclerotiorum* and *Botrytis cinerea* (Hadas, Goldberg, Pines, & Prusky, 2007; K. S. Kim, Min, & Dickman, 2008; Williamson, Tudzynski, Tudzynski, & van Kan, 2007).

3. Reactive Oxygen Species (ROS): ROS such as hydrogen peroxide (H_2O_2) are induced by DON biosynthesis during the defense response in wheat (Ponts, Pinson-Gadais, Verdal-Bonnin, Barreau, & Richard-Forget, 2006). H_2O_2 accumulation could lead to two opposite wheat responses. It might favor *F. graminearum* growth by causing programmed cell death and it may help the plant to stay alive by favoring antimicrobial pathways of plant defense (Desmond et al., 2008). However, it has not demonstrated yet which response is dominant and needs further investigations.
4. Phenolic Acids: Ponts et al. (2011) have shown that ferulic and coumaric acids increase the amount of DON biosynthesis, while p-hydroxybenzoic acid decreases the toxin production. On the other hand, Hamzehzarghani et al. (2005, 2008) have shown that FHB-resistant wheat varieties contain greater amounts of cinnamic and ferulic acids than susceptible ones, suggesting that these phenolic compounds can contribute to FHB resistance. Additional studies are needed to clarify the activities of phenolic compounds towards *F. graminearum* and FHB.

Other studies have brought a preliminary understanding of the response to FHB in susceptible and resistant wheat varieties, leading to some working hypotheses that will require further investigations. It has been proposed that there are two phases in the defense response against FHB in resistant wheat varieties. In the first phase, jasmonic acid (JA) and ethylene signaling pathways would be implicated in a nonspecifically coordinated antifungal defense leading to

a reduction of fungal growth and sporulation (Gottwald, Samans, Lück, & Friedt, 2012). Meanwhile, the second and more crucial phase would specifically contribute to fungal mycotoxin (DON) detoxification and protease (subtilisin-like proteases) inhibition (Gottwald et al., 2012). Other studies have conversely suggested that the JA and ethylene signaling pathways adversely increase wheat susceptibility (Ding et al., 2011).

Systemic acquired resistance (SAR) is an induced defense mechanism which can make plants resistant to a range of pathogens. Both salicylic acid (SA) and accumulation of PR proteins are essential factors in the SAR mechanism (Durrant & Dong, 2004). *Phenylalanine ammonia lyase* (*Pal*), *Enhanced disease susceptibility 1* (*Eds1*), *Natriuretic peptide receptor 1* (*Npr1*) and *Glucose transporter 2* (*Glut2*) are some of the genes involved in the SA signaling pathway. The role of the *Arabidopsis Npr1* (*AtNpr1*) gene is fundamental in SAR regulation. It has been demonstrated that down-regulation of the *AtNpr1* gene increases *Arabidopsis*' susceptibility to infection by various microorganisms (Dong, 2004). Accordingly, the gene's up-regulation enhances the resistance of *Arabidopsis* to pathogens (Cao, Li, & Dong, 1998). In addition to the effect of SA/*Npr1*, Makandar et al. (2010) have shown that the presence of JA signaling is also critical in *Arabidopsis* FHB resistance. JA initially suppresses the SA signaling in the early FHB infection stage, while increasing plant resistance through the later phases of infection.

In wheat, the SA signaling pathway has been proposed to regulate the defense strategy against FHB. It has been observed that a deleterious mutation of the gene *Pal*, which is a key enzyme in SA biosynthesis in the phenylpropanoid pathway, increases wheat susceptibility against FHB; this lends support to the role of the SA pathway in defense against FHB (Ding et al., 2011). *AtNpr1* expression in wheat conferred to the plants a rapid defense response and a higher FHB resistance level (Makandar, Essig, Schapaugh, Trick, & Shah, 2006). In addition,

another study by Makandar et al. (2012) has shown that, although both SA/*Npr1* and JA signaling contribute to FHB resistance mechanisms in wheat, the coincident or former activation of JA signaling can suppress SA activation, indicating that FHB resistance in wheat is very complex.

1.3.3 Types of FHB resistance

Producing FHB resistant wheat varieties is the most efficient solution not only to prevent FHB and mycotoxin contamination, but also to characterize resistance mechanisms and propose novel improvement strategies (McMullen, Jones, & Gallenberg, 1997). Schroeder and Christensen (1963) described the two most important types of FHB resistance when cereal plants encounter *F. graminearum* infection: a plant's ability to resist initial fungal infection, recognized as type I resistance, and resistance to disease spread through the spike, referred to as type II resistance. The other minor types of FHB resistance are tolerance (relative reduction of crop production), resistance to kernel infection and reduced DON mycotoxin accumulation (Mesterházy, 1995; J. D. Miller, Young, & Sampson, 1985). Not all scientists agree with the suggested first two minor types due to the difficulty in distinguishing between the effects of types I and II resistance on them. However, reduced DON accumulation is considered as resistance type III (Shaner, 2002). The amount of DON in the infected wheat grain varies significantly. For example, different *Fusarium* species produce various quantities of the mycotoxin. In addition, some wheat varieties (e.g. *Frontana*) have specific enzymes to degrade DON production and prevent its accumulation in the kernel (J. David Miller & Arnison, 1986). Lastly, some wheat varieties store the mycotoxin in their spike and prevent its penetration into the kernel (Bai & Shaner, 2004).

FHB resistance inheritance in wheat is quantitative and is affected by three factors: host, pathogen and environment. By this time, more than 100 DNA loci (Quantitative Trait Loci – QTL) related at various degrees to a phenotype of FHB resistance have been mapped. A great number of the studied QTL are related to type II resistance because type I is less stable as it might be influenced by non-genetic elements, and is also more difficult to screen due to the need to spray a fungal spore suspension during the flowering stage (Burt et al., 2015). The major QTL that has been identified in most of the FHB resistant wheat varieties of Chinese provenance is *Fhb1*; *Fhb1* is located on the short arm of chromosome 3B and is strongly related to type II resistance (Bai & Shaner, 2004).

1.3.4 FHB resistant species – Introducing *Thinopyrum elongatum*

In recent years, "*Praag 8*", "*Sumai 3*" and its derivatives, "*Frontana*", "*Wangshuibai*", "*Nyu Bai*" and "*Wuhan 1*" have been the main resistant wheat varieties used in breeding programs (Buerstmayr, Ban, & Anderson, 2009; Snijders, 1990). Due to the limited number of wheat genes/QTL that are efficiently used in breeding programs to improve FHB resistance, adding new exotic resistant sources can significantly help breeders to decrease wheat vulnerability to FHB by producing varieties having both currently explored mechanisms from wheat derivatives and resistance strategies from its wild relatives.

Some of the wheat wild relatives mentioned in the literature as FHB resistant species are: *Roegneria kamoji* (Weng, Wu, Chen, & Liu, 1993), *Elymus humidus*, *Elymus racemifer* (Ban, 1997), *Secale cereale*, *Aegilops speltoides* (Fedak et al., 2004) and *Thinopyrum junceiforme* (Jauhar & Peterson, 2001). Lately, researchers have found that *Thinopyrum elongatum* (2n=14, EE genome) is strongly resistant to FHB. This wild grass also called tall wheatgrass, is a wheat

relative carrying genetic resistance to FHB on the long arm of chromosome 7E (7EL) (Shen, Lingrang, & Ohm, 2004; Shen & Ohm, 2007; J.-R. Wang et al., 2010) (Figure 1.5).

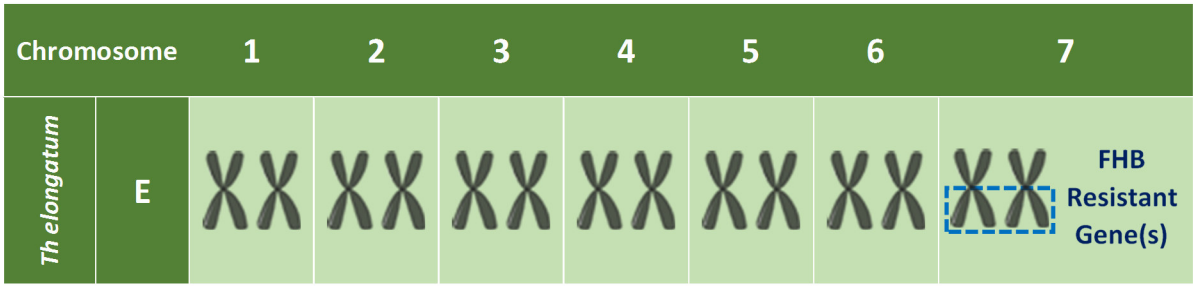

Figure 1.5: Th. elongatum diploid genome and the location of FHB resistant gene(s).

Th. elongatum has several other good agronomical characteristics including tolerance to drought (Roundy, 1985), salinity (Dvořák, Edge, & Ross, 1988) and cold environments, as well as resistance to leaf (Friebe, Jiang, Raupp, McIntosh, & Gill, 1996) and stripe rusts (Ma, Zhou, Dong, & Jia, 1999). *Th. elongatum* has longer spikes and more protein than wheat in its grains. Garg et al. (2009) have shown that chromosome 1 from *Th. elongatum* not only confers drought and salinity tolerance to wheat, but significantly modifies the wheat grain storage protein composition which results in high-quality final products. A later study has shown that wheat lines carrying a chromosome 4 from *Thinopyrum* species are highly resistant to necrotrophic eyespot and root pathogens (e.g. *Oculimacula yallundae* and *Rhizoctonia oryzae*) by increasing the plant's regrowth ability after senescence (Okubara & Jones, 2011). All of these traits make *Th. elongatum* an excellent source of new potential resistance genes for breeders to improve wheat.

1.4 Wheat and *Th. elongatum* genomic relationship

Poaceae is a large grass family that contains monocotyledon flowering plants including cereals. According to the information retrieved from the NCBI taxonomy browser ("Common

Taxonomy Tree," n.d.), *Thinopyrum* species have closer evolutionary relationship with *T. aestivum* comparing to the other species such as *Oryza sativa* (Rice), *Zea mays* (Maize), *Secale cereale* (Rye), *Hordeum vulgare* (Barley) and *Brachypodium distachyon* (Figure 1.6).

Different studies have shown that the E genome of *Th. elongatum* was closest to the wheat D genome. A study using EST-SSR (expressed sequence tag-simple sequence repeat) and PLUG (PCR-based landmark unique gene) markers showed many common bands between the wheat D and *Th. elongatum* E genomes; these same molecular markers amplified the most distinct bands for wheat B genome compared to *Th. elongatum* E genome, suggesting that these two genomes had the least homology with one another (Hu et al., 2012). Another experiment using genomic Southern and *in situ* hybridization techniques confirmed the same relationships (Liu, Li, & Zhang, 2007). In addition, these experiments showed that genomic rearrangements and exchanges in *Th. elongatum* and wheat substitution lines were mostly probable with the wheat D genome, although it sometimes happened with the A and rarely with the B genomes.

Close evolutionary association and high synteny between chromosomes 7D and 7E of wheat and *Th. elongatum* in addition to its ability to confer high protection against FHB from a resistant source located on 7EL chromosome, possibly at a single QTL, built a great interest in this wild species.

More recently, advances in molecular biotechnology have offered various methods to develop molecular markers making the use of genetic markers feasible in modern breeding programs. For instance, molecular marker assisted-breeding is a complementary application to select desired individuals based on their genomic DNA patterns in addition to their phenotypes (Jiang, 2013). Although specific markers have been developed for *Th. elongatum,* including some *SSR, EST-SSR* and *PLUG* markers, it is perceived that there are not enough of them to allow identification of beneficial resistance genes.

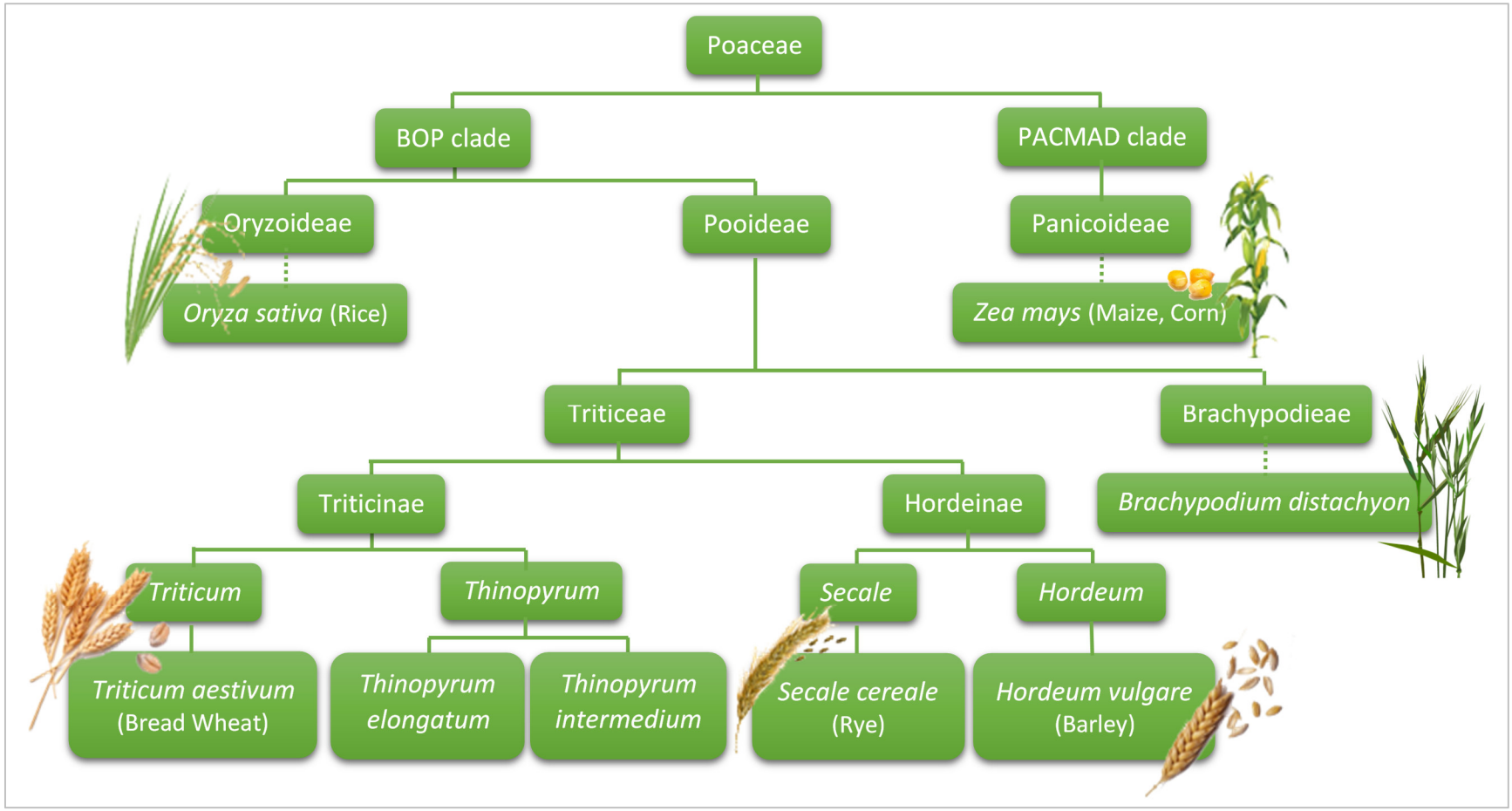

Figure 1.6: Schematic representation of the phylogenetic tree in the grass family (Poaceae).

1.5 The role and use of *Ph1* locus in wheat breeding

Some attractive characteristics (e.g. disease resistance genes) of wild wheat relatives, such as *Th. elongatum,* tempted geneticists to cross these grasses with wheat. Producing several resistant lines by transferring desirable genes from exotic germplasm to wheat made this strategy somewhat attractive in breeding programs. Although homoeologous chromosomes from different germplasm carrying the desirable traits can be relatively stable in wheat as additional chromosomes, introgression and chromosome pairing happened rarely between alien and wheat chromosomes. Scientists identified the pairing homoeologous (*Ph1*) locus on the long arm of chromosome 5B as the main inhibition factor for chromosome pairing between wheat and wild species (Riley & Chapman, 1958, 1964). A wheat line derived from the Chinese Spring variety and carrying an inactivated form of the *Ph1* locus, CS-*ph1b*, was developed (Sears, 1977) and utilized for crosses as an efficient solution to overcome the pairing issue and allow introgression of exotic DNA into wheat chromosomes (Figure 1.7).

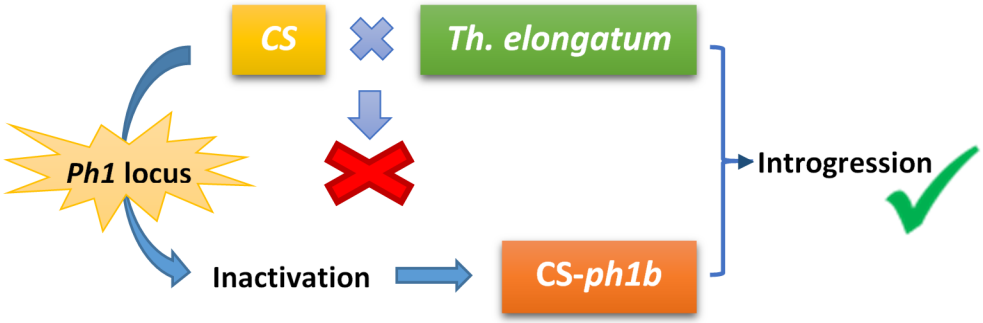

Figure 1.7: Ph1 locus role in a breeding program.

1.6 Development and characterization of CS-7E derived lines

Chinese Spring (CS) is an FHB-susceptible wheat variety. By crossing CS with *Th. elongatum,* many addition lines containing one exotic chromosome and a full complement of wheat chromosomes were produced, including lines containing chromosome 7E or approximately its long or short arm (CS-7E, CS-7EL and CS-7ES lines) (Dvořák, 1979; Dvořák & Knott, 1974). A series of substitution lines where chromosome 7E replaces one of the wheat chromosomes 7 has also been developed: CS-7E(7A), CS-7E(7B) and CS-7E(7D) (Dvořák, 1980) (Figure 1.8).

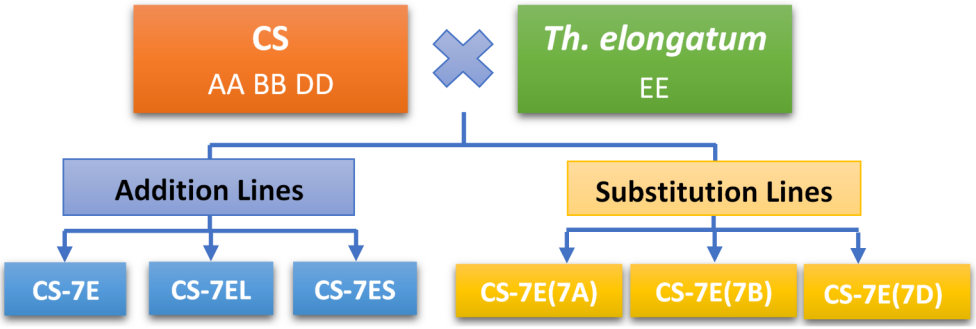

Figure 1.8: Examples of addition and substitution lines obtained from CS and Th. elongatum hybridization.

Inoculation experiments in the greenhouse have shown that CS-7E and CS-7EL have a high level of resistance to FHB when compared to CS, CS-7ES and CS lines carrying other *Th. elongatum* chromosomes (J.-R. Wang et al., 2010), suggesting that the resistance of *Th. elongatum* to FHB is produced by genetic element(s) on 7EL chromosome. Miller et. al. (2011) have performed *F. graminearum* inoculation experiments with CS and the CS-7EL addition line. Visual and microscopic observations have shown that fungal growth in the inoculated floret, as estimated by the appearance of a brown color on the wheat tissues, became visible after four days post inoculation (DPI) in CS inoculated florets, while browning in CS-7EL

became visible only after 10-14 DPI. In addition, in CS, the fungus spread through the rachis much more intensely and earlier than in CS-7EL addition line (Figure 1.9).

The observations also showed that the CS-7EL heads have longer internodes compared to those of CS (Figure 1.10). In addition, the resistant line displayed infection symptoms only in the inoculated spikelets most of the time and only 20% of the infected spikes displayed visible signs of disease in their rachis. From these experiments, it was proposed that the rachis played a key role against the fungal spread in CS-7EL. It is possible that longer internodes and the presence of an unknown dark brown material secretion in the node of the inoculated florets contribute to the FHB resistance associated with the rachis in CS-7EL (S. S. Miller et al., 2011).

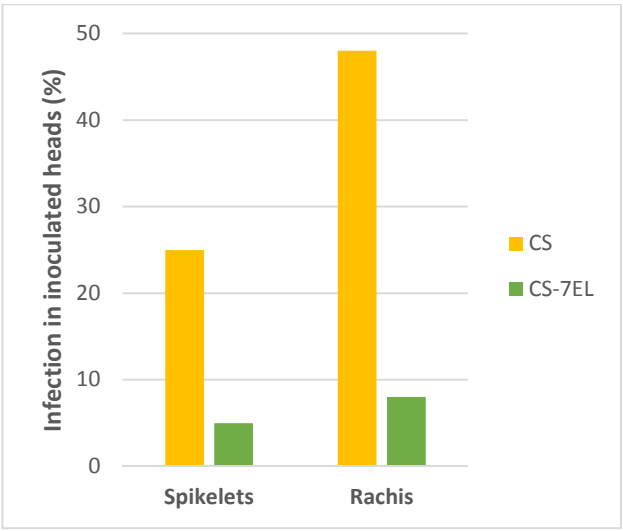

Figure 1.9: Comparing average infection levels in inoculated heads at 21 DPI for CS and CS-7EL. Modified from (S. S. Miller et al., 2011).

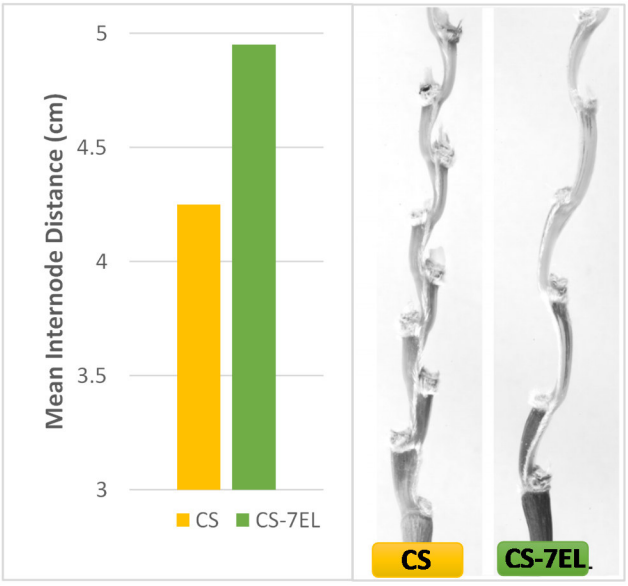

Figure 1.10: Comparing the mean internode distances between CS and CS-7EL lines. Modified from (S. S. Miller et al., 2011).

1.7 Towards identification of the FHB resistant gene(s) on the 7EL chromosome of *Th. elongatum*

Recently, a multidisciplinary project has been initiated to identify candidate gene(s) responsible for the mechanism of resistance to FHB contributed by the 7EL chromosome of *Th. elongatum.* Many complementary studies were initiated towards this goal and are described below (Thérèse Ouellet et al., 2016).

Developing markers associated with the 7E chromosome is essential to distinguish between the genomes of *Th. elongatum* and wheat. At the beginning, scientists tried to select 7E-specific markers from the existing wheat markers. Shen et al. (2004) used SSRs and cleaved amplified polymorphic sequences located on wheat group 7 homoeologous chromosomes, with the aim of identifying the 7E-specific polymorphisms. However, only a few of the examined markers specifically amplified for the 7E chromosome. In addition, Hu et al. (2012)

identified forty-three EST and PLUG markers specific to *Th. elongatum* chromosomes. In a more recent study, Chen et al. (2013), developed eighty-nine specific markers associated with specific length amplified fragments (SLAF) of *Th. elongatum* by using high-throughput sequencing technology. From these, sixty-one markers were specifically designed for *Th. elongatum* 7E chromosome; some of them have been used in this project.

In an effort to identify 7EL genes, a global profiling experiment using RNA-Seq was performed on rachis tissues of *F. graminearum* and water-treated (control) wheat heads of both CS and CS-7EL lines (Gou et al., 2016). Gou et al. (2016) designed a bioinformatics strategy to identify a list of candidate 7EL-expressed genes from the assembled RNA-Seq data. After eliminating all known wheat sequences, two criteria were used: 1. candidate 7EL-expressed sequences had to have 85-95% identity to wheat sequences (based on the information from published sequences at the time), and 2. the location of their closest homolog in the completely sequenced genome of the model cereal *Brachypodium distachyon* had to be preferentially on chromosome 1 or 3 (where homology with wheat chromosome 7 is found; Kumar, Balyan, & Gupta, 2012). Primers were designed for the best candidate 7EL-expressed genes (total of 135 genes) and tested by PCR assay using DNA from CS, CS-7EL and CS-7ES. 7EL-specific primers were identified for 48 genes and were used in this project.

In parallel to the marker design mentioned above, a draft genomic sequence of the 7EL chromosome fragment has been determined by DNA-Seq of a laser-enriched 7EL DNA fraction by collaborators Drs D. Konkin and A. Sharpe (NRC, Saskatoon) (T. Ouellet et al., 2016). This genomic sequence will allow the design of additional 7EL-specific markers and the identification of additional expressed genes from 7EL in the RNA-Seq data.

Another complementary study aimed at integrating the smallest possible fragment of 7EL that still carries resistance to FHB into a wheat chromosome 7. A collaborator of Dr. Ouellet's lab,

Dr. George Fedak (AAFC, Ottawa, Canada), has crossed the substitution line CS-7E(7D), which contains two 7E/no 7D chromosomes, with CS-*ph1b* (Figure 1.11). F_1 plants were backcrossed (BC) to CS-*ph1b* to develop lines homozygous for *ph1b*; a total of 556 BC_1F_1 progeny were produced (Fedak et al., 2014). DNA from the BC_1F_1 progeny was tested with *Ph1b*-specific markers (Qi, Friebe, Zhang, & Gill, 2007) and 43% (239 progeny) were *ph1b* homozygous recessive. BC_1F_2 progeny (called families), from selected plants that were *ph1b* homozygous recessive, were evaluated for resistance to FHB and for evidence of crossover between chromosome 7E and 7D. BC_1F_3 progeny were then evaluated for FHB resistance and also characterized with 7E-specific markers (Chen et al., 2013; Gou et al., 2016) to identify plants with small 7E introgressions that are still resistant to FHB.

The resistant BC_1F_3 progeny had different sizes of introgressed 7E in their 7D chromosomes. At the onset of the work described in this thesis, some of the BC_1F_3 progeny had been tested. Of these, three plants showed very promising results as they successfully amplified a smaller set of the 7E specific markers and still showed resistance to FHB in an initial test: plants 64-8-2, 64-8-17 and 64-8-27* (T. Ouellet et al., 2016). Characterization of BC_1F_4 families from these three plants was needed to confirm and follow up on the initial results and possibly find FHB resistant plants with a reduction in the size of their introgressed 7E fragment. In parallel, additional $BC_1F_{2\text{-}4}$ families continued to be tested in separate projects.

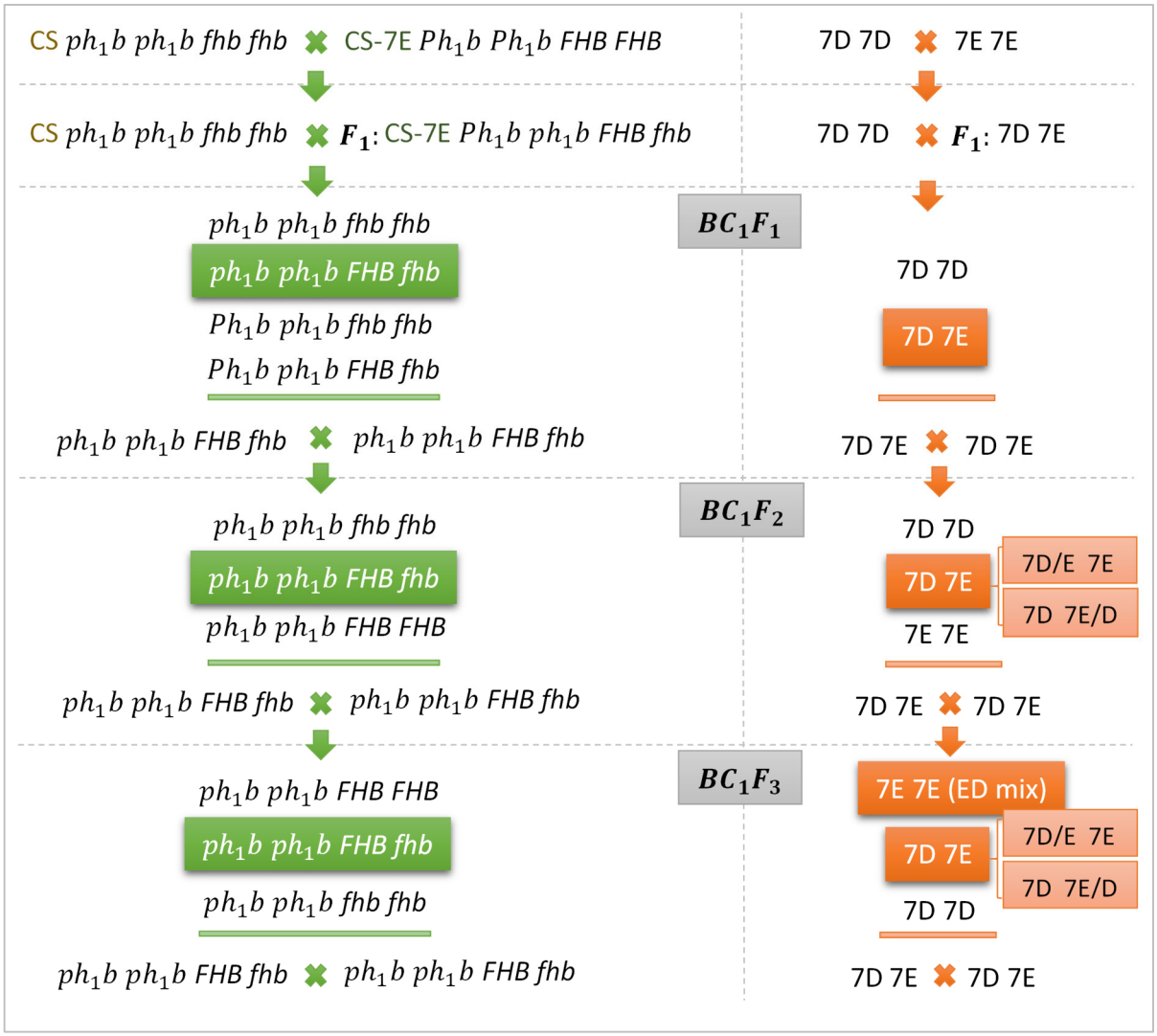

Figure 1.11: Schema summarizing the crossing events, up to BC_1F_3 in developing lines with fragments of 7E introgressed into the wheat chromosome 7D.
Personal communication from Dr. G. Fedak.

1.8 Statement of research and specific objectives

The long-term goal of the research is to identify the smallest fragment of 7EL chromosome of *Th. elongatum* that could be a novel source of resistance to FHB. Although *Th. elongatum* contains resistance genes, other traits (e.g. grain size) will pose a challenge for breeders.

Therefore, it is critical to identify the smallest possible fragment of 7EL chromosome possessing the functional element(s) responsible for FHB resistance.

Within a larger project, the specific objectives of this research were:

I.I Characterize five *Th. elongatum* accessions with differential response to FHB:

- Determine FHB resistance phenotype in these five accessions.
- Estimate the DNA polymorphism between the five accessions using 7E-specific markers.

I.II Characterize three BC_1F_4 families: 64-8-2, 64-8-17 and 64-8-27*

- Identify progeny carrying the same or smaller 7EL fragment compared to the BC_1F_3 plants using 7E-specific markers.
- Identify lines carrying a full 7D chromosome and the ones containing only 7D/7E chromosomes using wheat-specific markers.
- Determine FHB-resistance phenotype in progeny.

I.III Design additional 7EL-specific markers paired with homoeologous 7DL-specific markers that are either:

- Physically associated with selected 7E-specific markers from the previous objective.
- Presumed to be in the neighborhood of selected 7E-specific markers from the previous objective, when using genetic cross-walking between wheat and 7EL chromosomes.

I.IV Propose a genetic order for previous and novel 7E-specific markers that show a positive association with resistance to FHB.

2 MATERIALS AND METHODOLOGY

A brief description of required experiments for each of the objectives, listed in Chapter 1, is presented in the first section of this chapter. Then, complete details for materials and methods are provided in the second section.

2.1 Experimental highlights

2.1.1 Objective 1

Characterization of five *Th. elongatum* accessions with potentially differential response to FHB

a. Screening five *Th. elongatum* accessions and CS-7EL, CS-7ES and CS wheat lines with 48 markers for 7EL-specific expressed genes (Gou et al., 2016), and 25 7E chromosome-specific molecular markers (Chen et al., 2013) which specifically recognize either the short or long arm of the 7E chromosome of *Th. elongatum*.
    i. Growing CS-7EL, CS-7ES and CS seedlings and extracting DNA from fresh young leaves;
    ii. Extracting DNA from five different accessions of *Th. elongatum* (*1-72*, *1-73*, *1-74*, *1-86* and *'elongatum'*) (Plants were kindly provided by Dr. George Fedak);
    iii. Performing PCR assays with the mentioned eight DNA samples using a total of 73 markers;

iv. Determining if some of the markers have a distinct PCR band pattern between the five different *Th. elongatum* accessions and CS-7EL or CS-7ES wheat lines.

b. Rating fusarium head blight (FHB) progression in the same *Th. elongatum* accessions.

i. Preparing *F. graminearum* spores for plant inoculation;

ii. Inoculating the *1-72*, *1-73*, *1-74*, *1-86* and *'elongatum'* accessions in the greenhouse;

iii. Rating FHB symptom progression for each inoculated head at 5, 10, 15 and 21 days post inoculation (DPI);

iv. Identifying the most resistant and susceptible accessions.

2.1.2 Objective 2

Characterization of three BC_1F_4 families: 64-8-2, 64-8-17 and 64-8-27*

a. Screening three BC_1F_4 families using the same set of markers as described in Objective 1, as well as 34 wheat chromosome 7D-specific SSR markers.

i. Growing BC_1F_4 progeny of 64-8-2, 64-8-17 and 64-8-27* families;

ii. Extracting DNA from fresh young leaves;

iii. Performing PCR assays with 43 DNA samples from the three BC_1F_4 families and also CS-7EL, CS-7ES, CS and CS-7E(7D) (used specifically for the 7D-specific SSR markers) wheat addition and substitution lines;

iv. Identifying plants with the same or smaller 7E and 7D chromosome introgression comparing to the BC_1F_3 plants.

b. Rating FHB symptom progression in the BC_1F_4 progeny.

i. Preparing *F. graminearum* spores for plant inoculation;

ii. Performing inoculation of the wheat plants in the greenhouse;

iii. Rating FHB symptom progression in each inoculated head at 4, 8 and 12 DPI;

iv. Identifying the FHB resistant and susceptible plants.

c. Combining results from the "a" and "b" steps in order to identify the progeny having the smallest 7EL fragment and are still FHB resistant.

2.1.3 Objective 3

Designing additional 7EL-specific markers paired with homoeologous 7DL-specific markers

a. Markers physically associated with selected 7E-specific markers identified in the second objective.

I. Identifying the 7EL scaffold sequences associated with selected 7EL-specific expressed gene markers (Gou et al., 2016);

II. Identifying the 7EL scaffold sequences associated with Xgwm471 and Xgwm282 markers;

i. Amplifying the fragments from Xgwm282 and Xgwm471 markers;

ii. Cloning of the amplified fragments;

iii. Sequencing of the cloned fragments.

III. Designing new pairs of 7EL- and 7DL-specific primers.

b. Markers presumed to be in the neighborhood of selected 7E-specific markers from the second objective, using genetic cross-walking between wheat and 7EL (see 2.2.2.2 for the complete description).

I. Identifying the 7EL scaffold and 7ABD wheat contig sequences associated with selected 7EL-specific expressed gene markers;

II. Identifying corresponding and neighboring SNPs for wheat 7ABD contigs;

III. Identifying homoeologous 7ABD wheat contigs and 7EL scaffolds associated with selected neighboring SNPs;

IV. Designing new pairs of 7EL- and 7DL-specific primers.

c. Characterization of the novel 7EL- and 7DL-specific primer pairs.

2.1.4 Objective 4

Proposition of a genetic order for 7E-specific markers associated with FHB resistance

a. Retrieving 7EL scaffolds for 23 previously-designed markers from the 7EL draft genomic sequence database;

b. Finding the homoeologous 7ABD wheat contigs for 7EL scaffolds;

c. Retrieving the mapping data for the 7ABD wheat contigs from an in-house collection of publicly available Single Nucleotide Polymorphism (SNP) mapping data from the Axiom, iSelect, KASP chips and combine with mapping data obtained in Objective 3;

d. Estimating the location of previous and novel markers based on a compilation of the gathered information.

2.2 Materials and Methods

2.2.1 Characterization of five *Th. elongatum* accessions and three BC_1F_4 families

Figure 2.1 displays the methodology for Objectives 1 and 2. Further details of each step are discussed in the following subsections.

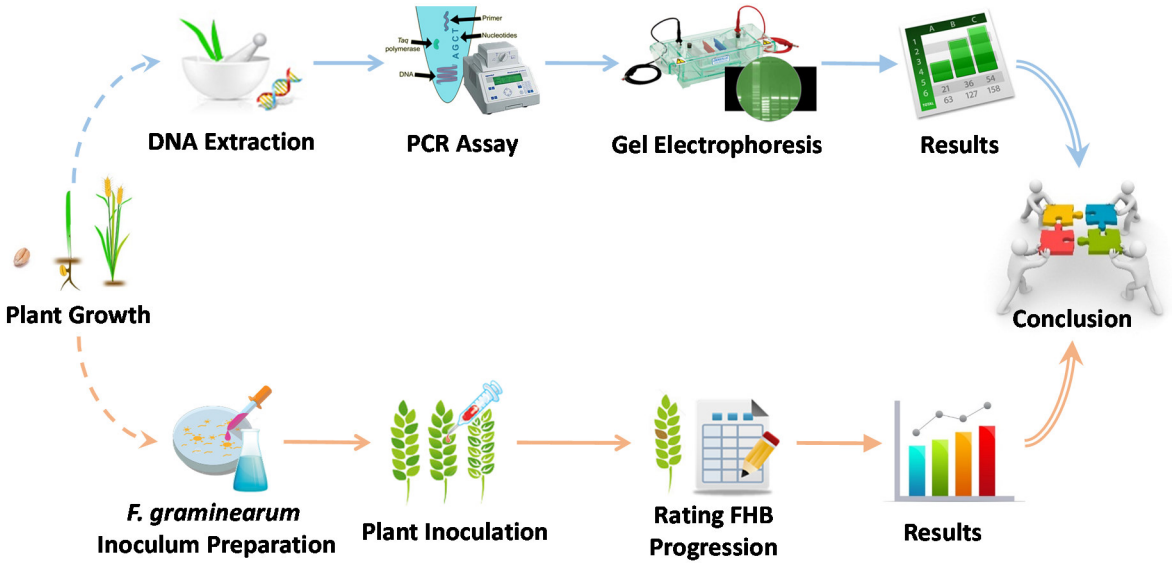

Figure 2.1: Methodology of first and second objectives: characterization of five Th. elongatum accessions and three BC1F4 families.

2.2.1.1 Plant material

Five *Th. elongatum* accessions were obtained and their identity confirmed by Dr. George Fedak (AAFC, Ottawa, Canada): *1-72, 1-73, 1-74, 1-86* and *'elongatum'*; they were the only confirmed *Th. elongatum* accessions that he was able to obtain following requests to many seed banks and scientist collections. Accessions *1-72* (Book No. 198–I, PI 531717) and *1-74* (Book No. 198–I, PI 531718) were originally collected in unspecified location(s) in France, *1-73* (Book No. 198–I, PI 531719) from Tunisia and *1-86* (Book No. 181, PI 383583) were harvested 50 km south of Kars, Turkey (US National Plant Germplasm System, "Plant Inventory Books," n.d.). The origin of *'elongatum'* is not known. Mature plants for those accessions were kindly donated by Dr. G. Fedak and Danielle Wolfe (ORDC, Ottawa, Canada).

BC_1F_4 progeny from three BC_1F_3 plants 64-8-2, 64-8-17 and 64-8-27* (the asterisk was used to differentiate between two different 64-8-27 progeny that were identically named in experiments by different individuals), that showed promising results in previous experiments

by L. Gou, Danielle Wolfe and Teresa Kim Nguyen (ORDC, Ottawa, Canada), were characterized (see Figure 1.11 for crossing schema). Those BC_1F_3 plants were successfully amplified for a smaller number of 7EL-specific markers when compared to the other BC_1F_3 plants and were FHB resistant. Twenty, ten and twenty seeds from families 64-8-2, 64-8-17 and 64-8-27* respectively were kindly provided by Dr. G. Fedak.

CS, an FHB susceptible wheat variety, CS-7ES, an addition line that contains the short arm of chromosome 7E from *Th. elongatum,* and CS-7EL, an FHB resistant addition line that contains the long arm of chromosome 7E, served as control plants. Seedlings of the CS-7EL, CS-7ES and CS lines were grown for DNA extraction. Five CS-7EL and five CS seedlings were also grown as control plants during the inoculation experiment.

All seeds were germinated prior to the sowing (Figure 2.2, left panel); seven seeds from family 64-8-17 did not germinate. Seedlings and mature plants were grown in a growth cabinet with a regime set at 16 hr light (20 °C)/8 hr night (15 °C) (Figure 2.2, right panel).

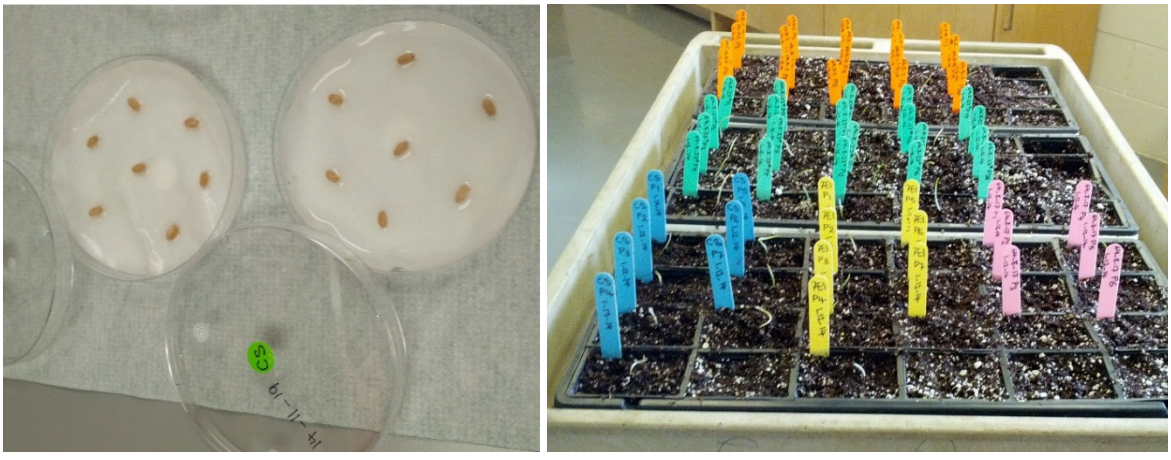

Figure 2.2: Illustration of growing plant materials.
Left: seed germination set up, right: transfer of seedlings to soil.

At week ten, each BC_1F_4 plant was vertically split in half. In case a crossing with regular CS would be required to stop recombination occurring in the *ph1b* background and fix the genotype,.one half was kept in a cold room (4 °C) in order to prevent the plant from entering the flowering stage. The other half was moved to a bigger pot and maintained in the same growing conditions mentioned above.

2.2.1.2 Genomic DNA extraction

Fresh young leaves were harvested from mature plants or from seedlings 14 days after planting. Immediately after harvest, leaves were flash-frozen in liquid N_2, then ground to a fine powder using a mortar and pestle. Genomic DNA from these plants was extracted using the "Illustra Nucleon Phytopure Genomic DNA Extraction Kit" (GE Healthcare Life Sciences) following the manufacturer's protocol. The RNA digestion optional step at the beginning of the extraction procedure was included. The DNA pellets were resuspended in 100 µl of 1x Tris-acetate-EDTA (TAE) buffer [40 mM Tris (pH 7.6), 20 mM acetic acid, 1 mM EDTA]. DNA concentrations were measured using a Nanodrop ND-1000 spectrophotometer (Software V.3.8.1, Thermo Scientific) and DNA quality assessed by electrophoresis on 0.9% agarose gel (Mandel Scientific) containing ethidium bromide and 1x TAE buffer in a Bio-Rad Sub-Cell GT Cell System containing 1x TAE buffer. Samples were resolved at 100-130 V. The gels were scanned in a Molecular Imager® Gel Doc™ XR+ System (Bio-Rad Laboratories), under UV Trans Illumination (302 nm) and analyzed with Image Lab™ 5.1 software (Bio-Rad Laboratories) (freely available at http://www.bio-rad.com/en-us/product/image-lab-software). The concentration of extracted DNA samples are presented in Table App-I.1 (section A and B). An example of electrophoresis results for several extracted genomic DNA samples is provided in Figure 2.3. In addition, DNA samples from BC_1F_3 plants was donated by L. Gou,

and CS-7E(7D) DNA was kindly provided by Danielle Wolfe to use as an additional control for the screening of the 7D-specific SSR markers.

Moreover, to screen the BC_1F_4 progeny with novel markers designed in Objective 3, fresh genomic DNA from CS-7E(7D) were needed. Five CS-7E(7D) seedlings were grown and their genomic DNA samples were extracted following the same procedure mentioned above. The concentrations of extracted DNA samples are presented in Table App-I.1 (section C). Many CS-7E(7D) DNA samples were prepared to provide reference stocks for other members of the lab.

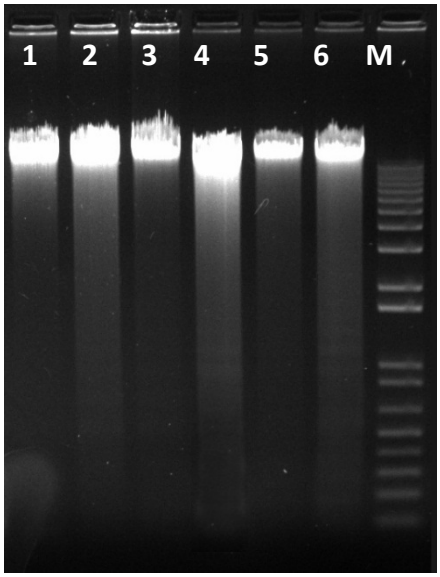

Figure 2.3: An example of extracted genomic DNA.
DNA samples are (1) 64-8-17-2, (2) 64-8-17-3, (3) 64-8-27-1, (4) 64-8-27*-2, (5) 64-8-27*-5, (6) 64-8-27*-6, (M) 1 Kb Plus DNA Ladder. PCR amplified fragments were separated on a 0.9% agarose gel.*

2.2.1.3 Polymerase chain reaction

First, 50 ng/µl working dilutions were prepared (Table App-I.1, sections A and B). For screening the BC_1F_4 progeny, a second series of working dilutions at 12 ng/µl were developed

from the first dilution series to simplify pipetting. The first and second dilution amounts for each progeny is presented in Table App-I.1 (section B).

For a single PCR reaction, a 10 µL reaction mix was prepared consisting of 1x PCR Buffer II (Applied Biosystems), 2.5 mM $MgCl_2$, 0.3 mM dNTP (ThermoScientific), 0.5 µM of each Forward and Reverse primer, 48-50 ng DNA sample and 0.625 U AmpliTaq Gold® DNA Polymerase (Applied Biosystems) (The multi reaction PCR template is presented in Table App-I.2). Reactions were performed in a Mastercycler Thermal Cycler (Eppendorf) with conditions set to denaturation at 94 °C for 4 minutes, followed by 35 cycles consisting of denaturation at 94 °C for 30 seconds, annealing at 50-60 °C for 30 seconds, elongation at 72 °C for 1 minute, with a final elongation at 72 °C for 5 minutes.

Forty-eight molecular markers for 7EL-specific expressed genes, which have been designed by a previous student in Dr. Ouellet's lab (Gou et al., 2016), and 25 7E chromosome-specific molecular markers (Chen et al., 2013) were used to screen the five *Th. elongatum* accessions and 43 BC_1F_4 progeny. In addition to the mentioned markers, 34 wheat chromosome 7D-specific SSR markers ("GrainGenes: A database for Triticeae and *Avena*," n.d., http://wheat.pw.usda.gov/cgi-bin/graingenes/browse.cgi?class=marker; accessed May 2015) were also tested for screening the BC_1F_4 progeny. The PCR amplification products (10 µl) were separated on 1.5% agarose gels. Finally, the PCR results were tabulated in Excel spreadsheets. If an amplicon was observed with a DNA sample, it was scored as 1, while the amplicon absence was recorded as 0. Scores of 0.5 and 0.25 indicated the presence of amplicon bands with lower intensity levels.

2.2.1.4 Plant inoculation with *F. graminearum*

***Fusarium graminearum* spore production:** 150 µl of a fresh *F. graminearum* macroconidia suspension (1 x 10^6 spores/ml) was used as inoculum from the wild type *F. graminearum* strain DAOM 233423 (Canadian Collection of Fungal Cultures, AAFC, Ottawa, Canada) and was transferred to 50 ml of CarboxyMethyl-Cellulose (CMC) medium (Cappellini & Peterson, 1965). After three days of shaking in the dark at 28 °C, the macroconidial spores were separated from the mycelia by filtration on Miracloth and washed three times by resuspending in sterile water followed by centrifugation at 14 °C, 4,200 rpm for ten minutes in order to obtain concentrated *Fusarium* spores free of CMC medium. Spores were counted using a hemocytometer and a fungal spore suspension at 1 x 10^5 spores/ml was prepared. Figure 2.4 shows *F. graminearum* macroconidia after harvest and the step of counting spores using a hemocytometer.

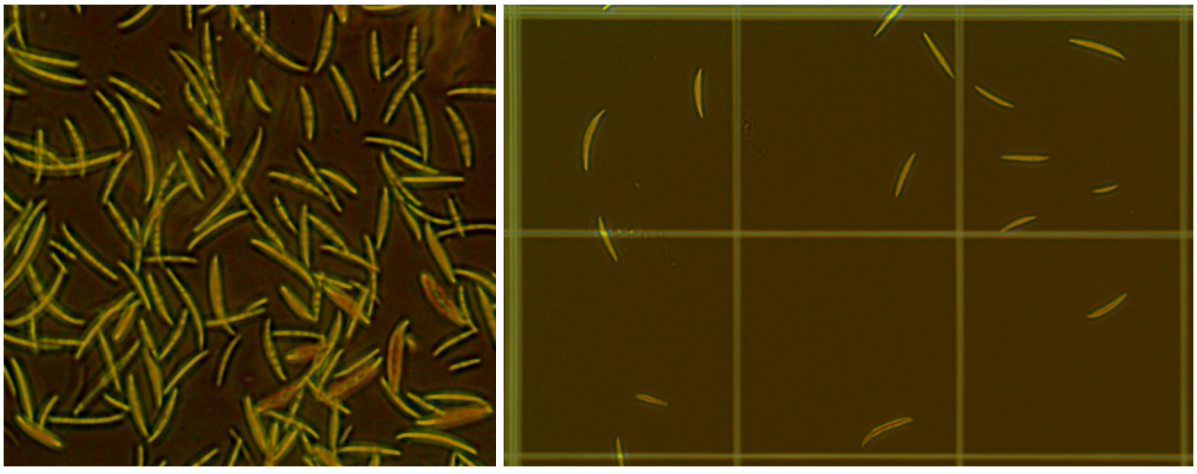

Figure 2.4: F. graminearum spore preparation for inoculation.
Left: F. graminearum ascospore stock, right: counting spores using a hemocytometer.

Plant inoculation: The *F. graminearum* fresh inoculum suspension was used to point-inoculate preferably the middle spikelet in each *Th. elongatum* or wheat spike; inoculations

were done at mid-anthesis, when the yellow anthers appeared out of the spikelets and before they became white (Figure 2.5, left panel and Figure 2.6, step 1). In our growth cabinet conditions (16 hr of light at 20 ℃ and 8 hr of dark at 15 ℃), *Th. elongatum* flowers extruded their anthers after nine hours of exposure to the light, and retracted them approximately two hours later, allowing for a narrow window of inoculation. However, in wheat, the flowering period lasted almost four days.

For each inoculated spike, ten µl of a *F. graminearum* spore suspension at 1 x 10^5 spores/ml was point-inoculated with a micropipette between the lemma and palea of one (*Th. elongatum* accessions) or two (BC_1F_4 progeny) floret(s) of one spikelet with extruded yellow anthers (Figure 2.5, right panel; Figure 2.6, steps 2). Plants were inoculated when most of their spikes were at the flowering stage to allow inoculation of more than one spike per plant because there was only one inoculation session per plant. In the experiments of this study, *F. graminearum* inoculations proceeded over nine days for the *Th. elongatum* accessions and fifteen days for the BC_1F_4 progeny, as individual plants entered the flowering stage at different times.

Figure 2.5: Example of a Th. elongatum spike.
Right: flowering florets ready for inoculation; left: inoculation with F. graminearum.

After inoculation, plants were transferred to the misting room and misted for 30 seconds every hour for two days during the light period, to provide high humidity conditions required by the fungus during the initial infection stage (Figure 2.6, step 3). Afterward, plants were moved to the non-misted side in the same cabinet which was kept at 75% humidity and 25 °C.

Lastly, FHB symptoms, observed as either browning or bleaching of tissues, were noted over time to track the disease progression signs in the inoculated plants. Training for inoculation and FHB symptom assessment was provided by a technician, Margaret Balcerzak (AAFC, Ottawa, Canada). For *Th. elongatum* accessions, disease ratings were performed at 5, 10, 15 and 21 DPI for every inoculated spike. BC_1F_4 progeny were rated at 4, 8 and 12 DPI; the last rating was done at 12 DPI because most wheat plants started to show maturing signs around fourteen days after the flowering stage making the FHB symptoms harder to evaluate.

The following FHB symptoms were tracked for each inoculated spike in *Th. elongatum* accessions: percentage of disease symptoms in inoculated and non-inoculated florets of each inoculated spikelet (scored as 0, 50 or 100%), percentage of inoculated spikelet with bleaching symptom (scored as 0, 50 or 100%), percentage of spikelets with bleaching symptom (total, above or below of inoculated spikelet) per (total, above or below) number of spikelets, percentage of infected internodes (total, above or below of inoculated spikelet) per (total, above or below) number of internodes.

The same parameters were scored for the BC_1F_4 progeny except for the inoculated spikelet, where both left and right florets were inoculated and scored as such. Finally, to assess the FHB responses of the *Th. elongatum* accessions and the BC_1F_4 progeny, one-way ANOVA (Analysis of variance) statistical test in Microsoft Excel software application was used.

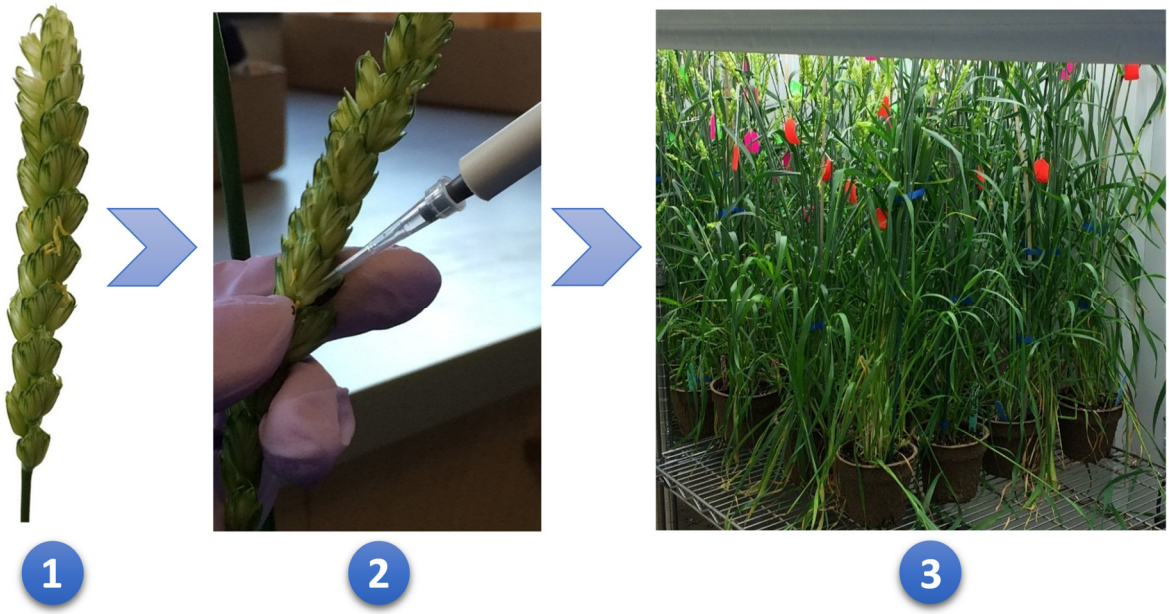

Figure 2.6: Wheat inoculation procedure with F. graminearum spores.
1) Wheat at flowering stage, 2) point inoculation between lemma and palea, 3) Inoculated plants in the misting room.

2.2.2 Designing additional 7EL-specific markers paired with homoeologous 7DL-specific markers

2.2.2.1 Designing additional markers physically associated with selected 7E-specific markers

2.2.2.1.1 Identifying the 7EL scaffold sequences associated with selected 7EL-specific expressed gene markers

The 7E genomic scaffolds that included the original EST contig sequences for markers Lu-9736, Lu-632-2, Lu-287-2 and Lu-387-2 (Gou et al., 2016) were identified in the 7EL_genomic_v150429_gapfilled database, containing all currently available 7EL genomic scaffolds of *Th. elongatum* (Konkin et al., 2016), using a local software application (Bigblast - ORDC Blast Server V2.93_2008_0929, 2008) built on BLASTN 2.2.17 (Altschul et al.,

1997). Only scaffolds with more than 97% identity with the original EST sequences were retained. Homologous 7EL scaffold sequences were extracted from the database using the "Extract sequences from a fasta file" software application (J. Hattori, personal communication).

2.2.2.1.2 Identifying the 7EL scaffold sequences associated with Xgwm471 and Xgwm282 markers

2.2.2.1.2.1 Amplifying the fragments from Xgwm282 and Xgwm471 markers

The sequence of the PCR fragments amplified by Xgwm471 and Xgwm282 had to be determined as that information was not publicly available. DNA from progeny 64-8-27*-2 and 64-8-27*-20 were used for PCR amplification with Xgwm282 and Xgwm471 markers respectively. For each PCR amplification, a 60 µL reaction mix was prepared consisting of 1x PCR Buffer II, 2.5 mM $MgCl_2$, 0.3 mM dNTP (ThermoScientific), 0.5 µM of each Forward and Reverse primer, 48 ng DNA sample and 0.625 U AmpliTaq Gold® DNA Polymerase (Applied Biosystems). Ten µL of amplification reactions were loaded on a 1.5% agarose gel and the remaining 50 µL were used for a PCR fragment purification procedure using the Quick PCR Purification Kit (Invitrogen) to remove small DNA molecules under 100 bp including primers and primer dimers. The protocol provided by the manufacturer was followed, except that elution was performed in water at pH 8 instead of elution buffer. The final DNA concentrations were as follows: Xgwm282 = 23.1 ng/ µL and Xgwm471 = 36.5 ng/µL.

2.2.2.1.2.2 Cloning of the amplified fragments from Xgwm282 and Xgwm471 markers

Due to the microsatellite origin of the markers which contain a number of repeated sequences, cloning the PCR products was done to increase the chance of obtaining a successful DNA sequence. The "pGEM®-T Easy Vector System" protocol was followed. To begin, A-Tailing

was done to insert and ligate the PCR amplicon to a pGEM-T Easy vector. For each PCR amplicon, a 10 µL reaction mix was prepared consisting of 1x Taq DNA Polymerase Reaction Buffer, 2.5 mM $MgCl_2$, 0.2 mM dATP (ThermoScientific), 6 µL of amplicon (≈0.2 Kb) and 5 U Taq DNA Polymerase (Fermentas). The final amplicon concentrations became 13.8 and 21.9 ng/µL respectively for Xgwm282 and Xgwm471 markers. The reactions were incubated at 70 °C for 30 minutes. Then, each A-tailed PCR amplicon was ligated into pGEM®-T Easy vector following the protocol provided by pGEM®-T Easy Vector System I using 2x Rapid Ligation Buffer and 3 Weiss units/µL of T4 DNA ligase (Promega).

Ten cm diameter petri dishes containing 40 g/L of Luria-Bertani (LB) agar, Miller (Difco Laboratories) and 0.1 g/L of Ampicillin (Sigma) were prepared. Then, 0.01 mmol IPTG and 1 mg X-Gal were added to each petri dish and spread over the surfaces, allowing to absorb for 30 minutes prior to use. Transformations into One Shot® TOP10 Chemically Competent Cells (Invitrogen) were performed following the manufacturer's protocol. Twenty, 50 and 100 µL of each transformation reaction were spread onto separate LB media petri dishes and incubated at 37 °C for 24 hours. The successful insertion turned the color of colonies to white as they interrupted the lactose operon reading frame and made it non-functional, while the blue colonies indicated the absence of an insertion. Twelve white colonies were selected for each marker and each single colony was resuspended in 12 µL of sterile water.

PCR amplifications using M13 primers were performed to screen for insertion in the selected colonies (M13 Forward sequence: 5´-d(CGCCAGGGTTTTCCCAGTCACGAC)-3´, and M13 Reverse sequence: 5´-d(TCACACAGGAAACAGCTATGAC)-3'). For each PCR amplification, a 25 µL reaction mix was prepared consisting of 1x Taq PCR Buffer, 1.5 mM $MgCl_2$, 0.2 mM dNTPs (ThermoScientific), 0.5 µM of each M13 Forward and Reverse Primer, 5 µL of resuspended colony and 0.625 U AmpliTaq gold® DNA Polymerase (Applied

Biosystems). The amplifications' conditions were set to denaturation at 94 °C four minutes, followed by 35 cycles which consisted of denaturation at 94 °C for 30 seconds, annealing at 54 °C for 30 seconds, extension at 72 °C for one minute and a final extension at 72 °C for five minutes. The amplified PCR products were loaded on a 2 % agarose gel. Based on the predicted size of the PCR products, the ten best-resuspended colonies were selected.

The 7 µL leftover of each colony was added to a 3.5 ml culture tube containing 25 g/L LB broth, Miller (Difco Laboratories) and 100 µg/ml ampicillin, and were placed in a shaker at 37 °C for 16-18 hours. To prepare plasmids, 3 ml of each bacterial culture was extracted using the "QIA Prep® Spin Miniprep Kit" (Qiagen). The protocol provided by the manufacturer was followed except that elution of the plasmids was done in H_2O at pH 8 instead of the provided buffer. Finally, the concentration of each plasmid was measured using a Nanodrop ND-1000 spectrophotometer (Software V.3.8.1, Thermo Scientific).

In order to visually check the insertion in the plasmids, a 15 µL digestion reaction containing 1x EcoR1 Buffer, 7.5 U of EcoR1 (Thermo Scientific) and 6 µL of the extracted plasmids were prepared and incubated at 37 °C for 60 minutes. Samples were then loaded on 1.5% agarose gel.

2.2.2.1.2.3 Sequencing of the cloned fragments

Using the plasmid DNA, sequencing reactions were performed. For each sequencing reaction, a 10 µL mix was prepared containing 1x Seq. Buffer V3.1, 0.125x BigDye® Terminator v3.1 Cycle Mix (Applied Biosystems™), 0.16 µM M13 Forward Primer, H_2O and 0.5-1 µL of the plasmid DNA. The sequencing reaction conditions were set to denaturation at 94 °C for four minutes, followed by 30 cycles which consisted of denaturation at 94 °C for 30 seconds, annealing at 54 °C for 30 seconds, extension at 72 °C for one minute and a final extension at

72 °C for five minutes. The sequencing reactions were sent to the Microbial Molecular Technologies Laboratory service group (ORDC, Ottawa), which are using a 3130XL ABI Sanger sequencing system to separate the sequencing fragments. The obtained DNA sequences were analyzed and assembled using Chromas and SeqMan Pro (Lasergene V 12, DNASTAR, Inc., Madison, Wisconsin, USA) software tools.

The 7EL genomic scaffold that contained the sequences for the Xgwm282 fragment was identified as described in 2.2.2.1.1.

2.2.2.1.3 Designing new 7EL- and 7DL-specific primers with physical association to selected 7E-specific markers

Sequence of the 7EL scaffolds containing the contig sequences for Lu-9736, Lu-632-2 and Xgwm282 were used to design physically associated novel markers. The "EditSeq" software application (Lasergene; DNASTAR) was used to identify the location of the associated 7E-specific marker contig sequences within the 7EL scaffold to determine candidate positions for designing new sets of markers. The new locations varied depending on the 7EL scaffold sizes and the position of the previous markers. When a previous marker was located in the middle of the associated 7EL scaffold, new markers were designed for each end of the scaffold; when a previous marker was closer to one end of the associated 7EL scaffold, the other end of the scaffold was used to design new markers (Figure 2.7).

Two steps were used to increase the chances of identifying sequences specific to the 7E chromosome of *Th. elongatum* and absent or with low homology to wheat 7A, B and D chromosomes. First, intergenic or intron sequences were identified by aligning the candidate region sequences against a database containing a local assembly of wheat ESTs (Hattori, Ouellet, & Tinker, 2005) using the "Bigblast" software (Figure 2.8).

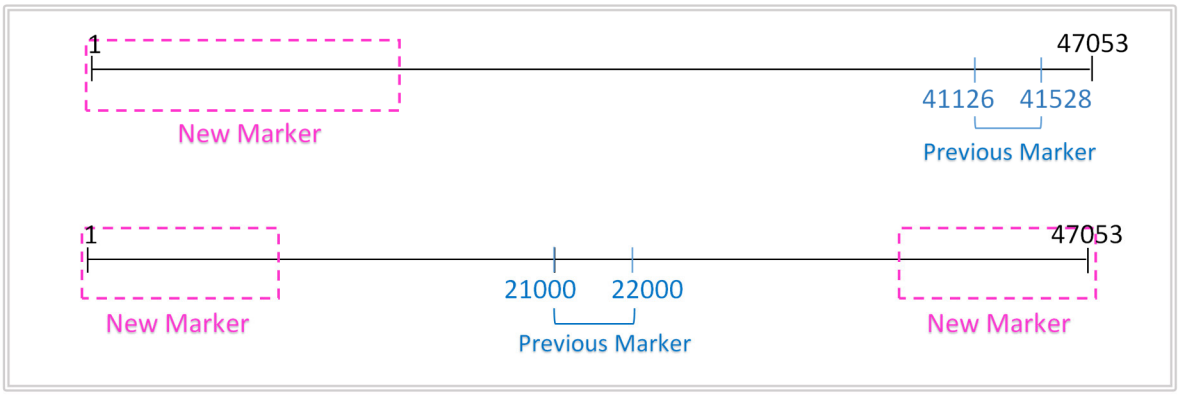

Figure 2.7: Hypothetical examples illustrating the design strategies for new markers physically associated with the previous 7EL-specific markers.

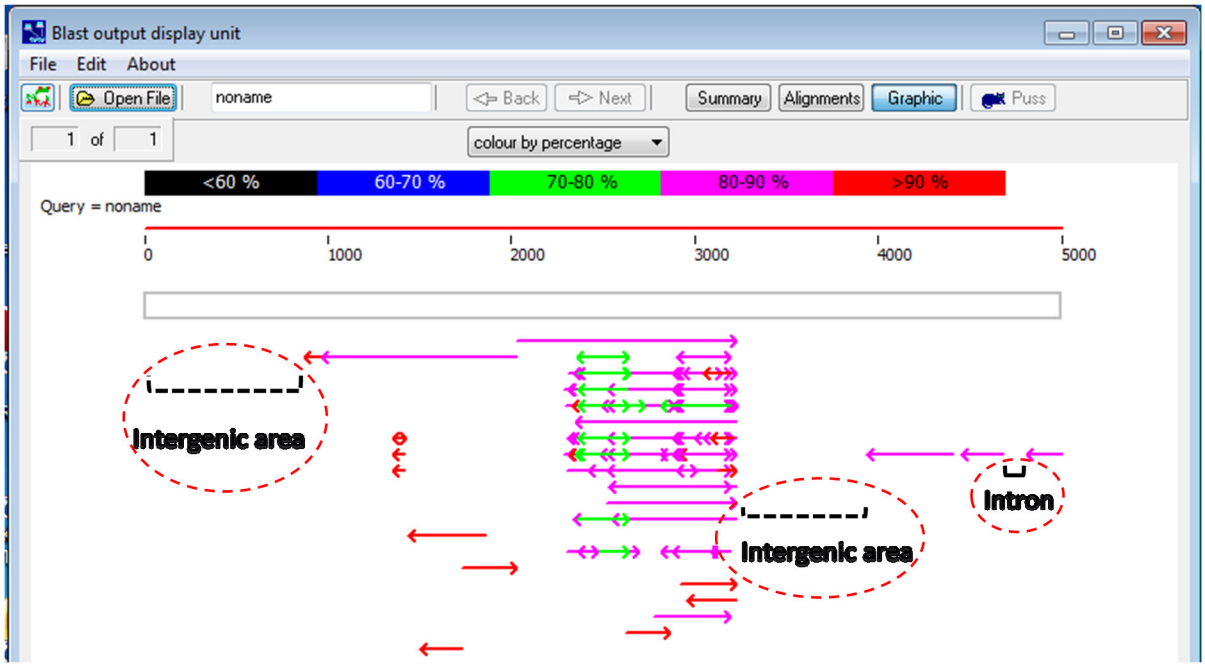

Figure 2.8: Detecting the intergenic and intron sequences in candidate regions for designing markers.

Second, sufficiently long 7EL region(s) with no or low homology to available wheat contigs, yet long enough to be able to design specific primer pairs, were identified by aligning the 7EL intergenic or intron sequences identified against the public wheat database using the Wheat URGI BLAST tool (BLAST 2.2.28+, Altschul et al., 1997, https://wheat-urgi.versailles.inra.fr/Seq-Repository/BLAST, accessed between June 2015 and March 2016);

the wheat genome information were collected from Wheat_Survey_v2_(IWGSC) sequence data (International Wheat Genome Sequencing Consortium (IWGSC), 2014).

The 7DL contig that had the highest identity (at least 85%) with the 7EL sequence was also used to design 7DL-specific markers, with attention to select candidate sequences located in the same or nearby (up to one Kb) regions to the novel 7EL-specific markers designed. Candidate 7DL sequences were aligned against all the wheat chromosome databases at URGI, except 7DL, and also against the 7EL_genomic_v150429_gapfilled database to select the most 7DL-specific regions for marker design.

Using the most specific sequences, new sets of 7EL- and 7DL-specific primer pairs were designed using a freely available online design tool ("PrimerQuest Tool, Integrated DNA Technologies (IDT)," n.d., http://www.idtdna.com/primerquest/home/index; accessed between July 2015 and February 2016). The parameters selected for the design were as follows: monovalent salt (Na^{+}): 50 (mM), primer DNA concentration: 200 (nM), divalent salt (Mg^{++}): 2.5 (mM), dNTP concentration: 0.8 (mM) and amplicon size: 250-600 (bp). For each set of marker, a maximum of four 7DL- and four 7EL-specific primer pairs were designed in the candidate regions. All of the electronically predicted amplicon sequences were further aligned against both wheat and 7EL databases, to double-check their specificity. To have the best set of markers at the end, the new primer pairs were designed in most of the candidate locations throughout the 7EL scaffolds. Primer specific nomenclature is as follows: for instance for primer 3488-A1-7E, the first part (3488) indicates the associated 7EL scaffold; the second part (A1) refers to sequence region considered during the design of the primers; and the third part (7E) denotes the chromosome specificity for the primer pair, which in this case is 7EL-specific. Primers were synthesized by SIGMA-ALDRICH (The Woodlands, TX, USA).

2.2.2.2 Designing markers that are presumed to be in the neighborhood of selected 7E-specific markers

A strategy was designed to identify 7EL scaffolds located in the neighborhood of existing 7EL-specific markers, by identifying homoeologous wheat contigs with known genetic position in wheat 7ABD genomes, selecting neighboring wheat contigs, and finding their homoeologous 7EL scaffolds. The strategy is accordingly referred to as genetic cross-walking between wheat 7ABD and 7EL chromosomes and is described in detail in the following sections. In parallel, three additional sets of 7EL- and 7DL-specific markers were designed by Kelsey Joustra, an honor undergraduate student, with my direction and under the supervision of Dr. Thérèse Ouellet (Table App-I.4, highlighted in orange). K. Joustra focused on additional 7E-specific markers that successfully amplified in FHB resistant plants of family 64-8-2.

2.2.2.2.1 Identifying the 7EL scaffold and 7ABD wheat contig sequences associated with selected 7EL-specific expressed gene markers

The EST contig sequences of twelve markers which amplified in FHB resistant plants of family 64-8-17 and 64-8-27* were collected from Gou et al. (2016). Their homologous 7EL scaffolds were retrieved as described in 2.2.2.1.1 (Figure 2.9, step 1). For the progression of this objective, an in-house database prepared by Dr. Jiro Hattori (ORDC, Ottawa, Canada) was then used. The database contained wheat mapping information gathered from public sources, including SNP mapping data from the 35K Axiom array ("CerealsDB, tools for the analysis of the wheat genome," n.d.-a, http://www.cerealsdb.uk.net/ cerealgenomics/CerealsDB/axiom_download.php, consulted October 2015), the 960 KASP assay chip ("CerealsDB, tools for the analysis of the wheat genome," n.d.-b, http://www.cerealsdb.uk.net/cerealgenomics/CerealsDB/ kasp_download.php, consulted

October 2015), as well as from the 90K iSelect array (including a consensus genetic map; S. Wang et al., 2014). The database also associates the SNP mapping information to wheat contigs and 7EL scaffolds (provided by the 7EL_genomic_v150429_gapfilled database and Wheat_Survey_v2_(IWGSC) sequence data and determined by BLAST match). This database is referred to as "wheat/7EL cross-walking" throughout this study.

The wheat contigs homoeologous to the 7EL scaffolds associated with selected 7EL-specific markers were identified using the "wheat/7EL cross-walking" database (Figure 2.9, step 2). To prevent any possible errors, all of the results were checked manually by aligning the 7EL scaffold sequences against the wheat 7ABD databases at URGI. For two of the markers with no homologous 7EL scaffolds (Lu-287-2 and Lu-387-2), the homoeologous wheat chromosome 7 contigs were identified by aligning the contig sequences from the markers against the wheat 7ABD databases at URGI. The wheat contigs with homoeology percentages lower than 85% were eliminated.

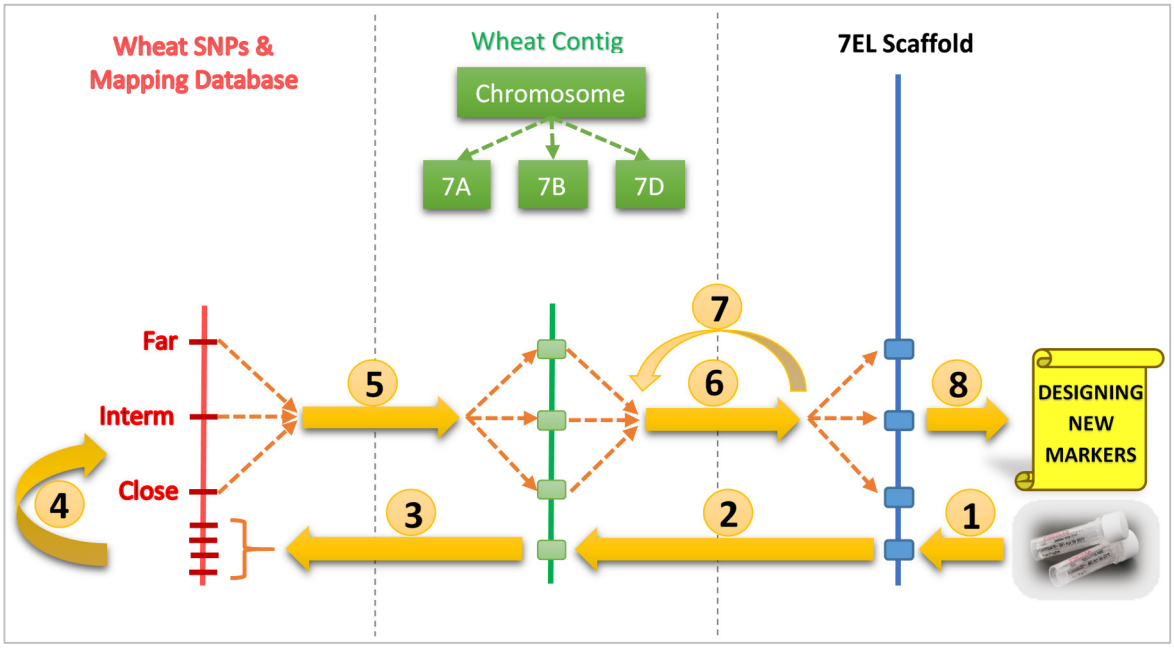

Figure 2.9: Genetic cross-walking between 7EL scaffolds and 7ABD wheat contigs, an eight steps bioinformatics procedure.

2.2.2.2.2 Identifying corresponding and neighboring SNPs for wheat 7ABD contigs

The mapping data in the "wheat/7EL cross-walking" database was used to determine the genetic position of the wheat contigs associated with 7EL scaffolds of interest (Figure 2.9, step 3). The mapping information in the "wheat/7EL cross-walking" database is organized by datasets (e.g. Axiom array mapping data for the Avalon × Cadenza population). So the mapping data could be extracted from seven individual datasets and one consensus dataset, each having to be considered separately. Assuming that 7E and 7ABD genes were located in similar genetic positions on their respective chromosomes, the comparison between datasets with common SNPs suggested an approximate genetic position for each 7EL-specific marker in the third step.

Schematic representations from separate datasets were drawn using an online software ("Flowchart Maker & Online Diagram Software," n.d., https://www.draw.io/, accessed between October 2015 and March 2016) to visually collate the information collected. The length of the chromosomes in each schema was estimated based on the largest genetic position in each dataset (Table 2.1).

Neighboring wheat contigs associated with SNPs located in close, medium and far distances relative to the original wheat contigs were identified (Figure 2.9, steps 4 and 5). However, the rest of the objective was only followed with the closely located SNP neighbors to keep the workload manageable. For the neighboring contigs selection, the focus was on those associated with SNPs present in a larger number of individual mapping datasets, providing extra confidence in their genetic location as well as those associated with the expected chromosome (e.g. contig 7BL6641439, which was associated with SNPs on the 7D chromosome, was not retained).

Table 2.1: Largest genetic position values (cM) for different datasets.
Mapping population are Avalon x Cadenza (AxC), Savannah x Rialto (SxR) and Synthetic x Opata (SxO). The consensus map was constructed with the iSelect assay for populations from the crosses of BT-Schomburgk x AUS33384 (BTxAUS), Chara x Glenlea (ChaxGlen), W7984 x Opata M85 (OpxSyn), Sundor x AUS30604 (SunxAUS), Westonia x Kauz (WesxKauz), Young x AUS33414 (Yo/AUS) (S. Wang et al., 2014).

Array	Crossing Parents	7A	7B	7D
Axiom	AxC	246.8	526.3	9.3
	SxR	342.8	111.4	69.1
	SxO	1562.1	1036.9	1699
iSelect	AxC	457	166.5	251
	SxR	298	75.5	128.6
Consensus Map		716.95	603.94	534.39
KASP	AxC	183.7	71	117.5
	SxR	164.5	52.9	122.2

2.2.2.2.3 Identifying homoeologous 7ABD wheat contigs and 7EL scaffolds associated with selected neighboring SNPs

7EL scaffolds homoeologous to the selected neighboring wheat contigs were identified from the "wheat/7EL cross-walking" database and the level of identity was manually checked against the 7EL_genomic_v150429.gapfilled database using the "Bigblast" software (Figure 2.9, step 6). In some cases, additional 7EL scaffolds with high homoeology to the wheat contigs were found in the manual searches. As the manual procedure for identity check was time-consuming, a software was designed (Mohammad Hossein Tekieh, personal communication) to represent the level of identity between 7DL contigs and 7EL scaffolds by visualising the position and percentage of identity of the sequence fragments from the 7DL contig onto the 7EL scaffold and vice versa. Guidelines used to help identify the homoeologous pairs can be found in "Guidelines used for homoeology check between *Th. elongatum* 7EL scaffolds and wheat contigs" in Appendix I.IV.

Because the progeny in this study had 7E chromosome fragments introgressed into 7DL, the designing focus for wheat markers was on 7DL-specific ones. So, when neighboring wheat contigs from 7AL or 7BL were shown to be homoeologous to a novel 7EL scaffold, the homoeolog 7DL wheat contigs were identified using the 7ABD databases at URGI (Figure 2.9, step 7). Using "Bigblast" software, the identified 7DL contigs were aligned against the 7EL_genomic_v150429.gapfilled database to ensure that the new 7DL contigs also had good homology with the novel 7EL scaffolds identified.

2.2.2.2.4 Designing new markers presumed to be in the neighborhood of selected 7E-specific markers

The procedure mentioned in 2.2.2.1.3 was applied to design new primer pairs using the specified 7EL scaffolds and 7DL contigs from the previous step (Figure 2.9, step 8). Three additional 7DL-specific primer pairs were designed for Lu-8964 because information available at the time indicated that no 7DL-specific marker was available close to that position.

2.2.2.3 Characterization of the novel 7EL- and 7DL-specific primer pairs

To screen the designed primers, the control DNA samples CS-7EL, CS-7ES, CS and CS-7E(7D) were used in PCR amplifications. The CS-7E(7D) substitution line played a very important role in the screening procedure, as among the tested DNA control samples this was the only one supposed to have no PCR amplification for 7D-specific primers (due to substitution of 7D with 7E chromosome) while expected to show a PCR amplification band for 7EL-specific primers.

For each forward and reverse primer pair, stock solutions at a concentration of 100 µM were prepared following the volume recommended by SIGMA, then ten µM working dilutions were prepared. To select the best performing 7EL- and 7DL-specific markers, PCR amplifications

were performed with each primer pair and the control DNA samples plus negative control. The PCR amplifications were performed using the same template and conditions as described in 2.2.1.3. For some of the designed primer pairs, optimization of PCR by increasing the number of cycles (additional two or three cycles) and decreasing the annealing temperature by 4 °C, was performed to increase their specificity. Table 2.2 shows the expected PCR results with each control DNA for 7EL- and 7DL- specific primer pairs.

Table 2.2: Expected PCR results from 7EL- and 7DL-specific primer pairs using the control DNA samples.

Primer Pairs	CS-7EL	CS-7ES	CS-7E(7D)	CS	H_2O
7EL-Specific	+	-	+	-	-
7DL-Specific	+	+	-	+	-

The primer pairs identified as 7EL- and 7DL- specific, were used as markers to screen the 43 BC_1F_4 progeny. The PCR template and conditions presented in 2.2.1.3 were followed.

2.2.3 Proposition of a genetic order for 7E-specific markers associated with FHB resistance

To propose a genetic order including novel and previously described 7E-specific markers, 7EL scaffolds and homoeologous 7ABD wheat contigs associated with previously used 7E-specific markers associated with FHB resistance were identified as presented in 2.2.2.2.1 (Figure 2.10, steps 1 and 2). Amplicon sequences for 7E chromosome-specific molecular markers from Chen et al. (2013), were kindly provided by Dr. Sylvie Cloutier (see Appendix II/ accompanying electronic file, sheet "Chen et al. Amplicon Sequences"). No homologous 7EL scaffold was identified for 3757-1. Only wheat contigs which were homologous to a 7EL

scaffold in a region proximal to that of the associated 7EL markers were used for SNP identification; schematic representations were done as described in 2.2.2.2.2 (Figure 2.10, step 3). Mapping information from previous and novel markers was combined.

Finally, to propose a genetic order, the relative position of each marker was determined based on the combination of data collected. For some of the markers, it was not possible to suggest a specific order based on the available mapping data; therefore, an area rather than a specific position was indicated (Figure 2.10, step 4).

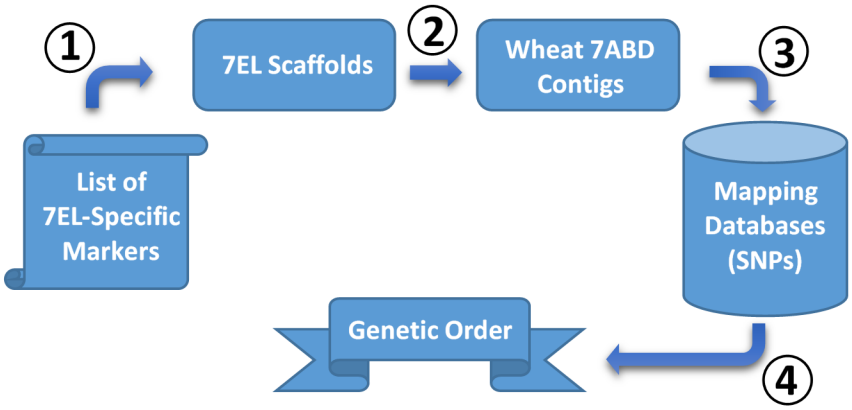

Figure 2.10: Four steps in providing a genetic order for the 7EL-specific markers associated with FHB resistance.

3 RESULTS

The aims of this research project were divided into four objectives as was mentioned in 1.8. Compiled results with preliminary analysis are presented for each specific objective in this chapter.

3.1 Objective 1: Characterization of five *Th. elongatum* accessions with differential response to FHB

The goal of this objective was to estimate the level of DNA polymorphism between five *Th. elongatum* accessions and also identify the most resistant and susceptible accessions that would be potential parents for the development of a mapping population.

3.1.1 Investigating DNA polymorphism between five *Th. elongatum* accessions using 7E-specific markers

To estimate the DNA sequence polymorphism between five *Th. elongatum* accessions, PCR assays were performed using 73 7E-specific markers (Chen et al., 2013; Gou et al., 2016). An example of PCR results is shown in Figure 3.1 and the complete results of the PCR screening are presented in Appendix II (see accompanying electronic file, sheet "*Th. elongatum*|7E-speci. Markers").

For most markers, the *1-72*, *1-73*, *1-74* and *'elongatum'* accessions had similar amplicons as those observed in the CS-7EL or CS-7ES lines. However, accession *1-86* showed differences regarding the presence or the absence of amplicon in 44 out of 73 tested markers. A few

markers showed differences between the *1-72*, *1-73*, *1-74* and *'elongatum'* accessions or in compare to CS-7EL:

- "p7es-56" showed a 400 bp amplicon for CS-7EL and each *Th. elongatum* accession except *1-73*.
- "p7es-77" showed a weak 400 bp amplicon for CS-7EL and each *Th. elongatum* accession except *'elongatum'*.
- "p7el-78" showed a 400 bp amplicon for CS-7ES and each *Th. elongatum* accession except *'elongatum'*.
- "Lu-138-1" showed a complex result. A 400 bp amplicon was observed for CS-7EL, two amplicons of 1600 and 1000 bp were observed for *1-72* and *1-74*, a 1600 bp band for *'elongatum'*, a 650 bp band for *1-86* and no band for *1-73*.

The PCR screening results indicated a close genetic relationship between the CS-7EL wheat addition line and the *1-72*, *1-73*, *1-74* and *'elongatum'* accessions.

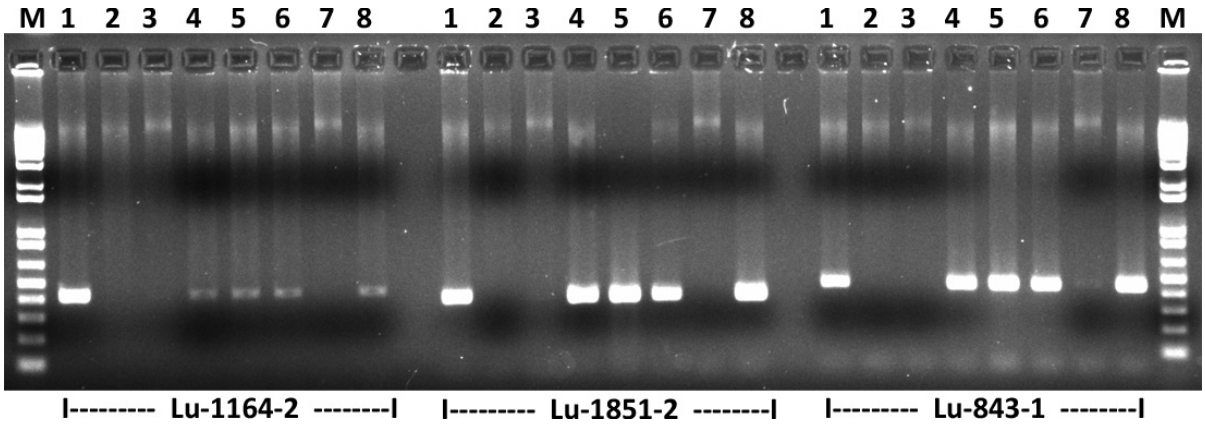

Figure 3.1: An example of PCR results for the screening of five Th. elongatum accessions. DNA samples were (1) CS-7EL, (2) CS-7ES, (3) CS, (4) 1-72, (5) 1-73,(6) 1-74, (7) 1-86, (8) 'elongatum',(M) 1 Kb Plus DNA Ladder. Scoring is done as mentioned in 2.2.1.3. PCR amplified fragments were separated on a 1.5% agarose gel.

3.1.2 Evaluating disease progression in five *Th. elongatum* accessions

To determine the FHB resistance phenotype of each *Th. elongatum* accession, rating of FHB symptom progression was done in plants inoculated with *F. graminearum* spores. The number of inoculated spikes for each *Th. elongatum* accession is provided in Table 3.1. The FHB progression parameters and rating system are illustrated in Figure 3.2 and Table 3.2. Disease ratings for FHB symptoms were performed at 5, 10, 15 and 21 days post inoculation (DPI) (Figure 3.3). The raw scoring data for each parameter is provided in Appendix II (see accompanying electronic file, sheet "*Th. elongatum*|FHB screening").

The disease rating results suggest that *Th. elongatum* accessions are highly resistant to *F. graminearum* when compared to CS. In fact, the *Th. elongatum* inoculated spikes were still mostly green even after 21 DPI, while most spikes from CS plants at this point were usually bleached (Margaret Balcerzak, AAFC, Ottawa, Canada, personal communication). Although no CS-7EL addition line was screened for FHB infection in this objective, a later experiment in Objective 2 shows very comparable results associated with FHB resistant between the *Th. elongatum* accessions and CS-7EL.

Table 3.1: Number of inoculated spikes with F. graminearum inoculum for each Th. elongatum accession.

Accession	*1-72*	*1-73*	*1-74*	*1-86*	*'elongatum'*
Number of Inoculated Spike	35	32	25	15	3

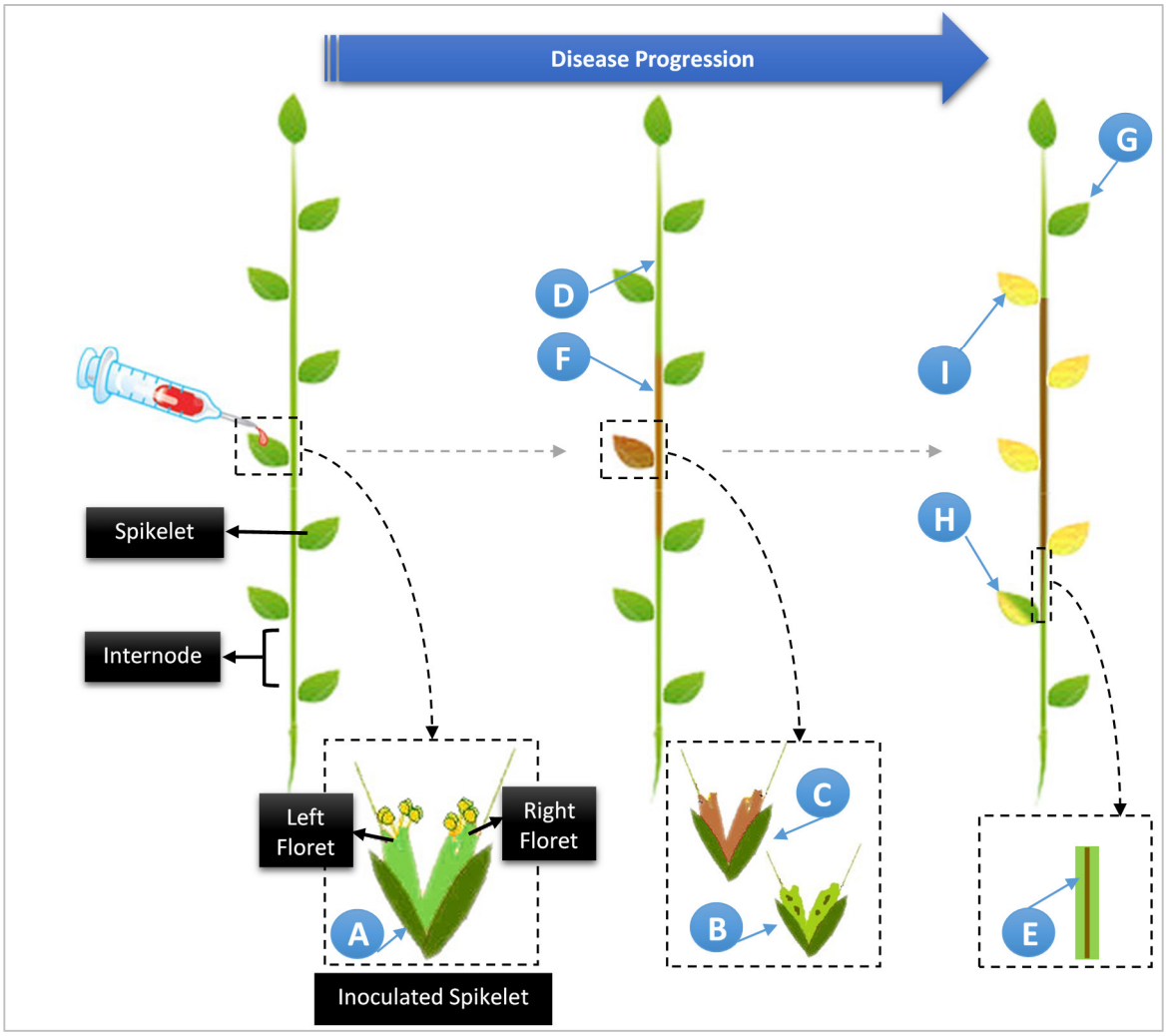

Figure 3.2: Illustration of the F. graminearum inoculation and the FHB progression symptoms. Only one floret in each spikelet was inoculated in Th. elongatum. Letters A, B and C indicating FHB symptoms in the inoculated floret and respectively represent healthy, partially infected and fully infected florets; letters D, E and F indicating FHB symptoms in the internode and respectively represent healthy, partially infected and fully infected internodes; letters G, H and I indicating FHB symptoms in the spikelet and respectively represent healthy, partially bleached and fully bleached spikelets (see Table 3.2).

Table 3.2: Example of rating of FHB symptoms for each inoculated floret, internode or spikelet as illustrated in Figure 3.2.

Rating	Inoculated Floret	Internode	Spikelet
0	A	D	G
0.5	B	E	H
1	C	F	I

After 5 Days

After 10 Days

After 21 Days

Figure 3.3: Evaluating FHB disease progression in Th. elongatum accessions at 5, 10 and 21 DPI.

Figure 3.4 compares the FHB disease progression in the internodes and spikelets of five *Th. elongatum* accessions at 21 DPI. The disease symptoms observed at 21 DPI had developed progressively over time, as can be seen in Figure App-I.4 and Figure App-I.5. Accessions with higher percentage of inoculated spike with healthy internodes and spikelets (interval of 0-20% infection) were considered FHB resistant; this included accessions *1-72*, *1-74* and *'elongatum'*. There was no accession with high percentages of inoculated spikes with heavily infected internodes and bleached spikelets (intervals of 61-80% and 81-100%) in the majority of inoculated spikes; if any, they would have been considered FHB susceptible. Accessions with a significant number of inoculated spikes with infection in the intervals of 21-40% and 41-60% were considered moderately susceptible; these included accessions *1-73* and *1-86*, with *1-73* presenting the most infection symptoms.

Parameters collected for the inoculated spikelets show that the infection can progress from the inoculated floret to the non-inoculated floret within a spikelet even in the most resistant accessions (Figure App-I.2). However, more than half of the inoculated spikelets in two of the most resistant accessions (*1-72* and *'elongatum'*) did not develop bleaching (Figure App-I.3), suggesting that the level of infection in the inoculated spikelets is lower in those accessions.

Among the four diploid accessions inoculated with *F. graminearum*, *'elongatum'* accession showed the highest resistance to FHB. However, only three spikes were inoculated for this accession; hence, the confidence in the results is lower for this accession. Additional inoculations would be required to confirm the disease rating results, but the work was not pursued as the cytogeneticist excluded that accession from future work because of low fertility and dwarfism. Disease ratings for the tetraploid accession *1-86* showed that the inoculated spikelets bleached very fast, although the browning symptoms of infection were slow to

progress; this may be associated with its spike morphology, with thinner stem and rachis and smaller spikelets when compared to the diploid accessions tested.

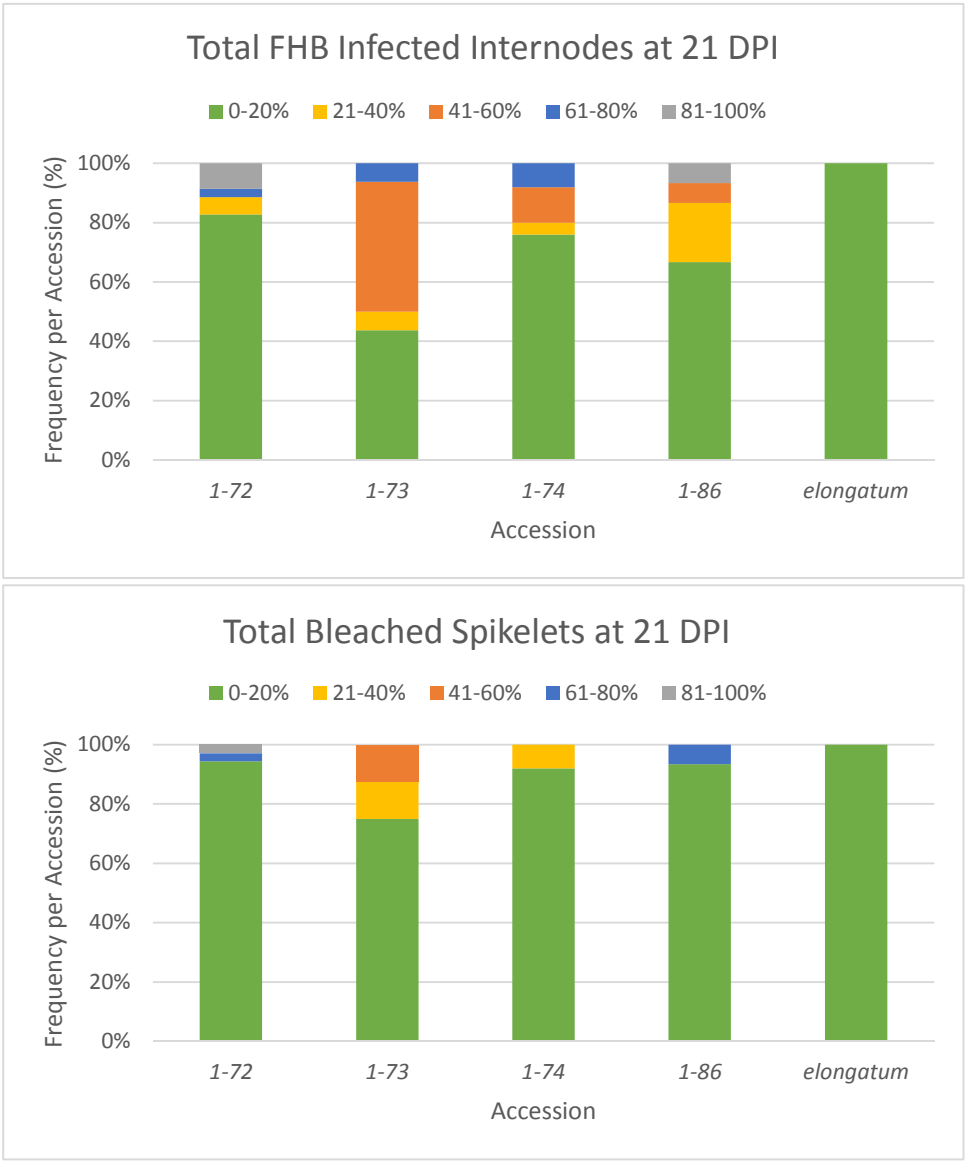

Figure 3.4: Comparing FHB progression in the internodes (upper panel) and spikelets (lower panel) of inoculated spikes from five Th. elongatum accessions at 21 DPI.
Frequency (in %) of spikes with infected internodes or bleached spikelets in each of five intervals (e.g. 0-20%) of infection over the whole spikes are presented.

Regarding the most FHB resistant accession after *'elongatum'*, as shown in Figure 3.4, *1-72* and *1-74* accessions seem to have the same level of FHB resistance. However, both FHB infection in non-inoculated florets and bleaching symptom parameters in the inoculated spikelets suggest *1-72* is more resistant than *1-74*.

For a more precise interpretation, statistical analysis was performed separately on both total FHB infected internode and total bleached spikelet parameters at 21 DPI for the *Th. elongatum* accessions *1-72*, *1-73*, *1-74* and *1-86*. *'elongatum'* was removed as not enough data was available for this particular accession to be included in the statistical analysis. The other four accessions were compared with each other. Results obtained from the one-way ANOVA indicated that variations within the accessions were too high to perceive small differences between them as the F ratio was lower than the F-critical ratio in both parameters, and the P-values were higher than 0.01 (Table 3.3). No statistically meaningful differences was detected between those accessions in their response to FHB. As a result based on statistical analysis, there was insufficient difference to choose any two accessions as potential parents for a *Th. elongatum* FHB-Susceptible × FHB-Resistant mapping population.

Table 3.3: One-way ANOVA on total FHB infected internode and total bleached spikelet parameters at 21 DPI for 1-72, 1-73, 1-74 and 1-86 accessions.

Parameter	Source of Variation	Sum of Square	degree of freedom	Mean Square	F Ratio	P-value	F critical Ratio
Total FHB infected internodes	Between accessions	0.575	3	0.192	2.490	0.064	2.693
	Within accessions	7.926	103	0.077	-	-	-
	Total	8.501	106	-	-	-	-
Total bleached spikelet	Between accessions	0.179	3	0.060	2.651	0.053	2.693
	Within accessions	2.321	103	0.023	-	-	-
	Total	2.500	106	-	-	-	-

3.2 Objective 2: Characterization of three BC_1F_4 families: 64-8-2, 64-8-17 and 64-8-27*

The goal of this objective was to identify the resistant progeny from three selected BC_1F_3 plants (64-8-2, 64-8-17 and 64-8-27*) in addition to determine if any FHB resistant progeny had a smaller introgressed 7EL chromosome fragment than the BC_1F_3 individuals due to recombination between the introgressed 7E and 7D chromosome.

3.2.1 Evaluating FHB progression in three BC_1F_4 families

FHB symptom progression was observed at 4, 8 and 12 DPI following inoculation of one spikelet with *F. graminearum* spores. The FHB progression parameters and rating system were as illustrated in Figure 3.2 and Table 3.2. The only difference was that in BC_1F_4 progeny both left and right adjacent florets in each spikelet were inoculated.

As shown in Figure 3.5, there was a range of observed disease symptoms, from very resistant to highly susceptible plants in the families tested. Detailed results for the different disease progression measurements, including presence of FHB symptoms in both left and right inoculated florets of each inoculated spikelet (scored as 0 = healthy, 0.5 = partially infected or 1 = fully infected), number of inoculated spikelets with bleaching symptom (scored as 0 = healthy, 0.5 = partially bleached or 1 = fully bleached), number of spikelets with bleaching symptom (total, above or below the inoculated spikelet) and percentage of spikelets with bleaching symptoms per spike, number of infected internodes (total, above or below the inoculated spikelet) and percentage of internodes with infection per spike, are provided in Appendix II (see accompanying electronic file, sheet "BC_1F_4 Family|FHB screening"). As variation in FHB disease symptoms between spikes of the same plant were observed, even for

the susceptible CS variety, the result for the head showing the highest FHB symptoms was selected for the purpose of analysis; this was considered representing best the potential for FHB susceptibility for individual plants. In addition, because of the variation in disease symptom progression between spikes of a same plant, the results from progeny with two or less inoculated spikes were treated with less confidence.

Figure 3.5: Example of disease progression in inoculated spikes of BC_1F_4 plants at 12 DPI. Far left represents the most resistant to the far right which is the most susceptible plant.

As all of the measured parameters followed a very similar trend in each progeny regarding the plants' response to FHB, the percentage of bleached spikelets per inoculated spike at 12 DPI was selected to illustrate the results for all progeny (see accompanying electronic file, sheet "BC_1F_4 Family|FHB screening"). Figure 3.6 shows that among the 43 progeny from families 64-8-2, 64-8-17 and 64-8-27*, fourteen, one and fifteen plants respectively showed a resistant phenotype against *F. graminearum*. There is a clear difference between plants with resistant and susceptible phenotypes, similar to the differences in symptoms observed between the FHB

resistant line CS-7EL and the FHB susceptible variety CS. For most of the resistant progeny, the percentages of bleached spikelets per spike were close to the one observed for CS-7EL. However, progeny 64-8-2-[1, 9, 19] and 64-8-27*-[12, 16, 20] had higher percentages of bleached spikelets (14 to 25%), suggesting that they might be partially resistant or the potential for FHB susceptibility is not fully expressed. It should be noted that in this pathosystem, there is a risk of observing false FHB resistant phenotype in an individual spike, as it can be seen for one inoculated head of CS while the other two heads from the same plant showed FHB susceptible phenotype (see Appendix II/ accompanying electronic file, sheet "BC_1F_4 Family|FHB screening" – FHB progression results of first CS plant, third inoculated spike). Although the progeny with 14 to 25% spikelet bleaching were considered FHB resistant in this study, as there is still major differences comparing to susceptible plants, more screening in the next generation would be required to confirm the results obtained.

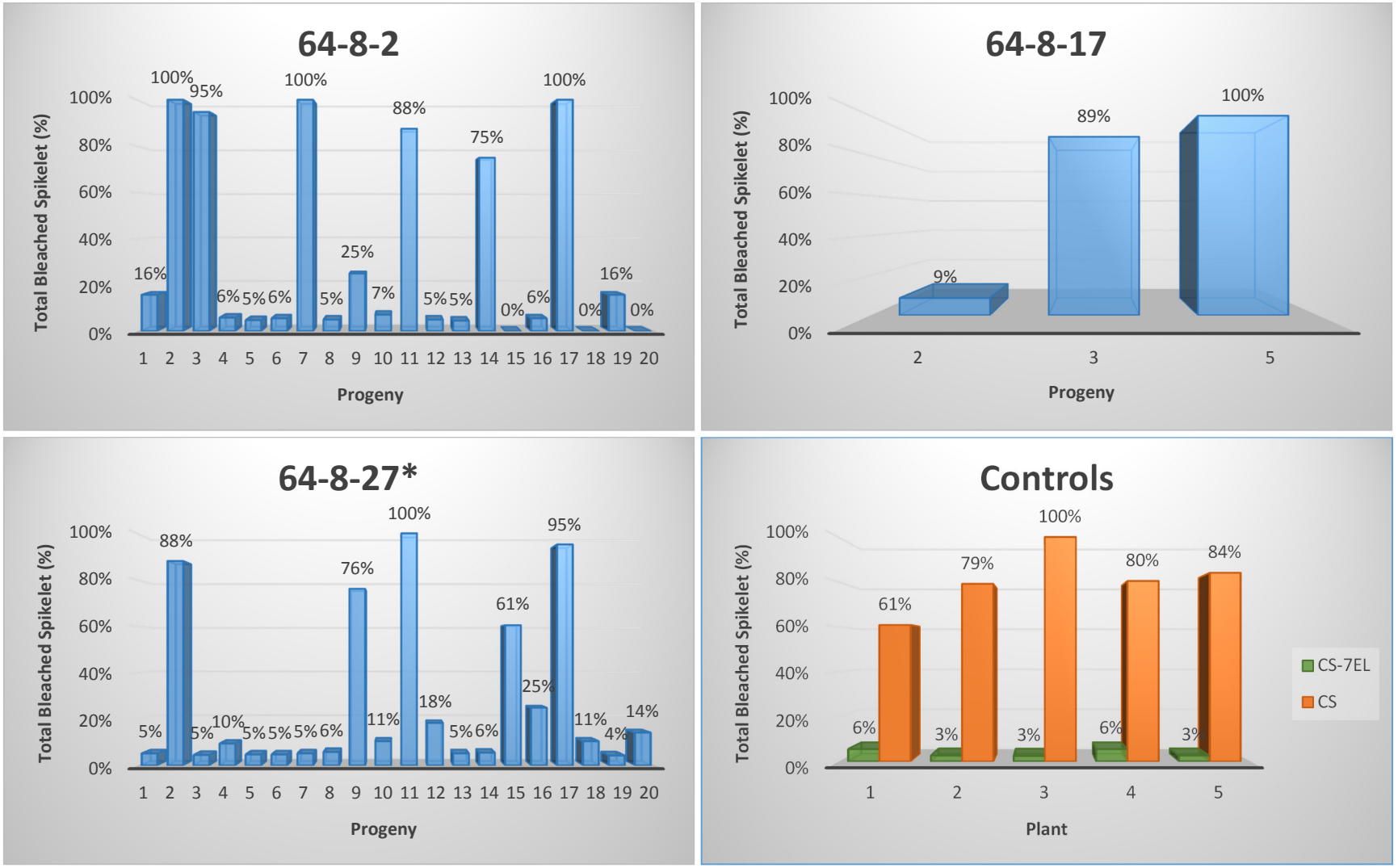

Figure 3.6: Percentage of bleached spikelets per inoculated spike for progeny of three BC_1F_4 families and control plants at 12 DPI.

The difference between plants with FHB-resistant and -susceptible phenotypes was also confirmed by statistical analysis. Both total FHB infected internode and total bleached spikelet parameters at 12 DPI for families 64-8-2 and 64-8-27* were statistically tested. Family 64-8-17 was not included as an insufficient number of progeny was screened. Progeny in each family were divided into two groups, one containing introgressed 7EL fragment and the other without 7EL introgression in their genomes based on the results obtained from screening with the novel 7EL-specific markers designed in this project (see section 3.3.3). To test if data from both families could be combined, one-way ANOVA was used. The results obtained are presented in Table 3.4. For the total FHB infected internode parameter at 12 DPI, there was a significant difference ($F > F\ crit$; $P\text{-value} < 0.01$) between the progeny with an introgressed 7EL fragment from the two families; therefore, they cannot be combined for further statistical analysis. However, no significant difference was observed in both groups of progeny for the total bleached spikelets at 12 DPI ($F < F\ crit$; $P\text{-value} > 0.01$) allowing to combine measurements for both families from this parameter. An additional one-way ANOVA test on the combined groups for the second parameter demonstrated that there is a significant difference between the progeny with introgressed 7EL fragment comparing to those without 7EL introgression in their genomes (Table 3.5).

Table 3.4: One-way ANOVA on families 64-8-2 and 64-8-27 containing progeny with introgressed 7EL fragment and progeny without 7EL introgression for total FHB infected internode and total bleached spikelet parameters at 12 DPI.*
This test is to verify if data from the two families can be combined.

Status	Source of Variation	Sum of Square	degree of freedom	Mean Square	F Ratio	P-value	F critical Ratio
Total FHB infected internodes at 12 DPI							
Progeny with introgressed 7EL fragment	Between families	0.240	1	0.240	8.977	0.004	3.978
	Within families	1.875	70	0.027	-	-	-
	Total	2.116	71	-	-	-	-
Progeny without introgressed 7EL fragment	Between families	0.319	1	0.319	2.333	0.136	4.149
	Within families	4.379	32	0.137	-	-	-
	Total	4.698	33	-	-	-	-
Total bleached spikelets at 12 DPI							
Progeny with introgressed 7EL fragment	Between families	0.01031	1	0.01031	3.87659	0.05292	3.977779
	Within families	0.18614	70	0.00266	-	-	-
	Total	0.19645	71	-	-	-	-
Progeny without introgressed 7EL fragment	Between families	0.30599	1	0.30599	2.02601	0.1643	4.149097
	Within families	4.83304	32	0.15103	-	-	-
	Total	5.13903	33	-	-	-	-

Table 3.5: One-way ANOVA for combined data from families 64-8-2 and 64-8-27 to compare differences between progeny with introgressed 7EL fragment and progeny without 7EL introgression for total bleached spikelets at 12 DPI.*

Source of Variation	Sum of Square	degree of freedom	Mean Square	F Ratio	P-value	F critical Ratio
Between groups	6.041	1	6.041	117.757	8.4E-19	3.932
Within groups	5.335	104	0.051	-	-	-
Total	11.377	105	-	-	-	-

Figure 3.7 compares disease progression in the rachis by measuring the percentage of infected internodes for three different resistant and susceptible progeny, one of each per family, after 4, 8 and 12 days of inoculation. Each selected progeny is representing the main FHB progression trend in its family. Similar trends between the three families were observed within the FHB resistant and susceptible groups; however, progeny 64-8-17-2 showed a higher percentage of infected internodes at 12 DPI when compared to 64-8-2-8 and 64-8-27*-14. In

addition, at 8 DPI, family 64-8-17 showed respectively the highest and lowest FHB progression potential in the internodes of its resistant and susceptible progeny when compared to the other two families. All three FHB susceptible progeny reached the maximum of 100% infected internodes in their inoculated spikes at their last rating day, confirming that 12 DPI was an appropriate time point for the final assessment of the disease progression.

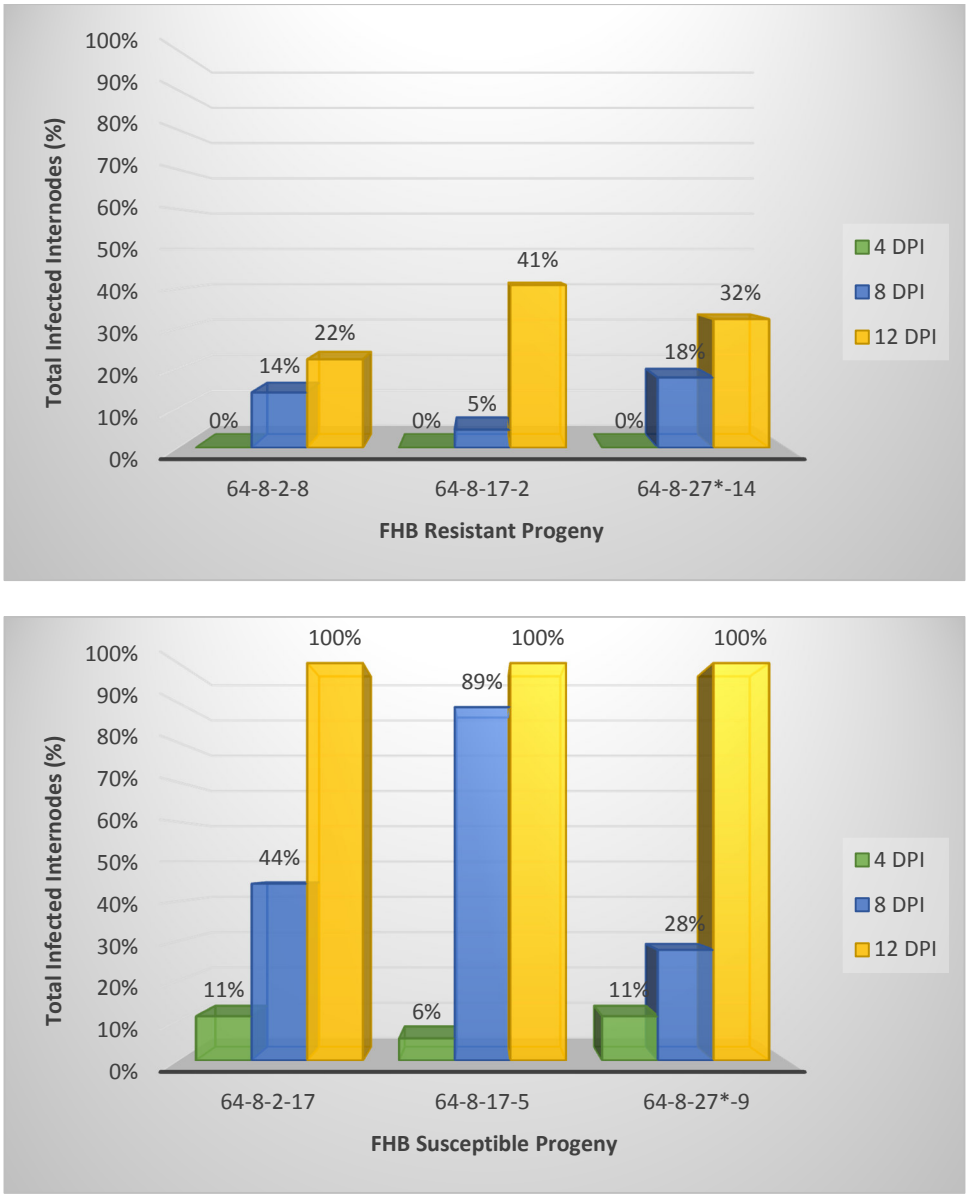

Figure 3.7: Percentage of infected internodes for three different resistant and susceptible progeny from each family at 4, 8 and 12 DPI.

By comparing the same progeny in Figure 3.6 and Figure 3.7 at 12 DPI, different percentages of disease progression are obtained for the bleached spikelets and infected internodes, especially in the resistant progeny. For instance, in progeny 64-8-2-8, 22% of the internodes were infected but only 5% of spikelets showed the bleaching symptom.

3.2.2 Identifying the smallest fragment of 7EL chromosome containing FHB resistance gene(s)

In order to identify the smallest fragment(s) of 7EL chromosome which is (are) associated with FHB resistance in the tested progeny, PCR assays were performed using 73 7E-specific markers (Chen et al., 2013; Gou et al., 2016). An example of PCR results is shown in Figure 3.8, and the complete results of the PCR screening are presented in Appendix II (see accompanying electronic file, sheet "BC_1F_4 Family|7E-speci. Markers").

Remnants of DNA from the selected BC_1F_3 plants from previous students was used to compare genotypes between the three selected BC_1F_3 and progeny plants, to detect novel recombination events. Unfortunately, no amplification or ambiguous results were obtained for some of the markers with weak DNA amplification, possibly because the leftover DNA samples were old. However, consistent amplifications in many progeny within families for most positive markers made it possible to estimate the genotypes of the selected BC_1F_3 plants. It was estimated that 54, 28 and 29 7E-specific markers were successfully amplified for BC_1F_3 plants 64-8-2, 64-8-17 and 64-8-27*, respectively. Results were not always in perfect accordance with the previous students' outcomes.

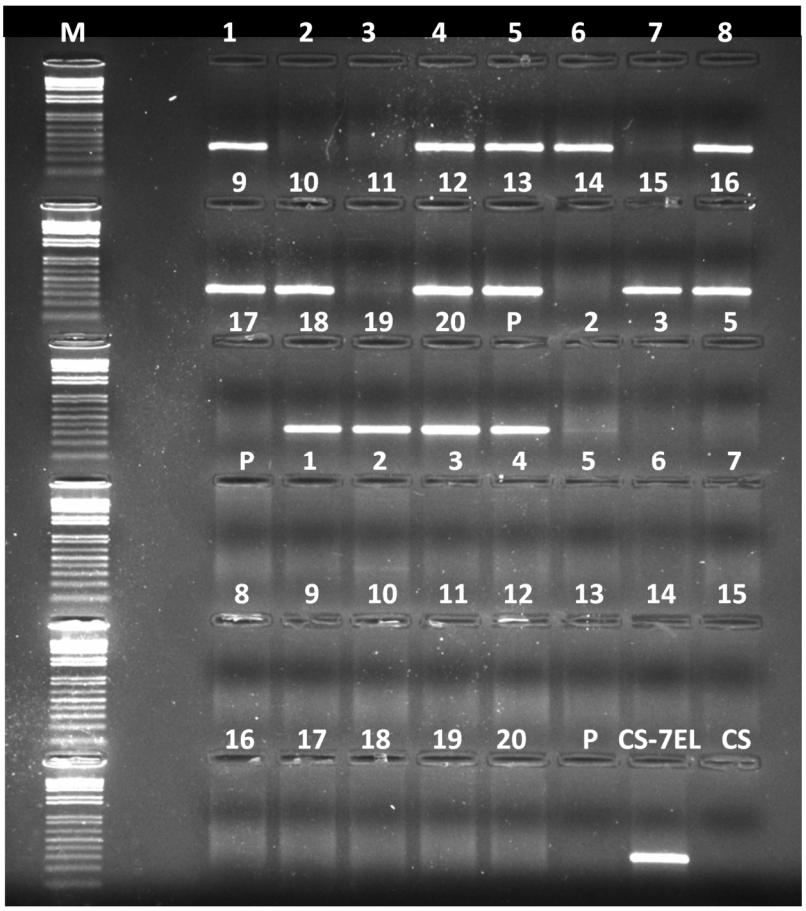

Figure 3.8: An example of PCR results in the genotyping of three BC_1F_4 families for marker Lu-1700-1. Progeny 1 to 20 of family 64-8-2; progeny 2, 3 and 5 of 64-8-17; and progeny 1 to 20 of 64-8-27 are successively represented from top to bottom, followed by the respective individual BC_1F_3 plants. P= DNA from BC_1F_3 plants. Control DNA samples were CS-7EL and CS, (M) 1 Kb Plus DNA Ladder. PCR amplified fragments were separated on a 1.5% agarose gel.*

A combination of the genotyping and phenotyping data for the BC_1F_4 progeny is summarized in Table 3.6. The progeny for each family were categorized based on their different genotypes by comparing the profile of 7E-specific markers which were successfully amplified in the BC_1F_3 and BC_1F_4 generations. Most of the progeny had the same or a very close marker profile as their individual BC_1F_3 plants (12 progeny each from families 64-8-2 and 64-8-27* and one progeny from family 64-8-17). However, variant genotypes showing medium or large deletions in the 7E fragment of the selected BC_1F_3 plants were observed in some progeny; suggesting that recombination between the introgressed 7E fragment that was present in the

BC_1F_3 plant and the 7D chromosome had occurred. For example, in family 64-8-2, two progeny were successfully amplified for 26 and 30 of the markers that showed an amplification in plant 64-8-2, while six progeny had only three to eleven of the markers successfully amplified for plant 64-8-2. Progeny from families 64-8-2 and 64-8-17 contain only 7EL DNA while progeny from family 64-8-27* contain some part of 7ES DNA (successfully amplified for markers p7es-23 and p7el-34), in addition to 7EL DNA.

Table 3.6: Summary of PCR and disease rating results for the BC_1F_4 families.
The first column contains the three selected BC_1F_3 plants. The second column shows different genotypes that were observed in BC_1F_4 progeny based on the PCR results obtained with 7E-specific markers. Most progeny had the same genotype, or very close to it, as the BC_1F_3 plant; some progeny had a genotype significantly different from the BC_1F_3 plant (variant) and were tentatively categorized either as "Medium Deletion" or "Large Deletion". The third column shows the number of markers which were successfully amplified for each genotype category. The fourth column contains the number of $BC1F_4$ progeny in each category. The last column provides an overall FHB resistance score, based on results for the disease rating parameters described in the previous section, with "R" for resistant and "S" for susceptible.

BC_1F_3 Plant	**BC_1F_4 Genotype**		**# of Marker**	**# of BC_1F_4 Progeny**	**Disease Rating**
64-8-2	~ Same as 64-8-2		<=54, >=35	12	R
	Variant	Medium Del.	=26 & 30	2	R
		Large Del.	<=11, >=3	6	S
64-8-17	~ Same as 64-8-17		=28	1	R
	Variant	Large Del.	=6 & 3	2	S
64-8-27*	~ Same as 64-8-27*		<=29, >=18	12	R
	Variant	Medium Del.	=9 & 10	2	S
		Large Del.	<=7, >=4	6	3 R's 3 S's

Some uncertainties exist in the genotype of each progeny due to weak amplification signals (indicated by scorings of 0.25 and 0.5 in Appendix II (see accompanying electronic file, sheet "BC_1F_4 Family|7E-speci. Markers"). Some of those weak signals are due to markers that produce less than optimum amplification (e.g. Lu-3836-1) and some are due to the poor quality of DNA for some samples (e.g. progeny 64-8-2-9). We were careful to not over-interpret those results when assigning the genotype category for each progeny.

The genotyping results suggest that progeny 64-8-2-1 and -19 (categorized in the "Medium Deletion" genotype) have lost some part of 7EL fragment compared to the plant 64-8-2 while remaining FHB resistant, yet the size of 7EL fragment is still quite big in both of these progeny. All eight progeny from the families 64-8-2 and 64-8-17 and three from 64-8-27* that showed large deletions in the 7EL fragment were susceptible to FHB. Surprisingly, three other progeny from 64-8-27* (10, 13 and 20) lost a big part of the 7EL fragment integrated into the BC_1F_3 plant yet showed an FHB resistant phenotype. At the time, these three plants with a resistant phenotype were considered good candidates to follow-up in the next generation. It was noticed that these three progeny had the same genotype profile with 7E-specific markers as did progeny 64-8-2-14 and 64-8-1-3 yet the latter two were susceptible to FHB (Table 3.4).

Table 3.7: PCR results with 7E-specific markers for progeny 10, 13 and 20 from family 64-8-27 with FHB resistant phenotype and two susceptible progeny, 64-8-2-14 and 64-8-17-3.*

Marker	64-8-2	64-8-17	64-8-27*		
	14	3	10	13	20
p7es-23	0	0	1	0	0
Xgwm471	1	1	1	1	1
Xgwm282	0.25	0.5	0.5	0.5	0.5
Lu-9736	0.5	0.25	0.5	0.25	0.5
Lu-387-2	1	1	1	1	1
Lu-632-2	0.5	0.25	0.25	1	1
Lu-287-2	1	1	0.5	1	1
Phenotype	**Susceptible**		**Resistant**		

One possible interpretation of those results is that the integrated fragments of the 7E chromosome in each of the three families are different. While having a common region identified by the six 7E-specific markers, the FHB resistant gene(s) in resistant plants would be present in a different area of the integrated 7E fragment (Figure 3.9) which would not be carrying any of the 7EL-specific markers. Therefore, it was assumed that 7EL gene/locus responsible for the FHB resistant phenotype might be close to the markers with successful amplification. Furthermore, these results also suggested that there was no 7EL-specific marker available to distinguish between FHB susceptible and resistant plants. Designing additional 7EL-specific markers associated with FHB resistance became necessary for further analysis (see Section 3.3 below).

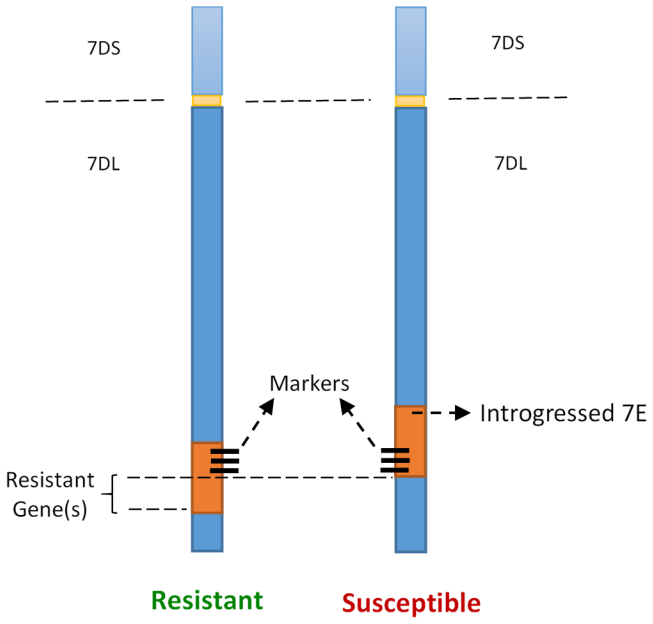

Figure 3.9: A proposed interpretation of the results presented in Table 3.7, different introgression of 7EL fragments into resistant and susceptible plants.

3.2.3 Determining possible deletion of 7D chromosome

Determining the extent of the 7D chromosome still present in the progeny was done using wheat chromosome 7D-specific SSR markers. An example of PCR results is shown in Figure 3.10 and the complete results of the PCR screening are presented in Appendix II (see accompanying electronic file, sheet "BC_1F_4 Family|Wheat SSR Markers"). The results were sorted based on the approximate genetic position of wheat SSR markers (available at GrainGenes, A Database for Triticeae and Avena website; http://wheat.pw.usda.gov/cgi-bin/graingenes/browse.cgi?class=locus; accessed June 2015).

Based on the genetic positions of the 35 markers, results suggest that most of the studied plants in the BC_1F_4 generation still have a full 7DL, except for seven progeny:

- Approximately 3/4 of 7DL is missing in progeny 8, 18 and 20 from 64-8-2 family;
- Approximately half of 7DL is missing in 64-8-27*-5;
- A very small segment of 7DL is missing in progeny 2, 3 and 5 from 64-8-17 family.

The results obtained with the SSR markers suggest that the introgressed 7E fragment in families 64-8-2 and 64-8-27* is still quite big yet containing FHB resistance locus/loci. All three progeny from family 64-8-17 are missing a small fragment close to the tip of the long arm of 7D, yet one contains a large fragment of 7EL and the other two successfully amplified for few 7E markers and are susceptible to FHB. More investigation would be required to understand the results obtained with the 7D markers in that family.

The results with the control DNA samples suggest that some of the tested wheat SSR markers were not specific to 7D, because an amplicon was detected in absence of the 7D chromosome in CS-7E(7D) (e.g. wmc526) or no amplification was detected for CS (e.g. bar111). Finally, false negative PCR results may explain the absence of amplicons for a few of the wheat SSR

makers in some progeny (e.g. 64-8-2-1); it was considered that there was a deletion in 7D only when two or more consecutive SSR markers had no amplification.

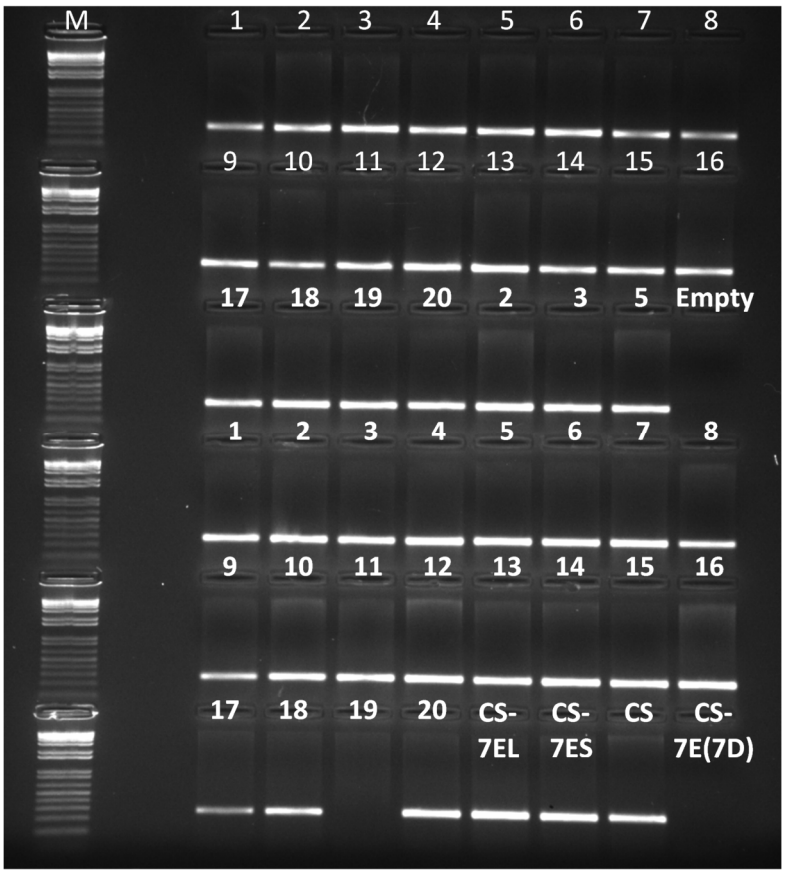

Figure 3.10: An example of PCR results in determining possible deletion of the 7DL chromosome in progeny from three BC_1F_4 families for marker cfd 41.
Progeny 1 to 20 of family 64-8-2; progeny 2, 3 and 5 of 64-8-17; and progeny 1 to 20 of 64-8-27 are successively represented from top to bottom. Control DNA samples were CS-7EL, CS-7ES, CS and CS-7E(7D), (M) 1 Kb Plus DNA Ladder. PCR amplified fragments were separated on a 1.5% agarose gel.*

3.3 Objective 3: Designing additional 7EL-specific markers paired with homoeologous 7DL-specific markers

3.3.1 Designing additional markers physically associated with the selected 7E-specific markers identified in the second objective

In the first approach for designing new pairs of markers, it was assumed that resistant gene(s) might be located in regions very close to one/some of the six 7E-specific markers identified in the second objective (Table 3.7). These markers were successfully amplified in three progeny with a resistant phenotype, 64-8-27*-[10, 13, 20], and also in susceptible progeny 64-8-2-14 and 64-8-17-3. In a first step, the 7EL genomic scaffold sequences associated with the selected markers were identified. No homolog 7EL scaffolds were identified for markers Lu-287-2 and Lu-387-2 in the 7EL_genomic_v150429_gapfilled.

As no sequence was available for Xgwm471 and Xgwm282, cloning and sequencing of the PCR amplicons was performed. Although these were wheat 7D SSR markers, they had been reported to amplify a 7EL fragment (Shen et al., 2004). After the transformation procedure, twelve white colonies (for each amplicon) containing transformed DNA fragments were screened in order to verify that the amplicon fragments were successfully inserted (Figure 3.11). The expected and observed sizes for the amplicons after cloning in *E. coli* are presented in Table 3.8. Most colonies had an amplified fragment of the expected size. From each group, ten colonies were chosen for sequencing.

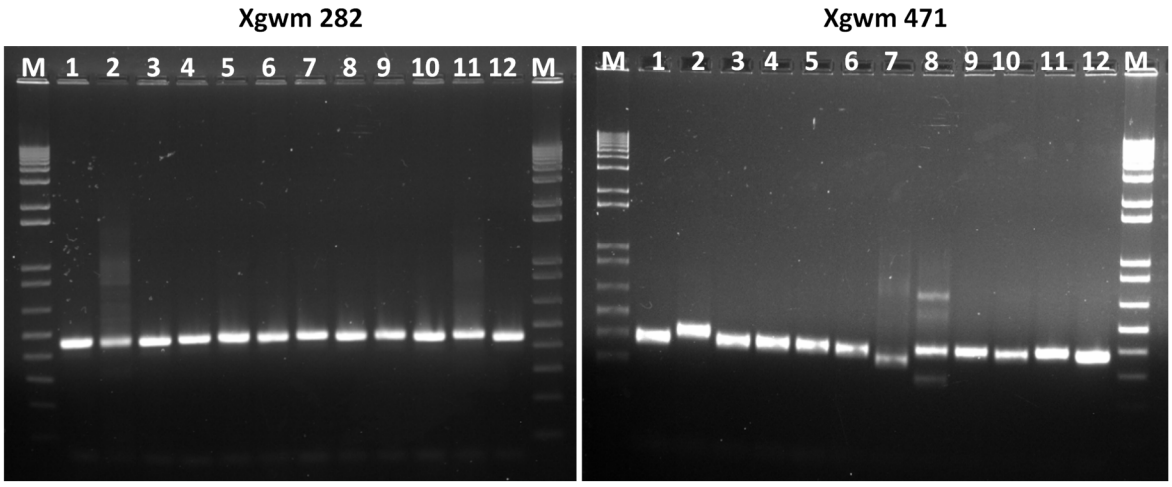

Figure 3.11: PCR amplification products from DNA of E. coli colonies containing cloned fragments obtained from amplification with markers, Xgwm282 and Xgwm471.
Colonies # 2 & 11 from the Xgwm282 and # 5 & 8 from the Xgwm471 were not used in the following analysis, (M) 1 Kb Plus DNA Ladder. PCR amplified fragments were separated on a 2% agarose gel.

Table 3.8: Expected and observed sizes of amplified fragments after cloning in E. coli.

Marker	Expected amplification size (bp)	Observed amplification size (bp)
Xgwm282	461	~ 450
Xgwm471	341	~ 250-350

Following plasmid preparation from the selected transformed *E. coli* colonies, the cloned fragments were visualized using EcoR1 restriction enzyme digestion prior to the PCR sequencing procedure (Figure 3.12).

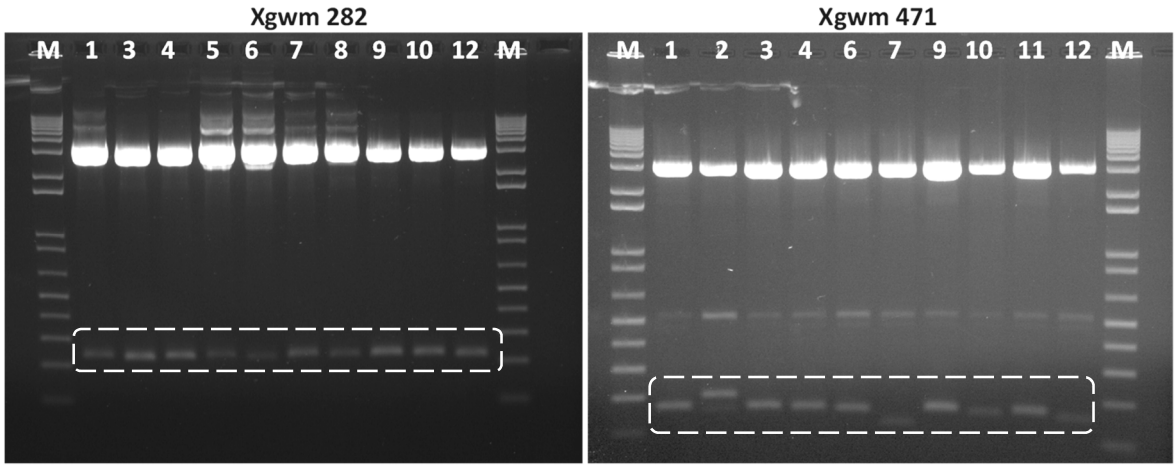

Figure 3.12: EcoR1 digested plasmids from E. coli colonies transformed with amplicons obtained with Xgwm282 and Xgwm471.
The upper bands, at 3018 bp, are the vector DNA and the insertion fragments are shown within dashed boxes, (M) 1 Kb Plus DNA Ladder. Digested plasmids were separated on a 1.5% agarose gel.

The sequence chromatograms from different clones containing amplicons from Xgwm282 and Xgwm471 were analyzed individually regarding the formation and separation of the peaks with good quality scores. The sequencing results for clones from the Xgwm282 amplicon were unambiguous and the 225 bp consensus sequence is presented in Figure 3.13. The 7EL scaffold associated with the sequence for Xgwm282 was identified. The consensus sequence for clones from the Xgwm471 amplicon contained many ambiguities. A possible explanation for the multiple sequencing results might be the simultaneous amplification of two or more homoeologous sequences by the markers in the DNA. The sequence for Xgwm471 was not retained.

TTCGATTTTGGCCGTGTAAGGCAGCAAGCCAGCAAGTCACCAAAACAAAACTCGTGTAT

TTGTACATGTTGAGAGAGAGAGAGAGAGAGAGAGAGAGAGAGAGAGAGAGAGAG

AGAGAGAGAGAGAGAGAGAGGAGCCGAGGGATTCAGCTCCAACAGACAGAGAAG

CACTGGTTCAGCTAAACTTCACTGCTAGTGTTGTGTGTGAATGAGAAATCGAAT

Figure 3.13: Sequence for the Xgwm282 amplicon.

Once 7EL scaffolds were identified for many of the selected markers in Table 3.7 and the position of the markers within the corresponding scaffolds noted, novel 7EL-specific primer pairs were designed on those scaffolds following the strategy illustrated in Figure 2.7. The homoeologous 7DL contigs for the 7EL regions selected for primer design were also identified and used to design 7DL-specific primer pairs positioned in similar locations as the homoeologous 7EL target regions. The data collected from the bioinformatics analysis and the new markers designed are summarized in Table 3.9. In total, 24 7EL- and 18 7DL-specific primer pairs were designed. The complete list of designed primer pairs along with their

sequences, amplicon sizes, annealing temperatures and number of amplification cycles are presented in Table App-I.3.

After testing the designed primer pairs by PCR with control DNA samples (CS-7EL, CS-7ES, CS, CS-7E(7D) and a negative control), the eight best markers with a clear specific band for either 7EL or 7DL were selected (Table App-I.3, in bold format). An example of PCR results for 7EL and 7DL-specific markers is shown in Figure 3.14. As markers Lu-9736 and Xgwm282 were located close to one end of their homologous 7EL scaffold (Table 3.9), only one set of 7EL- and 7DL-specific new markers were retained for each of them. On the other hand, two sets of new markers were selected, one at each end of scaffold 154, as marker Lu-632-2 was located in the middle of the scaffold.

Table 3.9: Summarized data collected from the first approach for marker design, for markers physically associated with selected previous markers.
The left-hand side of the table provides 7EL scaffolds associated with the indicated previous markers, with their sizes and the locations of the previous markers on the scaffolds. The right-hand side of the table provides information about the new7EL- and 7DL-specific primer pairs including: the name and location of the scaffold regions used to design the novel 7EL primer pairs, and the number of primer pairs (#) designed in that location. Primer pair naming is as following: (1) name of associated 7EL scaffold (e.g. 3488), (2) the sequence region used for the design (e.g. A) plus the specific primer pair reference numbers (e.g. A(1:2) means primer pairs A1 and A2), (3) the specificity of the primer pair (e.g. 7EL or 7DL-specific).

Previous Markers		7EL Scaffolds		New Primer Pairs					
Name	Location on 7EL Scaffold (bp)	Name	Size (bp)	Region	Location on 7EL Scaffold (bp)	7EL-Specific Name	#	7DL-Specific Name	#
Lu-9736	5610 - 5850	3488	23798	A	22398 - 23798	3488-A*(1:2)*-7E	2	3488-A*(1:2)*-7DL	2
				B	13798 - 15098	3488-B*(1:4)*-7E	4	3488-B*(1:3)*-7DL	3
Lu-632-2	105470 - 107339	154	204341	A & E	67201 - 72320	154-A*(1:4)*-7E	4	154-E*(1:3)*-7DL	3
				C	72321 - 76658	154-C*(1:2)*-7E	2	154-C*(1:2)*-7DL	2
				D	161921 - 166920	154-D*(1:4)*-7E	4	154-D*(1:4)*-7DL	4
				B	181921 - 192160	154-B*(1:4)*-7E	4	-	-
Xgwm282	9865 - 10019	2506	39786	A	24788 - 29787	2506-A*(1:4)*-7E	4	2506-A*(1:4)*-7DL	4
Xgwm471	-	-	-	-	-	-	-	-	-
Lu-287-2	-	-	-	-	-	-	-	-	-
Lu-387-2	-	-	-	-	-	-	-	-	-

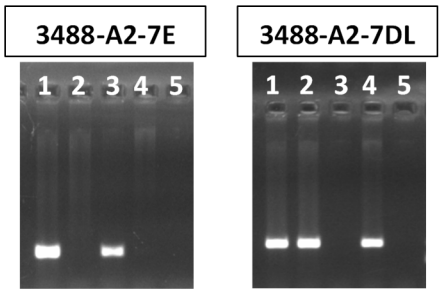

Figure 3.14: Example of PCR results with 7EL and 7DL-specific markers.
DNA samples are (1) CS-7EL, (2) CS-7ES, (3) CS-7E(7D), (4) CS and (5) negative control. PCR amplified fragments were separated on a 1.5% agarose gel.

Discrepancies were noted between the results obtained with the novel designed markers and the previous ones after testing the new 7EL markers on the BC_1F_4 progeny (Appendix II, see accompanying electronic file, sheets "BC_1F_4 Family|7E-speci. Markers" and "BC1F4 Family|Novel Markers"). PCR amplifications were optimized for markers Lu-9736, Lu-632-2 and Xgwm282 (Appendix II, see accompanying electronic file, sheet BC1F4.family|Novel Markers). An increased in PCR annealing temperature by 2 degrees (from 55 to 57°C) for Lu-9736 improved the 7EL specificity of the marker. Results for Lu-9736 were exactly the same as marker 3488-A2-7E. Surprisingly, for both 154-A1-7E and 154-D2-7E, no amplification was obtained in any of the progeny, leading to further investigation. The PCR test with the associated marker Lu-632-2 was redone with the BC_1F_4 and control DNA samples, with separation on agarose gel for a longer time. Three bands of different sizes were observed, with only one of them specific to the 7EL. None of the progeny showed the 7EL-specific band for this marker, confirming the results obtained with the two new 7EL-specific markers, 154-A1-7E and 154-D2-7E. Finally, new PCR amplifications were performed for the SSR marker Xgwm282, which had been reported as having a specific band for the 7EL chromosome (Shen et al., 2004). When separating the amplification products using a longer running time, no 7EL-

specific band was observed. Although this marker was no longer 7EL-specific in our amplification conditions, the associated 2506-A4-7E marker is a 7EL-specific marker. No further experiment was performed with the Lu-632-2 and Xgwm282 markers.

3.3.2 Designing markers that are presumed to be in the neighborhood of selected 7E-specific markers from the second objective

In the second approach for designing new pairs of markers, new sets of 7EL- and 7DL-specific markers were designed on different scaffolds potentially located in the neighborhood of several existing 7E-specific markers that had successful PCR amplification in FHB resistant plants of the family 64-8-27* (Lu-287-2, Lu-387-2, Lu-9736, Lu-1700, 2506-A4-7E) and family 64-8-2 (Lu-138-1, Lu-387-22, Lu-632-2, Lu-1851-1, Lu-5846-1, Lu-129-21, Lu-3836-1). Following the genetic cross-walking strategy (see 2.2.2.2 for the complete description) between wheat 7ABD and 7EL chromosomes (Figure 2.9), a group of 7EL scaffolds were identified as possibly located in the neighborhood of existing 7E-specific markers with associated 7EL scaffolds. Briefly, 7EL scaffolds homologous to the EST contig sequences associated with twelve selected markers were identified and their sequence retrieved. No homologous 7EL scaffolds were identified for Lu-287-2, Lu-387-2 and Lu-5846-1. Then, using the "wheat/7EL cross-walking" database, the wheat contigs homoeologous to the 7EL scaffolds associated with selected 7EL-specific markers were identified. For most of the 7EL scaffolds, all three homoeologous 7A, 7B and 7D wheat contigs were found. The genetic position of the wheat contigs associated with 7EL scaffolds of interest was collected from many publicly available mapping datasets that were collated in the "wheat/7EL cross-walking" database. Each homoeologous wheat contig was associated with zero to fifteen SNPs. In total, 85 SNPs were associated with wheat contigs homoeologous to 7E-specific markers Lu-287-2,

Lu-9736, Lu-1700, Lu-387-22, Lu-1851-1, Lu-129-21, Lu-3836-1. The mapping data were extracted from seven individual and one consensus datasets. The results from step one to three of the genetic cross-walking strategy are summarized in Table App-I.5. Bioinformatics analysis with markers 2506-A4-7E, Lu-138-1, Lu-632-2 and Lu-5846-1 were discontinued at this stage due to the absence of homoeologous wheat contigs with mapping information. It should be noted that, to reduce the size of K. Joustra's project, mapping data for the last seven 7E-specific markers were collected only from the consensus dataset (markers highlighted in orange in Table App-I.5).

To better illustrate the collected mapping data, schematic representations were constructed to display the information collected from separate datasets (Figure App-I.6 and Figure App-I.7). Only chromosomes with mapping data related to the 7E-specific markers were represented. Using those schemas, thirty neighboring regions (R) were selected as candidate locations to design new markers in the neighborhood of the selected 7E-specific markers (Figure 3.15). Neighboring regions between SNPs associated with the same wheat contigs and in between different datasets were given the same neighboring region (R) number.

Using the neighboring regions defined, wheat contigs associated with SNPs located in close, intermediate and far distance to the original wheat contigs were identified and the sequence of their homoeologous 7EL scaffolds retrieved from the relevant database. In total, 114 7EL scaffolds homoeologous to the selected neighboring wheat contigs were selected. The results obtained from step four to six of the "wheat/7EL cross-walking" strategy are presented in Table App-I.6. The candidate regions 23, 25 and 28, assessed by K. Joustra, were dropped along the procedure because no homoeologous 7EL scaffold was available for wheat contigs in R23, and there were no neighboring SNPs in the database for R25 and R28.

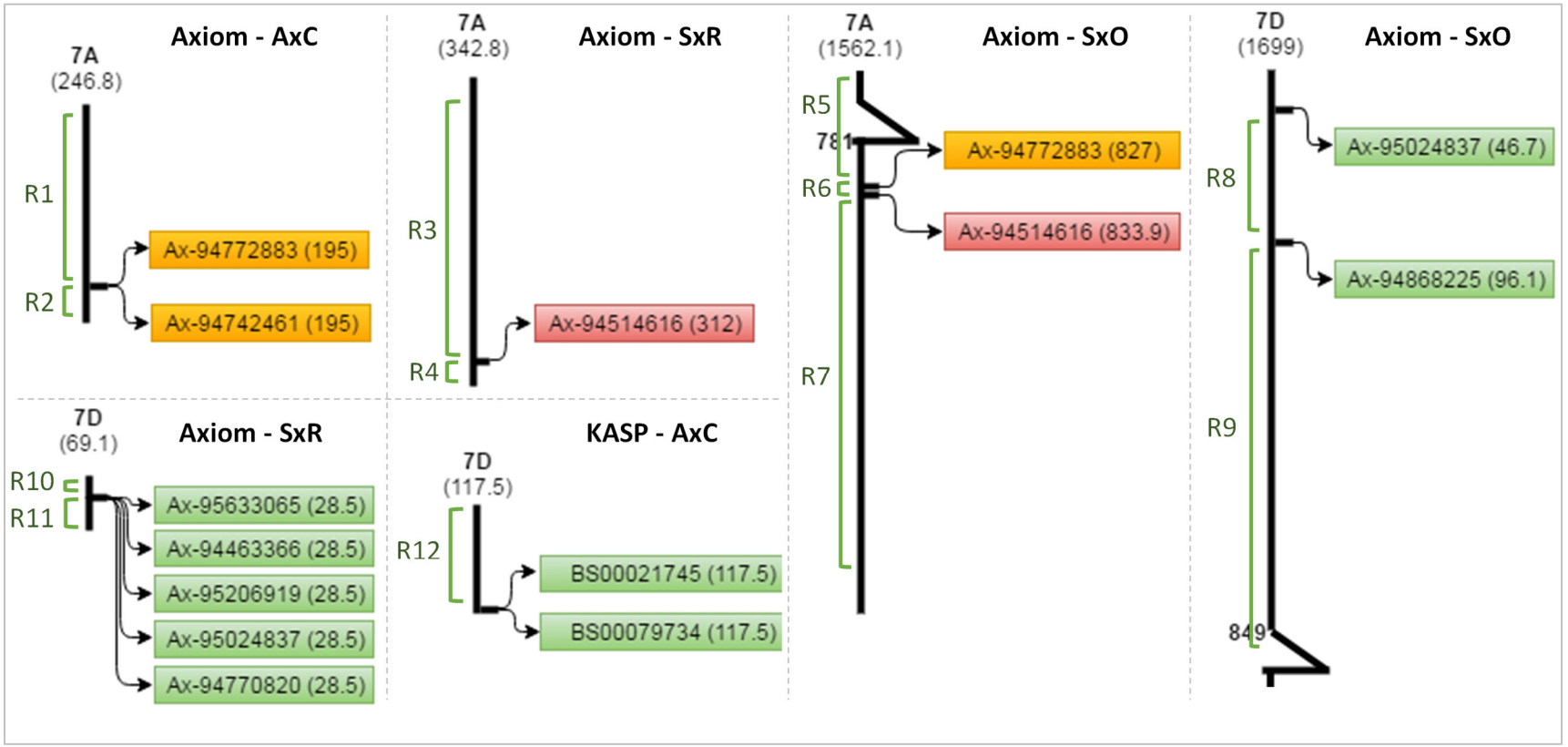

Figure 3.15: Candidate neighboring regions (R) defined by the SNPs associated with wheat contigs homoeologous to previously used 7E-specific markers. The regions marked with orange brackets were analyzed by K. Joustra. The genetic positions of the SNPs, in cM, in the respective datasets are shown in the bracket next to the SNP name; when many SNPs were found in the same position in a dataset, the number of SNPs found is indicated instead of their name. SNPs in boxes of similar color represent SNPs associated with the same wheat contig. Mapping data were from publicly available datasets produced with the Axiom, iSelect and KASP assays for populations from the crosses of Avalon x Cadenza (AxC), Savannah x Rialto (SxR) and Synthetic x Opata (SxO) (top panel) and from a consensus dataset produced with the iSelect assay (S. Wang et al., 2014) (bottom panel). The complete maps and the significance of the colors are available in Figure App-I.6 and Figure App-I.7.

(Figure 3.15 continues on next page)

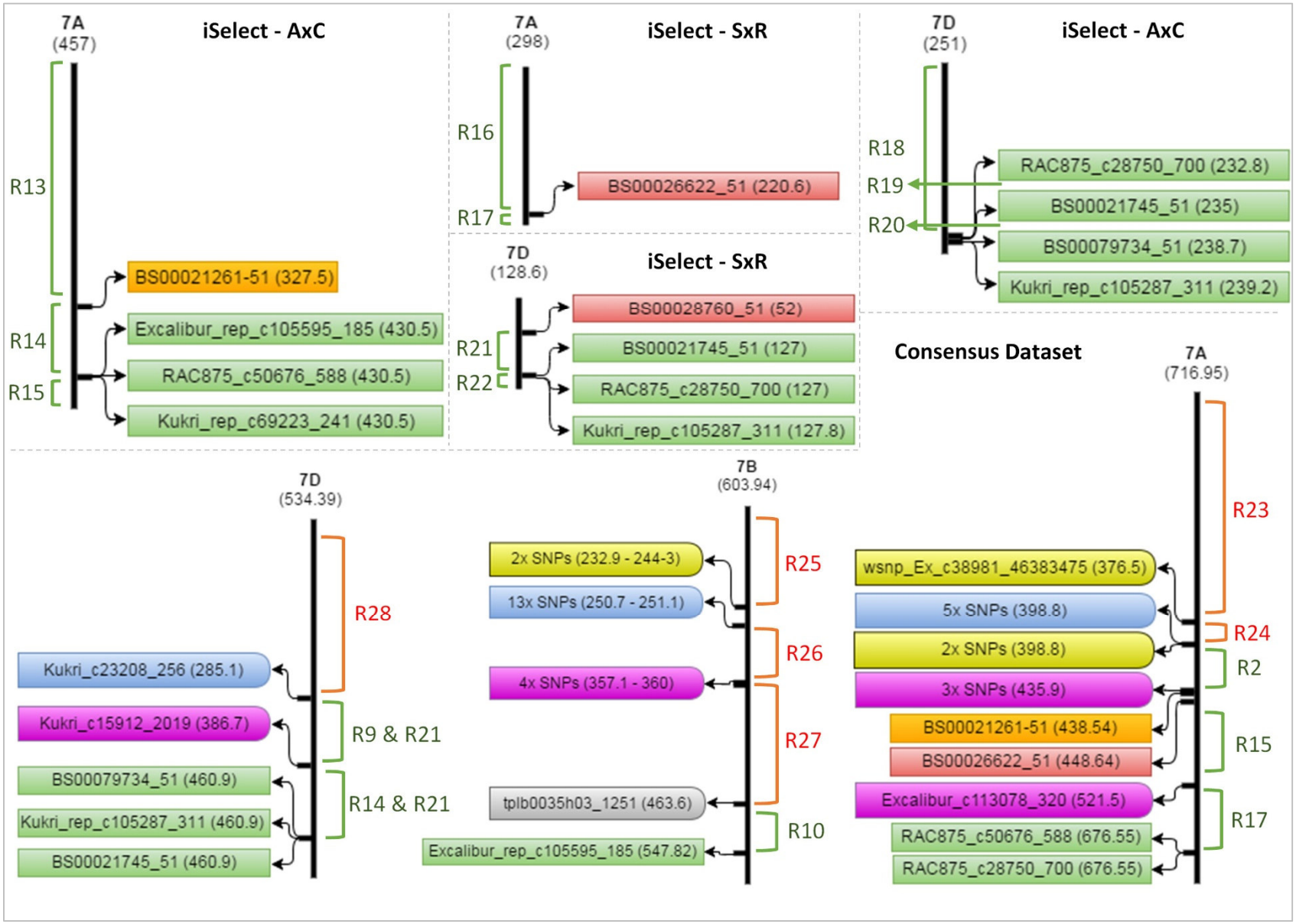
7A
(457)
iSelect - AxC
R13
R14
R15
BS00021261-51 (327.5)
Excalibur_rep_c105595_185 (430.5)
RAC875_c50676_588 (430.5)
Kukri_rep_c69223_241 (430.5)
7A
(298)
iSelect - SxR
R16
R17
BS00026622_51 (220.6)
7D
(128.6)
iSelect - SxR
R21
R22
BS00028760_51 (52)
BS00021745_51 (127)
RAC875_c28750_700 (127)
Kukri_rep_c105287_311 (127.8)
7D
(251)
iSelect - AxC
R18
R19
R20
RAC875_c28750_700 (232.8)
BS00021745_51 (235)
BS00079734_51 (238.7)
Kukri_rep_c105287_311 (239.2)
Consensus Dataset
7A
(716.95)
R23
R24
R2
R15
R17
wsnp_Ex_c38981_46383475 (376.5)
5x SNPs (398.8)
2x SNPs (398.8)
3x SNPs (435.9)
BS00021261-51 (438.54)
BS00026622_51 (448.64)
Excalibur_c113078_320 (521.5)
RAC875_c50676_588 (676.55)
RAC875_c28750_700 (676.55)
7D
(534.39)
R28
R9 & R21
R14 & R21
Kukri_c23208_256 (285.1)
Kukri_c15912_2019 (386.7)
BS00079734_51 (460.9)
Kukri_rep_c105287_311 (460.9)
BS00021745_51 (460.9)
7B
(603.94)
R25
R26
R27
R10
2x SNPs (232.9 - 244-3)
13x SNPs (250.7 - 251.1)
4x SNPs (357.1 - 360)
tplb0035h03_1251 (463.6)
Excalibur_rep_c105595_185 (547.82)

The number of SNPs, wheat contigs and 7EL neighboring scaffolds was too large therefore the rest of this objective was focused on the wheat contigs and 7EL scaffolds associated with the SNPs located close to the previous 7E-specific markers. After checking sequence homology between wheat contigs and 7EL scaffolds, sequences with the highest ranking alignment for each of the eighteen homoeologous matches were selected to be used for the design of new markers. The list of selected wheat contigs and their homoeologous 7EL scaffolds is provided in Table 3.10. For candidate wheat contigs from either the 7AL or 7BL chromosomes, the homologous 7DL wheat contigs were identified, when available. No homologous 7D contigs were found for six of the selected 7A wheat contigs. As our priority was to develop pairs of 7DL- and 7EL-specific markers those were not pursued.

Table 3.10: Selected 7ABD wheat contigs, their homoeologous 7EL scaffolds and the associated 7DL contigs (when the selected contig was from 7A or 7B).
The results highlighted in orange were produced by K. Joustra.

	Selected Wheat Contig	7EL Scaffold	Associated 7D Contig
1	7DL3391547	2485	-
2	7DL3393572	507	-
3	7DL3352272	3571	-
4	7DL3315688	959	-
5	7DL3311341	1952	-
6	7DL3311257	2500	-
7	7DL3341845	1383	-
8	7DL3311538	2368	-
9	7AL4464798	455	N/A
10	7AL4557311	577	N/A
11	7AL4519433	480	N/A
12	7AL4442603	1384	N/A
13	7AL1206673	542	7DL3368356
14	7AL4554209	3201	N/A
15	7AL4550273	4231	N/A
16	7AL4373898	2096	7DL3393747
17	7BL6514240	1262	7DL3284342
18	7BL6630673	153	7DL3359758

In total, 118 primer pairs were designed for the targeted locations. The complete list of designed primer pairs along with their sequences, amplicon sizes, annealing temperatures and number of amplification cycles are presented in Table App-I.4. After testing of the designed primer pairs with control DNA samples, CS-7EL, CS-7ES, CS, CS-7E(7D) and a negative control, twelve 7DL- and fourteen 7EL-specific markers were identified as the best options. In several cases, either the designed 7DL- or 7EL-specific primer pairs did not specifically amplify; therefore, the complementary 7DL or 7EL markers do not always exist.

In addition to the markers designed above, 7DL-specific primer pairs associated with the 7EL-specific marker Lu-8964 were designed. The associated EST contig was identified on 7EL scaffolds 6092 (6243 bp length). Lu-8964 was located between 4347 to 4884 bp of that scaffold. The 7DL3376588 contig was identified as homoeologous and used to design 7DL-specific primer pairs within the region 8801-9547 bp. The marker obtained is named 6092-A2-7DL (Table App-I.3).

3.3.3 Screening of the BC_1F_4 progeny with the novel markers from approaches one and two

PCR assays were performed on the 43 BC_1F_4 progeny using the eight selected markers from the first design approach and 26 markers from the second approach, and the results are shown in Appendix II (see accompanying electronic file, sheet "BC_1F_4 Family|Novel Markers").

Results with the novel 7EL-specific markers supported and added precision to the results obtained in the second objective with previous markers. The novel 7EL-specific markers amplified successfully in resistant progeny except 64-8-27*-(10, 13, 20). Although these three progeny showed very low FHB symptoms, later results from their next generation by Margaret Balcerzak showed that the progeny were all susceptible. This suggested that the full potential

for FHB susceptibility was not detected in those three BC_1F_4 plants (64-8-27*-10, 13, 20). No amplification with the novel 7EL-specific markers was observed in any of the FHB susceptible progeny, suggesting that those did not contain an introgressed 7E fragment.

Results from the 7DL-specific markers also supported and added precision to the results obtained with the wheat SSR markers (Objective 2). Most of the 7DL-specific markers (11 out of 16) did not amplify progeny 8, 18, 20 from family 64-8-2, confirming the loss of the corresponding region of 7DL in those plants. In addition, progeny 64-8-27*-5 was missing almost half of the novel 7DL markers (7 out of 16). Progeny 64-8-2-19 did not amplify two of the 7DL-specific markers (154_E1_7DL and 153-A1-7DL), although those were not predicted to have a consecutive position in our proposed genetic order; additional experiments will be needed to confirm if these negative results really correspond to deletions in the 7D chromosome. In progeny 64-8-2-8, 18, 20 and 64-8-27*-5, when the 7EL-specific markers successfully amplified, the corresponding 7DL-specific markers were missing, and vice versa. The only exceptions were the markers 1383 and 2506; the 7EL- and the 7DL-specific markers for 1383 both successfully amplified in family 64-8-2, and those for 2506 in all progeny, as long as there was 7EL introgression in the plants.

3.4 Objective 4: Proposition of a genetic order for 7E-specific markers associated with FHB resistance

A predicted genetic order for the 7EL-specific markers has been proposed based on a compilation of the mapping information collected for wheat sequences homoeologous to the previous and novel 7E-specific markers. This genetic order will allow a better interpretation

of the PCR screening results and identification of the segments of 7EL chromosome from *Th. elongatum* introgressed into wheat 7DL chromosome.

In addition to the mapping data associated with the wheat sequences homoeologous to the 7EL-specific markers designed in this study, mapping data for wheat sequences homoeologous to thirty-one other 7E-specific molecular markers (Chen et al., 2013; Gou et al., 2016), were collected. According to the results obtained in the second objective, 23 of those markers were associated with FHB resistance in BC_1F_4 families. Eight additional markers (Lu-1974, Lu-114-21, Lu-485, Lu-1225302, Lu-193-2, p7es-1, p7es-16 and p7es-59) were selected to expand the genetic order beyond the markers which were successfully amplified in family 64-8-2, as they amplified in other 7E-introgressed materials (Dr. Thérèse Ouellet, AAFC, Ottawa, Canada, personal communication).

Following the procedure demonstrated in Figure 2.10, the 7EL scaffold containing 31 of the 7EL-specific markers used in Objective 2 and their homoeologous 7ABD wheat contigs with mapping information were identified. For each wheat contig, between one and nineteen associated SNPs were found (Table App-I. 7). The mapping information was used to draw two series of schematic representations. One series relates the position of the previous markers to the novel designed 7EL-specific markers, based on the SNP information associated with the homoeologous wheat contigs (Figure App-I. 8). The other series relates all SNP information associated with the previous markers to the novel markers (Figure App-I. 9).

The information contained in the two series of schematic representations was used to propose a genetic order for all of the markers for which there are associated SNPs and mapping data; presuming for this exercise that homoeologous sequences on 7ABD and 7E were organised in a similar genetic order (see discussion for more details) (Figure 3.16).

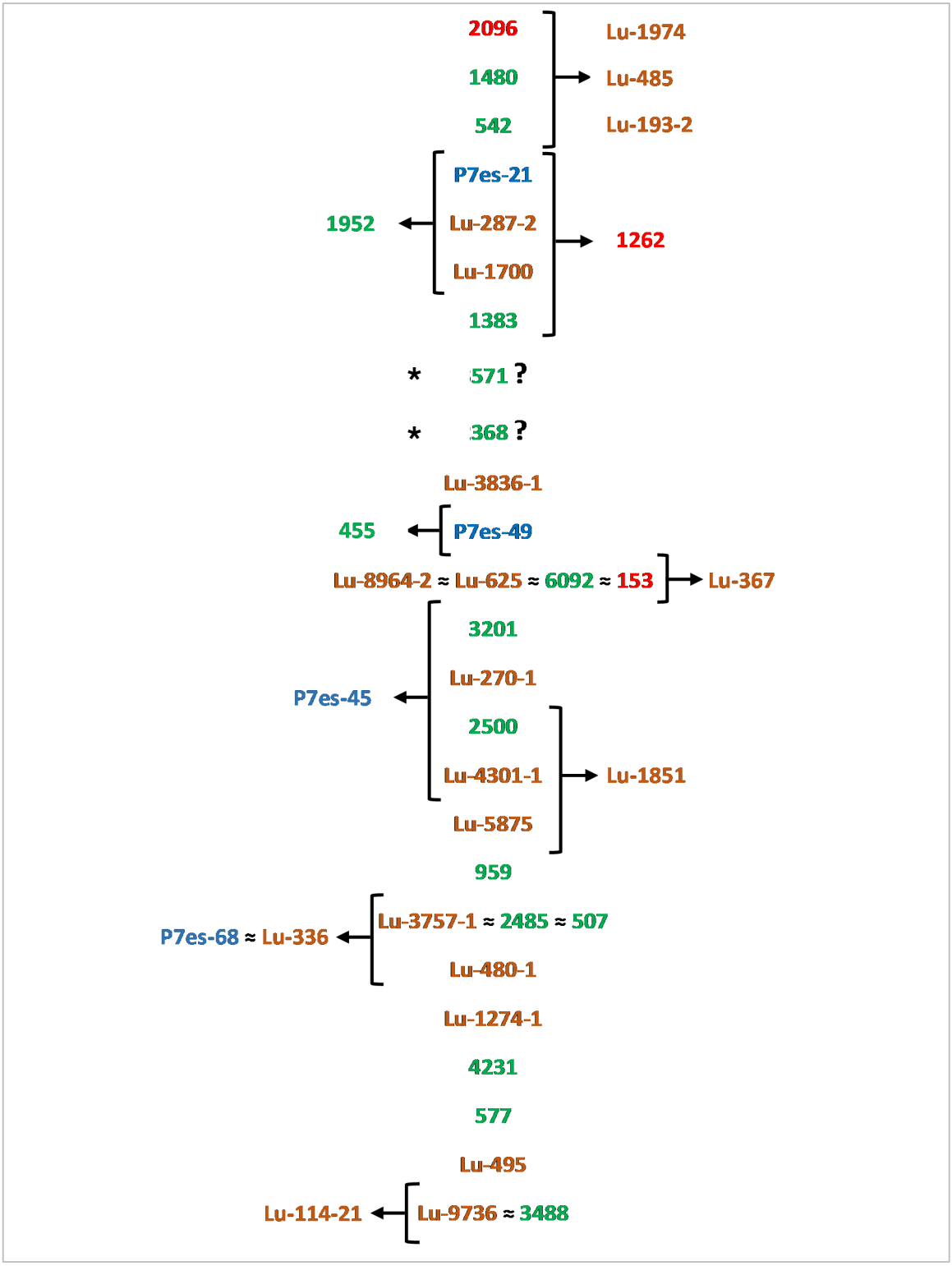

Figure 3.16: A proposed genetic order for previous and novel 7EL-specific markers.
7EL-specific expressed gene markers are brown (Gou et al., 2016); 7E chromosome-specific markers are blue (Chen et al., 2013); markers designed in this project are green; markers designed by K. Joustra are red. Only the first part of the marker name (associated 7E scaffold) in groups C and D is displayed. Genetic order for two markers with an asterisk (*) is based on the combination of genetic information and PCR results. [or] indicate incertitude in order for indicated markers.

For some of the markers, a precise ranking in the genetic order could not be established based on the available data and those are presented in Figure 3.16 using a vertical line to represent the approximate position where they might be located.

Based on the proposed genetic order presented in Figure 3.16, PCR results for previous and novel markers were combined and reorganized in Appendix II (see accompanying electronic file, sheet "All PCR Results in Order").

3.4.1 Interpretation of the reorganized PCR screening results

Analysis of the rearranged PCR screening results for the progeny of the three BC_1F_4 families using the proposed genetic order, combined with the results for other markers without mapping information, has revealed a number of 7DL/7EL introgression patterns which occurred in individual progeny. The introgression patterns were labeled alphabetically and are summarized in Table 3.11 and graphically illustrated in Figure 3.17. Individual patterns are presented in the following paragraphs.

Pattern A. This pattern was observed when DNA of the BC_1F_4 progeny did not amplify any of the 7EL-specific markers while successfully amplifying all 7DL-specific markers. Plants 64-8-2-[2, 3, 7, 11 and 14], 64-8-17-[3 and 5], 64-8-27*-[2, 9, 10, 11, 13, 15, 17 and 20] showed this pattern. Although there were some exceptions regarding the absence/presence of amplifications for a few 7DL- and/or 7EL-specific markers, these progeny were all categorized in the same group. It was considered more probable that the few 7DL-specific markers with no amplification in some of the progeny from families 64-8-2 and 64-8-27*, were due to failure of PCR amplification rather than to absence of very small segment(s) of 7DL chromosome. It needs to be further investigated in the next generation to make a conclusion. After many amplification experiments, it became evident that some 7EL-specific markers were less

consistent in their specificity which led to false positive results, including markers Lu-287-2, Lu-387-2, Lu-1851-2, Lu 632-2 and Lu-387-2. Optimization of these markers will be required to clarify interpretation. It is probable that no 7EL introgression occurred in those progeny.

Pattern B. This pattern represents only a small subset of BC_1F_4 progeny and was observed when plants had lost a relatively large part of both 7DL chromosomes (no amplification for a considerable portion of 7DL-specific markers) whereas amplified successfully for many of the 7EL-specific markers. Plants 64-8-2-[8, 18 and 20], 64-8-27*-5 showed this pattern. It is proposed that a segment of 7EL, possibly the same, was introgressed in both 7DL chromosomes in those plants, with the 7E fragment integrated into 64-8-27*-5 being smaller than the fragment in the 64-8-2 progeny. It is expected that no further recombination events between 7E and 7D would occur in those progeny, although all four progeny were shown to be resistant to FHB in the inoculation experiments.

Pattern C. This pattern was observed when the BC_1F_4 progeny amplified successfully for most of the 7EL- and 7DL-specific markers. Plants 4, 5, 6, 9, 10, 12, 13, 15 and 16 only from family 64-8-2 showed this pattern. Because most of the 7DL- and 7EL-specific markers successfully produced amplification in these progeny, it is proposed that a full copy (or at least the region tested with the available markers) of the 7DL chromosome and a large introgressed fragment of the 7EL chromosome are present in their genome. The inoculation experiment results showed that all of these progeny were FHB resistant.

Table 3.11: Six 7DL/7EL introgression patterns were observed in the genome of the BC_1F_4 progeny. See Figure 3.17 for a schematic representation.

Patterns				BC_1F_4 progeny		
Name	**7DL**	**7EL**	**FHB**	**64-8-2**	**64-8-17**	**64-8-27***
A	+	-	Susceptible	2, 3, 7, 11, 14	3, 5	2, 9, 10, 11, 13, 15, 17, 20
B	- (Partly)	+ (Large Frag.)	Resistant	8, 18, 20	-	5
C	+	+ (Large Frag.)	Resistant	4, 5, 6, 9, 10, 12, 13, 15, 16	-	-
D	+	+ (Smaller Frag.)	Resistant	-	2	1, 3, 4, 6, 7, 8, 12, 14, 16, 18, 19
E	+	+ (Medium Frag.)	Resistant	1, 19	-	-
F	+	+ (V. Small Frag.)	Susceptible	17	-	-

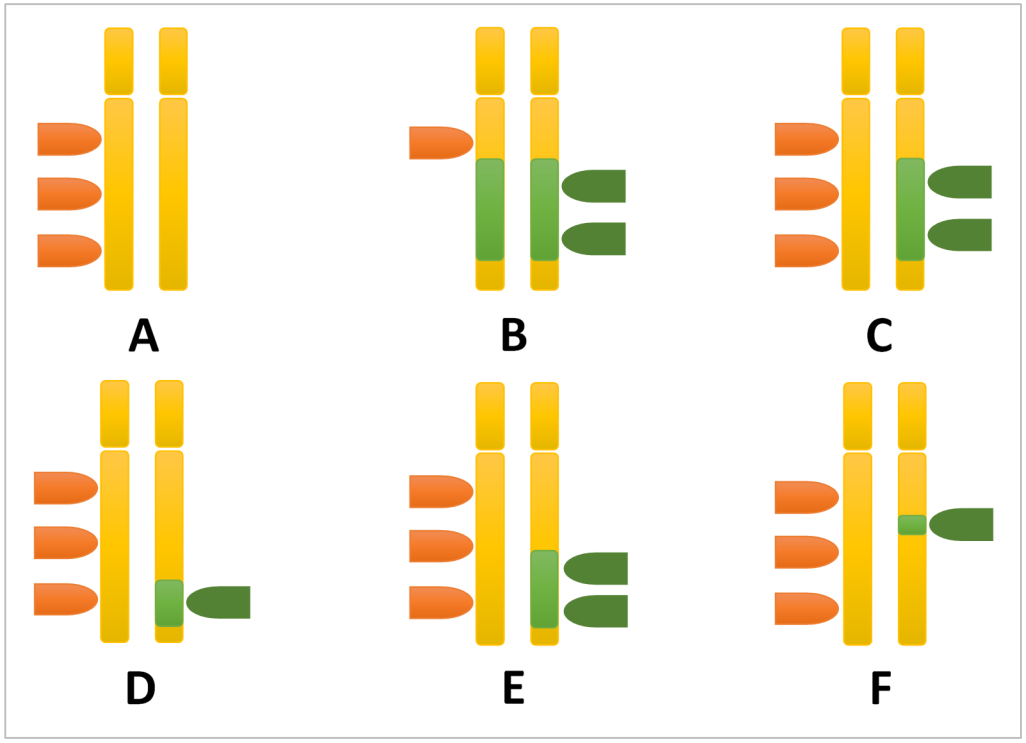

Figure 3.17: Schematic representation of six possible 7DL/7EL introgression patterns in the genome of different BC_1F_4 progeny.
See Table 3.11 for more details. The 7D chromosome is represented in yellow; green indicates introgressed 7EL chromosome fragments; orange and dark-green symbols on the left and right of the chromosomes respectively represent 7DL- and 7EL-specific markers.

Pattern D. This pattern includes the BC_1F_4 progeny which successfully amplified for all or most of the 7DL-specific markers, suggesting presence of a full 7DL chromosome in the genomes of the 64-8-27* progeny and possibly only a small deletion in the progeny from 64-8-17. Those progeny contain a smaller 7EL fragment comparing to the plants in pattern C. Progeny 64-8-17-2, 64-8-27*-[1, 3, 4, 6, 7, 8, 12, 14, 16, 18 and 19] showed this pattern. Although these progeny contain a smaller 7EL introgressed fragment, they were all FHB resistant.

Pattern E. This pattern is actually a subset of pattern C, where two progeny from family 64-8-2 amplified fewer 7EL-specific markers than those with pattern C. However, they still have larger 7EL introgressed fragment compared to the plants of pattern D. Plants 64-8-2-[1 and 19] showed this pattern. Despite repeating each experiment several times, most of the PCR amplifications for these two progeny were weak (rated as 0.5 or 0.25) and the negative results were spread through different areas of the chromosome arm; false negative results are highly probable for these two progeny. These results suggested that the DNA quality was not good enough and new DNA extractions would be needed; however, no more tissue was available. Further investigation has to be done with tissues from their next generation.

Pattern F. The last minor pattern was observed only for progeny 64-8-2-17. It successfully amplified all 7DL-specific markers except one and was positive for only ten 7EL-specific markers that present consistent specific results suggesting a very small 7EL introgressed fragment in its genome. As this progeny is FHB susceptible, the introgressed 7EL fragment is hypothesized to not contain the resistance gene(s).

4 DISCUSSION

The long-term goal of this research is to identify the smallest introgressed 7EL fragment of *Th. elongatum* that carries a novel source of resistance to FHB. Several objectives were defined to contribute to the long-term goal: 1) identification of *Th. elongatum* accessions that could be used as parents for a mapping population segregating for FHB resistance; 2) identification of BC_1F_4 progeny that carry the smallest introgressed 7EL fragment and are FHB resistant; 3) development of novel 7EL- and 7DL-specific markers that are associated with FHB resistance and finally 4) proposition of a genetic order for 7E-specific markers associated with FHB resistance. The key findings and accomplishments are summarized below.

In the first objective, five *Th. elongatum* accessions (*1-72, 1-73, 1-74, 1-86 and 'elongatum'*) were tested for their resistance to FHB and their genetic polymorphism. Among the five accessions, *1-86* showed high polymorphic PCR amplifications compared with other accessions and also CS-7EL or CS-7ES lines. It was subsequently found that this accession was tetraploid (4N) instead of diploid; the other four accessions were diploid. It was subsequently found that this accession was tetraploid (4N) instead of diploid; the other four accessions were diploid (Dr. George Fedak, AAFC, Ottawa, Canada, personal communication). The *Th. elongatum* accessions being inoculated in this project did not show adequate differences in response to FHB. In addition, very limited and insufficient polymorphism was observed between the accessions when using the genetic markers tested. Alternative methods to identify polymorphisms will have to be explored to characterize a

possible mapping population in further studies. No study on genetic diversity in the *Th. elongatum* species has been found to help interpret our results in a broader context.

In the second objective, a characterization of BC_1F_4 progeny from three families developed from an initial cross between CS-*ph1b* and the substitution line CS-7E(7D), a cross that favored introgression of *Th. elongatum* 7E fragments into wheat 7D chromosome. Thirteen plants, one from family 64-8-17 and 12 from family 64-8-27*, were identified as carrying the smallest 7EL fragment and still showing resistance to FHB among the 43 BC_1F_4 progeny examined. Based on the screening with genetic markers, all 13 progeny may contain the same 7EL fragment. However, it is possible that small differences in length could not be detected by available markers. Results for progeny 64-8-27*-5 with wheat 7D SSR and novel 7DL-specific markers suggest that the 7EL fragment introgressed into this progeny replaced about half of the 7DL chromosome arm. In the other 12 progeny of that group, homoeologous regions in the 7D and 7E chromosomes are still present, suggesting that there is capacity for additional recombinations between 7D and 7E in the next generations.

In the third objective, different strategies to develop additional 7EL-specific markers and their homoeologous 7DL-specific markers were used. Thirty-four novel genetic markers were designed, including 18 7EL and 16 7DL-specific ones. Among those, there are 12 pairs of markers for homoeologous sequence regions between 7EL and 7DL chromosomes. Although attempts were made, it was not always possible to develop corresponding pairs of markers on 7DL and 7EL chromosomes.

One of the strategies used to design novel 7EL-specific markers involved using genetic mapping information from wheat. Assuming a similar genetic position for 7EL and 7DL sequences, a genetic order was proposed in the fourth objective for the novel 7EL-specific markers. Using a similar strategy, the relative genetic order for some of previously designed

7E-specific markers (Chen et al., 2013; Gou et al., 2016) was also compiled. This improved greatly the interpretation of the screening data with genetic markers.

Triticum aestivum, as one of the most valuable cereal crops in the world, is threatened, both quantitatively and qualitatively, by the fungal disease fusarium head blight. Increasing host resistance to FHB is one of the strategies to manage the mycotoxin contaminated wheat problem. To complement the pyramiding of wheat genes/QTL associated with FHB resistance, an alternative strategy being tested is the introgression of FHB resistant loci from wild wheatgrass relatives into the *T. aestivum* genome.

Several investigations using crossing of exotic materials to wheat in order to genetically improve its sustainability against different diseases have been successful. For instance, the short arm of chromosome 1R (1RS) of rye (*Secale cereale* L., RR genome, 2n=2x=14) was successfully introgressed into the wheat chromosomes 1AL or 1BL. Due to the presence of beneficial and disease resistant genes located in 1RS, the plants obtained had a greater yield (specifically affected by the source of rye derivatives) and became resistant to powdery mildew, stem-, leaf- and stripe rust (W. Kim, Johnson, Baenziger, Lukaszewski, & Gaines, 2004). In another example, yellow dwarf disease resistance was transferred to wheat from *Thinopyrum intermedium* (2n=6x=42) (Ohm & Anderson, 2007). However, having the minimum possible length of exotic chromosome introgressed into the wheat genome, exempt from genes with a negative effect and possibly carrying only the gene(s) of interest, is not an easy process as the chance of recombination between wheat genomes and introgressed exotic chromosomes is naturally restricted (Shen & Ohm, 2007).

Despite many limitations, producing FHB resistant lines using exotic FHB resistant sources has been a focus for many research groups. *Roegneria kamoji* (Weng et al., 1993), *Elymus*

humidus, *Elymus racemifer* (Ban, 1997), *Aegilops speltoides*, *Secale cereale* (Fedak et al., 2004), *Thinopyrum junceiforme* (Jauhar & Peterson, 2001) are some of the wheat wild relatives which have been identified as having resistance to FHB. Shen et al. (2004) showed that CS-*Thinopyrum elongatum* substitution lines, 7E(7A, B, D), showed a strong type II resistance to FHB, suggesting that resistance gene(s) were located on chromosome 7E of *Th. elongatum* genome.

A QTL for FHB resistance has also been identified in wheat on the 7DL chromosome (Li, Bai, Wu, & Gu, 2011); however, it is in a different region of the chromosome than that one carrying the FHB resistance on chromosome 7EL of *Th. elongatum*. This suggests that the resistance on 7EL might be different from the one on 7DL. Characterization of the genes contributing to the 7DL and 7EL QTL will be required to determine if they act using similar or different mechanisms.

Thinopyrum ponticum is another wheatgrass that contains FHB resistance on the long arm of its chromosome 7E and the resistance has been transferred to wheat (Shen et al., 2004). Shen et al. (2007) developed a segregating mapping population in six generations from two distinct wheat-*Th. ponticum* substitution lines (7E(7D)) with different responses to FHB (one had type II FHB resistance and another was FHB susceptible). A QTL associated with FHB resistance was identified on the distal end of chromosome 7EL and several different specific markers for that specific region were developed. Although both *elongatum* and *ponticum* species are from the same *Thinopyrum* genus, none of the markers developed specifically for *Th. ponticum* were useful for *Th. elongatum* (Dr. George Fedak, personal communication). As a result, different 7E-specific markers developed specifically for *Th. elongatum* were used in this study to characterize the five different *Th. elongatum* accessions and also the progeny of BC_1F_4 generation.

As two different sources of *Th. ponticum* had contrasting responses to *Fusarium graminearum* (Shen et al., 2004), available *Th. elongatum* accessions were screened for their response to FHB in the current study. Although there were variations in their response, all accessions tested in this project were relatively resistant to FHB when compared to FHB-susceptible wheat. More *Th. elongatum* accessions will need to be screened in order to identify adequate parents to develop a mapping population segregating for FHB resistance.

Several years ago, series of substitution and addition lines carrying individual *Th. elongatum* chromosomes were created (Dvořák & Knott, 1974). The substitution line CS-7E(7D) from one of those series was used in Shen et al. (2004) experiments and also in the cross with a CS-*ph1b* for this project. A series of 7E/7D introgression plants were generated and characterized over generations, including three BC_1F_4 families in the current study. This is the first time that such a project is described as no mention of similar work could be found in the literature.

The FHB progression rating results for most of the BC_1F_4 progeny were consistent with the outcomes from screening with the 7EL-specific markers. However, in three progeny (64-8-27*-[10, 13 and 20]) there was ambiguity in interpreting the results. Although the DNA from those plants was successfully amplified only for 7E-specific markers that became recognized as not consistently specific, the plants had an FHB resistant phenotype. Further experiments revealed that the phenotype was really FHB susceptible. The difference in infection between different spikes of the same plant was observed frequently in this study, although lots of care was exercised to control inoculation conditions and consistency of it (e.g. control of temperature, light and humidity; control of wheat flowering stage for inoculation, amount of inoculum, etc.). A similar phenomenon has been observed in other projects; for example, it has been occasionally observed that one/some of the inoculated spikes did not get infected even in a very FHB susceptible wheat cultivar Roblin while the neighboring spikes were 100%

infected (Dr. Thérèse Ouellet, AAFC, Ottawa, Canada, personal communication). Attempts were made to inoculate many spikes for each plant to improve the accuracy of the disease rating; however, the limited number of spikes per plant and the often different flowering times for each spike made it so that only a few spikes could be inoculated for some progeny. Therefore, it was decided to analyze the phenotyping data using the spike showing the highest potential for FHB susceptibility as an indicator of the plant response to the disease, as no false positive results were expected for susceptible plants.

In a microscopy study, Miller et al. (2011) have shown that the progression of *F. graminearum* from the inoculated spikelet to the adjacent internodes and subsequently into the neighboring spikelets above and below the infected spikelet is considerably blocked in CS-7EL addition lines compared to CS. Longer internodes and secretion of an unknown brown material in the node tissue of CS-7EL were proposed as contributing factors to this blockage. Those results support our observations that the percentages of "infected internodes" were higher than the percentages of "spikelets with bleaching symptom" in the inoculated spikes of the resistant progeny; suggesting that the fungus is stopped in the node tissue located between the rachis and the spikelet in resistant plants. This leads to significant lower penetration of the infection into the neighboring spikelets.

Various markers have been used to characterize the size of the introgressed fragment from chromosome 7E of *Th. elongatum*. Some *SSR* markers developed for wheat have been shown to amplify the *Th. elongatum* 7E chromosome (Shen et al., 2004); several specific markers have been developed for *Th. elongatum,* including*, EST-SSR* and *PLUG* markers (Hu et al., 2012). More recently, sixty-one SLAF 7E-specifc markers (Chen et al., 2013) and forty-eight 7EL-expressed molecular markers (Gou et al., 2016) were designed for *Th. elongatum*. To

increase marker density in the 7EL region associated with FHB resistance, two strategies were developed to design additional 7EL-specific markers. It is hoped that a higher density of markers will eventually contribute to define a smaller 7EL region associated with FHB resistance. An important attribute of the novel 7EL-specific markers is that, as a new approach, many have a matching homoeologous 7DL-specific marker on wheat, facilitating the definition of the introgressed 7EL fragments in 7DL. This is a unique feature that was not found in any literature. Even though not all designed markers had both 7DL and 7EL types, they can still provide useful mapping information for either chromosome. It is important to note that, although the 7DL- and 7EL-specific pairs of markers were assumed to be in a similar location on each chromosome, it may not be the case for every pair designed. Lots of attention was applied to the selection of the homoeologous sequences; however, the absence of complete genomic sequence for the wheat and *Th. elongatum* genomes, and the absence of a genetic map for all wheat contigs and for 7E scaffolds altogether decrease the certainty of accuracy for the existing homoeology information between the two chromosomes.

Our assumption that wheat and *Th. elongatum* chromosome seven were largely syntenic, leading to most genes being in a similar location, is supported by related works discussed below. It has been shown that the model plant *Brachypodium distachyon* (2n=2x=10), with a small fully sequenced genome (~300 Mega-base pairs), has a closer relationship to Triticeae species compared to rice or maize (Huo et al., 2009; Kumar, Mohan, Balyan, & Gupta, 2009). In the same study, it was found that 77% of predicted *Brachypodium* genes were highly homoeologous to wheat ESTs. Kumar et al. (2012) have described the relationship between the chromosomes of wheat and *Brachypodium*. For instance, chromosome seven of wheat is highly syntenic to part of chromosome one and part of chromosome three of *Brachypodium*, suggesting that wheat and *Brachypodium* have evolved from a common ancestor. In another

study Hu et al. (2012) have also shown that the *Th. elongatum* E genome is closest to the D genome of wheat by comparing the locations of EST and PLUG molecular markers with polymorphic results between CS-*Th. elongatum* addition lines and CS.

Our proposed order for the 7EL-specific markers is also supported by complementary work done by collaborators (Tulpan, Leger, Konkin, & Ouellet, 2016). Working towards constructing a physical map of the 7EL of *Th. elongatum* genomic sequence, expressed sequences and predicted genes located on 7EL were used to identify orthologs in the evolutionary related plant species *Brachypodium distachyon* and *Sorghum bicolor.* Blocks of conserved orthologs common between 7EL and the two other species were identified. A subset of 7EL-specific expressed markers from Gou et al. (2016), for which we have determined a possible genetic order and that are common with their work, are present in a series of contiguous conserved blocks of orthologs. Their work supports the proposed genetic order presented in this research study.

The genetic order proposed in this study for the novel 7EL-specific markers and those from previous studies is adding an important advantage. Using this genetic order, the 7EL chromosome segments from *Th. elongatum* that are introgressed into wheat 7DL chromosome can be characterized more precisely for their content and size by interpreting the genetically ordered-PCR screening results of different progeny. For most of the markers, the predicted genetic order is consistent with the PCR screening results. However, for a few markers, such as the novel marker 1383-A3-7E, there is uncertainty about the markers' position as predicted genetic order and PCR results are not consistent; further investigation by screening other families with different introgression patterns may help resolve that uncertainty. It should be noted that evolutionary changes occurring between the genomes of different grasses may explain the uncertainty. Although the *Th. elongatum* genome is closely related to the D genome

of wheat, different types of mutations such as insertion, deletion, duplication and translocation in addition to variations in genome size, ploidy and number of chromosomes can affect the position of some DNA fragment regions in different species. Exceptions have been described where genes were not located where predicted by synteny. For instance, Kumar et al. (2012) showed most of the wheat chromosomes have high homology with two different chromosomes in *Brachypodium* (e.g. chromosome five of wheat is highly syntenic to part of chromosome four and part of chromosome one of *Brachypodium*). In addition, in the same study, there were a few genomic regions of wheat that were located outside of the syntenic blocks between wheat and *Brachypodium*. In another study based on the synteny comparison between chromosome 4A of the wheat genome, with the highest rate of rearrangement, and the full genome sequence of rice, *Brachypodium* and sorghum, only 29% of the genes had conserved location (Hernandez et al., 2012).

4.1 Conclusion

In conclusion, this study has contributed to identify a shorter fragment of 7EL chromosome of *Th. elongatum* that harbor a novel source of resistance to FHB among 43 characterized BC_1F_4 progeny. To better characterize the identified 7EL fragment, thirty-four novel markers were designed that were either 7EL- or 7DL-specific, including 12 pairs of markers from homoeologous regions of 7EL and 7DL chromosomes. For a more accurate interpretation of the screening data, a genetic order for the novel 7EL-specific markers and also some of the previously used 7E-specific markers (Chen et al., 2013; Gou et al., 2016) is recommended. In addition, response to FHB was characterized among *Th. elongatum* accessions.

4.2 Future Work

Further work to expand the results of this research study are proposed in the following paragraphs.

Once *Th. elongatum* accessions with sufficient differences in their FHB responses will be identified, they could be used as potential parents for a *Th. elongatum* FHB-Susceptible × FHB-Resistant mapping population. The results presented here clearly indicate that genetic mapping of a *Th. elongatum* segregating for FHB resistance could not be done using the 7E-specific markers tested in this study to characterize four diploid *Th. elongatum* accessions, as few of these markers were polymorphic among the four accessions. Other methods will need to be explored for that purpose. For instance, using SNP chips, such as those commercially available for wheat by Axiom and iSelect, to identify single nucleotide variations in the DNA of the four *Th. elongatum* accessions. This option assumes that some of the SNPs identified in wheat would also be present in *Th. elongatum*. Another approach is the sequencing of genes following exome capture. This approach compares sequence variations in the coding parts of genomes from different individuals. Basically in this approach, primer pairs specific to each exon of a species are hybridized with genomic DNA fragments; the hybridized primer/DNA fragments are then used for PCR amplification and sequencing using next generation sequencing technology. As there is only a partial *Th. elongatum* genomic sequence available, the wheat exome capture array would be used. Here, the assumption is that wheat and *Th. elongatum* coding sequences are sufficiently conserved for a subset of the primer pairs to bind to *Th. elongatum* DNA.

The characterization of BC_1F_4 progeny from three families allowed us to identify many plants from families 64-8-17 and 64-8-27* which had a short 7EL introgression. However, that

fragment is still representing about half of the 7EL chromosome arm. It would be desirable to identify FHB resistant plants with a smaller introgressed 7EL fragment. Screening of the next generation (BC_1F_5) of progeny for some of those plants might lead to smaller 7EL introgression in their FHB resistant progeny. However, there is a chance of not obtaining a smaller 7EL fragment as recombination might happen less frequently between the remaining 7EL fragment and the 7DL chromosome. Alternatively, characterizing additional $BC_1F_{2\text{-}4}$ families could provide different 7E/7D introgression patterns than the ones observed in this study. Identification of FHB resistant progeny carrying different yet overlapping 7EL fragments introgressed in the wheat 7D chromosome, or the identification of progeny with closely related marker patterns yet contrasting for FHB resistance, would be informative towards narrowing down the location of the FHB resistance gene(s). The genetic markers that were designed in this study would be used in the screening of other families.

Once FHB resistant progeny with small 7EL fragment are identified, or the location of the FHB resistance gene(s) is narrowed down, a more thorough examination of the target area in the 7EL genomic DNA would be required. Scaffolds corresponding to that area can be analyzed for the presence of genes based on bioinformatics annotation. By comparing genomic sequence and the previously obtained RNA sequence data from CS and CS-7EL, genes on those scaffolds which are expressed in CS-7EL head tissues can be identified. This information could be used to design new 7EL-specific markers closer to the resistance gene(s) and to identify candidate genes for the resistance. In addition, the expression of the candidate genes associated with FHB resistance could be determined in FHB resistant and susceptible progeny, to confirm their association with resistance. The FHB resistant progeny with very small 7EL fragment will then be stabilized by removing the *ph1b* mutation and provided as a germplasm for breeders.

It is possible that the available scaffolds for the 7EL genomic sequence would not cover fully the narrowed down target area for FHB resistance. In that case, cross-walking with the wheat chromosome 7 genomic sequences, as done in this project, would be used to complement the sequence information available for 7EL. The wheat genomic sequence and mapping information used in this study could now be supplemented with new sequencing data: organization of the contigs into scaffolds and genetically ordered whole-genome assemblies (Chapman et al., 2015; Poland, Brown, Sorrells, & Jannink, 2012; "Wheat Seq Repository: Assemblies," 2016).

REFERENCES

Agrios, G. N. (1997). *Plant Pathology* (4th ed.). London: Academic Press.

Alberta Fusarium Action Committee. (2012). *Alberta Fusarium graminearum Management Plan*. Edmonton, AB: Alberta Agriculture and Forestry, Government of Alberta. Retrieved from http://www1.agric.gov.ab.ca/$department/deptdocs.nsf/all/agdex5210

Altschul, S. F., Madden, T. L., Schäffer, A. A., Zhang, J., Zhang, Z., Miller, W., & Lipman, D. J. (1997). Gapped BLAST and PSI-BLAST: a new generation of protein database search programs. *Nucleic Acids Research*, *25*(17), 3389–3402. https://doi.org/10.1093/nar/25.17.3389

Bai, G., Desjardins, A. E., & Plattner, R. D. (2002). Deoxynivalenol-nonproducing *Fusarium graminearum* causes initial infection, but does not cause disease spread in wheat spikes. *Mycopathologia*, *153*(2), 91–98. https://doi.org/10.1023/A:1014419323550

Bai, G., & Shaner, G. (2004). Management and resistance in wheat and barley to Fusarium Head Blight. *Annual Review of Phytopathology*, *42*(1), 135–161. https://doi.org/10.1146/annurev.phyto.42.040803.140340

Ban, T. (1997). Evaluation of resistance to Fusarium head blight in indigenous Japanese species of Agropyron (Elymus). *Euphytica*, *97*(1), 39–44. https://doi.org/10.1023/A:1003078109694

Boenisch, M. J., & Schäfer, W. (2011). *Fusarium graminearum* forms mycotoxin producing infection structures on wheat. *BMC Plant Biology*, *11*(1), 110. https://doi.org/10.1186/1471-2229-11-110

Borrill, P., Adamski, N., & Uauy, C. (2015). Genomics as the key to unlocking the polyploid potential of wheat. *The New Phytologist*, *208*(4), 1008–1022. https://doi.org/10.1111/nph.13533

Brenchley, R., Spannagl, M., Pfeifer, M., Barker, G. L. A., D'Amore, R., Allen, A. M., … Hall, N. (2012). Analysis of the bread wheat genome using whole-genome shotgun sequencing. *Nature*, *491*(7426), 705–710. https://doi.org/10.1038/nature11650

Brown, N. A., Bass, C., Baldwin, T. K., Chen, H., Massot, F., Carion, P. W. C., … Hammond-Kosack, K. E. (2011). Characterisation of the *Fusarium graminearum*-Wheat Floral Interaction. *Journal of Pathogens*, *2011*, e626345. https://doi.org/10.4061/2011/626345

Brown, N. A., Urban, M., van de Meene, A. M. L., & Hammond-Kosack, K. E. (2010). The infection biology of *Fusarium graminearum*: defining the pathways of spikelet to

spikelet colonisation in wheat ears. *Fungal Biology*, *114*(7), 555–571. https://doi.org/10.1016/j.funbio.2010.04.006

Buerstmayr, H., Ban, T., & Anderson, J. A. (2009). QTL mapping and marker-assisted selection for Fusarium head blight resistance in wheat: a review. *Plant Breeding*, *128*(1), 1–26. https://doi.org/10.1111/j.1439-0523.2008.01550.x

Burt, C., Steed, A., Gosman, N., Lemmens, M., Bird, N., Ramirez-Gonzalez, R., … Nicholson, P. (2015). Mapping a Type 1 FHB resistance on chromosome 4AS of Triticum macha and deployment in combination with two Type 2 resistances. *TAG. Theoretical and Applied Genetics. Theoretische Und Angewandte Genetik*, *128*(9), 1725–1738. https://doi.org/10.1007/s00122-015-2542-9

Cao, H., Li, X., & Dong, X. (1998). Generation of broad-spectrum disease resistance by overexpression of an essential regulatory gene in systemic acquired resistance. *Proceedings of the National Academy of Sciences*, *95*(11), 6531–6536.

Cappellini, R. A., & Peterson, J. L. (1965). Macroconidium formation in sub-merged cultures by a non-sporulating strain of *Gibberella zeae*. *Mycologia*, *57*(6), 962–966. https://doi.org/10.2307/3756895

CerealsDB, tools for the analysis of the wheat genome. (n.d.-a). Retrieved July 29, 2016, from http://www.cerealsdb.uk.net/cerealgenomics/CerealsDB/axiom_download.php

CerealsDB, tools for the analysis of the wheat genome. (n.d.-b). Retrieved July 29, 2016, from http://www.cerealsdb.uk.net/cerealgenomics/CerealsDB/kasp_download.php

Chapman, J. A., Mascher, M., Buluç, A., Barry, K., Georganas, E., Session, A., … Rokhsar, D. S. (2015). A whole-genome shotgun approach for assembling and anchoring the hexaploid bread wheat genome. *Genome Biology*, *16*, 26. https://doi.org/10.1186/s13059-015-0582-8

Chen, S., Huang, Z., Dai, Y., Qin, S., Gao, Y., Zhang, L., … Chen, J. (2013). The Development of 7E Chromosome-Specific Molecular Markers for *Thinopyrum elongatum* Based on SLAF-seq Technology. *PLOS ONE*, *8*(6), e65122. https://doi.org/10.1371/journal.pone.0065122

Common Taxonomy Tree. (n.d.). Retrieved December 13, 2016, from https://www.ncbi.nlm.nih.gov/Taxonomy/CommonTree/wwwcmt.cgi

Curtis, B. C. (2002). Wheat in the world. In *Bread Wheat: Improvement and Production*. Rome: Food and Agriculture Organization of the United Nations. Retrieved from http://www.fao.org/docrep/006/y4011e/y4011e04.htm

Desjardins, A. E. (2006). *Fusarium mycotoxins: chemistry, genetics, and biology*. St. Paul, MN: American Phytopathological Society.

Desmond, O. J., Manners, J. M., Stephens, A. E., Maclean, D. J., Schenk, P. M., Gardiner, D. M., … Kazan, K. (2008). The Fusarium mycotoxin deoxynivalenol elicits hydrogen peroxide production, programmed cell death and defence responses in wheat. *Molecular Plant Pathology*, *9*(4), 435–445. https://doi.org/10.1111/j.1364-3703.2008.00475.x

Ding, L., Xu, H., Yi, H., Yang, L., Kong, Z., Zhang, L., … Ma, Z. (2011). Resistance to hemi-biotrophic *F. graminearum* infection is associated with coordinated and ordered expression of diverse defense signaling pathways. *PLoS ONE*, *6*(4), e19008. https://doi.org/10.1371/journal.pone.0019008

Dong, X. (2004). NPR1, all things considered. *Current Opinion in Plant Biology*, *7*(5), 547–552. https://doi.org/10.1016/j.pbi.2004.07.005

Durrant, W. E., & Dong, X. (2004). Systemic acquired resistance. *Annual Review of Phytopathology*, *42*, 185–209. https://doi.org/10.1146/annurev.phyto.42.040803.140421

Dvořák, J. (1979). Metaphase I pairing frequencies of individual *Agropyron elongatum* chromosome arms with *Triticum* chromosomes. *Canadian Journal of Genetics and Cytology*, *21*(2), 243–254. https://doi.org/10.1139/g79-028

Dvořák, J. (1980). Homoeology between *Agropyron elongatum* chromosomes and *Triticum aestivum* chromosomes. *Canadian Journal of Genetics and Cytology*, *22*(2), 237–259. https://doi.org/10.1139/g80-029

Dvořák, J., Edge, M., & Ross, K. (1988). On the evolution of the adaptation of *Lophopyrum elongatum* to growth in saline environments. *Proceedings of the National Academy of Sciences*, *85*(11), 3805–3809.

Dvořák, J., & Knott, D. R. (1974). Disomic and ditelosomic additions of diploid *Agropyron elongatum* chromosomes to *Triticum aestivum*. *Canadian Journal of Genetics and Cytology*, *16*(2), 399–417. https://doi.org/10.1139/g74-043

FAOSTAT. (2015). Retrieved September 22, 2016, from http://faostat3.fao.org/browse/rankings/commodities_by_regions/E

Fedak, G., Cao, W., Han, F., Savard, M., Gilbert, J., & Xue, A. (2004). Germplasm enhancement for FHB resistance in spring wheat through alien introgression. In S. M. Canty, T. Boring, K. Versdahl, J. Wardwell, & R. W. Ward (Eds.), *Proceedings of the 2nd International Symposium on Fusarium Head Blight* (pp. 56–57). East Lansing, MI: Michigan State University.

Fedak, G., Wolfe, D., Chi, D., Ouellet, T., Cao, W., & Xue, A. G. (2014). Process of transferring fhb resistance from *Thinopyrum elongatum* to spring wheat. Presented at the Second Canadian Wheat Symposium (Poster), Saskatoon, SK, Canada.

Flowchart Maker & Online Diagram Software. (n.d.). Retrieved July 29, 2016, from https://www.draw.io/

Friebe, B., Jiang, J., Raupp, W. J., McIntosh, R. A., & Gill, B. S. (1996). Characterization of wheat-alien translocations conferring resistance to diseases and pests: current status. *Euphytica*, *91*(1), 59–87. https://doi.org/10.1007/BF00035277

Gale, L. R. (2003). Population biology of *Fusarium* species causing head blight of grain crops. In K. J. Leonard & W. R. Bushnell (Eds.), *Fusarium Head Blight of Wheat and Barley* (pp. 120–143). St. Paul, MN: American Phytopathological Society.

Gardiner, D. M., Kazan, K., & Manners, J. M. (2009). Nutrient profiling reveals potent inducers of trichothecene biosynthesis in *Fusarium graminearum*. *Fungal Genetics and Biology*, *46*(8), 604–613. https://doi.org/10.1016/j.fgb.2009.04.004

Gardiner, D. M., Kazan, K., Praud, S., Torney, F. J., Rusu, A., & Manners, J. M. (2010). Early activation of wheat polyamine biosynthesis during Fusarium head blight implicates putrescine as an inducer of trichothecene mycotoxin production. *BMC Plant Biology*, *10*(1), 289. https://doi.org/10.1186/1471-2229-10-289

Gardiner, D. M., Osborne, S., Kazan, K., & Manners, J. M. (2009). Low pH regulates the production of deoxynivalenol by *Fusarium graminearum*. *Microbiology*, *155*(9), 3149–3156. https://doi.org/10.1099/mic.0.029546-0

Garg, M., Tanaka, H., Ishikawa, N., Takata, K., Yanaka, M., & Tsujimoto, H. (2009). *Agropyron elongatum* HMW-glutenins have a potential to improve wheat end-product quality through targeted chromosome introgression. *Journal of Cereal Science*, *50*(3), 358–363. https://doi.org/10.1016/j.jcs.2009.06.012

Gilbert, J., & Tekauz, A. (2000). Review: Recent developments in research on fusarium head blight of wheat in Canada. *Canadian Journal of Plant Pathology*, *22*(1), 1–8. https://doi.org/10.1080/07060660009501155

Gilchrist, L., & Dubin, H. J. (n.d.). Fusarium head blight. Retrieved January 13, 2015, from http://www.fao.org/docrep/006/y4011e/y4011e0j.htm#TopOfPage

Gottwald, S., Samans, B., Lück, S., & Friedt, W. (2012). Jasmonate and ethylene dependent defence gene expression and suppression of fungal virulence factors: two essential mechanisms of Fusarium head blight resistance in wheat? *BMC Genomics*, *13*(1), 369. https://doi.org/10.1186/1471-2164-13-369

Gou, L., Hattori, J., Fedak, G., Balcerzak, M., Sharpe, A., Visendi, P., … Ouellet, T. (2016). Development and Validation of *Thinopyrum elongatum*–Expressed Molecular Markers Specific for the Long Arm of Chromosome 7E. *Crop Science*, *56*(1), 354. https://doi.org/10.2135/cropsci2015.03.0184

GrainGenes: A database for Triticeae and *Avena*. (n.d.). Retrieved July 29, 2016, from http://wheat.pw.usda.gov/cgi-bin/graingenes/browse.cgi?class=marker

Green, R. E., Cornell, S. J., Scharlemann, J. P. W., & Balmford, A. (2005). Farming and the Fate of Wild Nature. *Science*, *307*(5709), 550–555. https://doi.org/10.1126/science.1106049

Hadas, Y., Goldberg, I., Pines, O., & Prusky, D. (2007). Involvement of Gluconic Acid and Glucose Oxidase in the Pathogenicity of *Penicillium expansum* in Apples. *Phytopathology*, *97*(3), 384–390. https://doi.org/10.1094/PHYTO-97-3-0384

Hamzehzarghani, H., Kushalappa, A. C., Dion, Y., Rioux, S., Comeau, A., Yaylayan, V., … Mather, D. E. (2005). Metabolic profiling and factor analysis to discriminate quantitative resistance in wheat cultivars against fusarium head blight. *Physiological and Molecular Plant Pathology*, *66*(4), 119–133. https://doi.org/10.1016/j.pmpp.2005.05.005

Hamzehzarghani, H., Paranidharan, V., Abu-Nada, Y., Kushalappa, A. C., Dion, Y., Rioux, S., … Marshall, W. D. (2008). Metabolite profiling coupled with statistical analyses for potential high-throughput screening of quantitative resistance to fusarium head blight in wheat. *Canadian Journal of Plant Pathology*, *30*(1), 24–36. https://doi.org/10.1080/07060660809507493

Hattori, J., Ouellet, T., & Tinker, N. A. (2005). Wheat EST sequence assembly facilitates comparison of gene contents among plant species and discovery of novel genes. *Genome / National Research Council Canada = Génome / Conseil National De Recherches Canada*, *48*(2), 197–206. https://doi.org/10.1139/g04-106

Hernandez, P., Martis, M., Dorado, G., Pfeifer, M., Gálvez, S., Schaaf, S., … Mayer, K. F. X. (2012). Next-generation sequencing and syntenic integration of flow-sorted arms of wheat chromosome 4A exposes the chromosome structure and gene content. *The Plant Journal: For Cell and Molecular Biology*, *69*(3), 377–386. https://doi.org/10.1111/j.1365-313X.2011.04808.x

Hu, L.-J., Liu, C., Zeng, Z.-X., Li, G.-R., Song, X.-J., & Yang, Z.-J. (2012). Genomic rearrangement between wheat and *Thinopyrum elongatum* revealed by mapped functional molecular markers. *Genes & Genomics*, *34*(1), 67–75. https://doi.org/10.1007/s13258-011-0153-7

Huo, N., Vogel, J. P., Lazo, G. R., You, F. M., Ma, Y., McMahon, S., … Gu, Y. Q. (2009). Structural characterization of *Brachypodium* genome and its syntenic relationship with rice and wheat. *Plant Molecular Biology*, *70*(1–2), 47–61. https://doi.org/10.1007/s11103-009-9456-3

International Wheat Genome Sequencing Consortium (IWGSC). (2014). A chromosome-based draft sequence of the hexaploid bread wheat (Triticum aestivum) genome.

Science (New York, N.Y.), *345*(6194), 1251788. https://doi.org/10.1126/science.1251788

Jansen, C., Wettstein, D. von, Schäfer, W., Kogel, K.-H., Felk, A., & Maier, F. J. (2005). Infection patterns in barley and wheat spikes inoculated with wild-type and trichodiene synthase gene disrupted *Fusarium graminearum*. *Proceedings of the National Academy of Sciences of the United States of America*, *102*(46), 16892–16897. https://doi.org/10.1073/pnas.0508467102

Jauhar, P., & Peterson, T. (2001). Hybrids between durum wheat and *Thinopyrum junceiforme*: prospects for breeding for scab resistance. *Euphytica*, *118*, 127–136.

JGI Genome Portal Help: What is a Scaffold. (n.d.). Retrieved September 8, 2015, from http://genome.jgi.doe.gov/help/scaffolds.html

Jiang, G.-L. (2013). Molecular Markers and Marker-Assisted Breeding in Plants. In S. B. Andersen (Ed.), *Plant Breeding from Laboratories to Fields*. InTech. Retrieved from http://www.intechopen.com/books/plant-breeding-from-laboratories-to-fields/molecular-markers-and-marker-assisted-breeding-in-plants

Kim, K. S., Min, J.-Y., & Dickman, M. B. (2008). Oxalic acid is an elicitor of plant programmed cell death during *Sclerotinia sclerotiorum* disease development. *Molecular Plant-Microbe Interactions: MPMI*, *21*(5), 605–612. https://doi.org/10.1094/MPMI-21-5-0605

Kim, W., Johnson, J. W., Baenziger, P. S., Lukaszewski, A. J., & Gaines, C. S. (2004). Agronomic Effect of Wheat-Rye Translocation Carrying Rye Chromatin (1R) From Different Sources. *Crop Science*, *44*(4), 1254. https://doi.org/10.2135/cropsci2004.1254

Konkin, D. J. F., Tan, Y., MacLachlan, R., Koh, K., Clarke, C., Condie, J., … Sharpe, A. G. (2016). Never Eat Shredded Wheat – Navigating through Reference and Survey Wheat Assemblies Using Diverse Mate-Pair Libraries. Presented at the Plant and Animal Genome XXIV Conference (Poster), San Diego, CA, USA: Plant and Animal Genome. Retrieved from https://pag.confex.com/pag/xxiv/webprogram/Paper21570.html

Kumar, S., Balyan, H. S., & Gupta, P. K. (2012). Comparative DNA Sequence Analysis Involving Wheat, Brachypodium and Rice Genomes Using Mapped Wheat ESTs. *Triticeae Genomics and Genetics*, *3*(3), 25–37. https://doi.org/10.5376/tgg.2012.03.0003

Kumar, S., Mohan, A., Balyan, H. S., & Gupta, P. K. (2009). Orthology between genomes of *Brachypodium*, wheat and rice. *BMC Research Notes*, *2*, 93. https://doi.org/10.1186/1756-0500-2-93

Li, T., Bai, G., Wu, S., & Gu, S. (2011). Quantitative trait loci for resistance to fusarium head blight in a Chinese wheat landrace Haiyanzhong. *TAG. Theoretical and Applied*

Genetics. Theoretische Und Angewandte Genetik, *122*(8), 1497–1502. https://doi.org/10.1007/s00122-011-1549-0

Liu, Z., Li, D., & Zhang, X. (2007). Genetic Relationships Among Five Basic Genomes St, E, A, B and D in Triticeae Revealed by Genomic Southern and *in situ* Hybridization. *Journal of Integrative Plant Biology*, *49*(7), 1080–1086. https://doi.org/10.1111/j.1672-9072.2007.00462.x

Ma, J. X., Zhou, R. H., Dong, Y. S., & Jia, J. Z. (1999). Gene location for resistance to wheat strip rust derived from *Lophopyrum elongatum* (Host). *Chinese Science Bulletin*, *44*, 65–69.

Makandar, R., Essig, J. S., Schapaugh, M. A., Trick, H. N., & Shah, J. (2006). Genetically engineered resistance to Fusarium head blight in wheat by expression of *Arabidopsis NPR1*. *Molecular Plant-Microbe Interactions: MPMI*, *19*(2), 123–129. https://doi.org/10.1094/MPMI-19-0123

Makandar, R., Nalam, V., Chaturvedi, R., Jeannotte, R., Sparks, A. A., & Shah, J. (2010). Involvement of Salicylate and Jasmonate Signaling Pathways in *Arabidopsis* Interaction with *Fusarium graminearum*. *Molecular Plant-Microbe Interactions*, *23*(7), 861–870. https://doi.org/10.1094/MPMI-23-7-0861

Makandar, R., Nalam, V. J., Lee, H., Trick, H. N., Dong, Y., & Shah, J. (2012). Salicylic acid regulates basal resistance to Fusarium head blight in wheat. *Molecular Plant-Microbe Interactions: MPMI*, *25*(3), 431–439. https://doi.org/10.1094/MPMI-09-11-0232

Market Analysis Group, Grains and Oilseeds Division, Food Value Chain Bureau. (2010). *Canada Wheat Sector Profile - Part One: Overview* (Market Outlook Report No. Volume 2 Number 6). Agriculture and Agri-Food Canada. Retrieved from www.agr.gc.ca/gaod-dco

McMullen, M., Bergstrom, G., De Wolf, E., Dill-Macky, R., Hershman, D., Shaner, G., & Van Sanford, D. (2012). A Unified Effort to Fight an Enemy of Wheat and Barley: Fusarium Head Blight. *Plant Disease*, *96*(12), 1712–1728. https://doi.org/10.1094/PDIS-03-12-0291-FE

McMullen, M., Jones, R., & Gallenberg, D. (1997). Scab of wheat and barley: a reemerging disease of devastating impact. *The American Phytopathological Society*, *81*, 1340–1348.

Mesterházy, A. (1995). Types and components of resistance to *Fusarium* head blight of wheat. *Plant Breeding*, *114*(5), 377–386. https://doi.org/10.1111/j.1439-0523.1995.tb00816.x

Miller, J. D., & Arnison, P. G. (1986). Degradation of deoxynivalenol by suspension cultures of the fusarium head blight resistant wheat cultivar Frontana. *Canadian Journal of Plant Pathology*, *8*(2), 147–150. https://doi.org/10.1080/07060668609501818

Miller, J. D., Young, J. C., & Sampson, D. R. (1985). Deoxynivalenol and Fusarium Head Blight Resistance in Spring Cereals. *Journal of Phytopathology*, *113*(4), 359–367. https://doi.org/10.1111/j.1439-0434.1985.tb04837.x

Miller, S. S., Watson, E. M., Lazebnik, J., Gulden, S., Balcerzak, M., Fedak, G., & Ouellet, T. (2011). Characterization of an alien source of resistance to Fusarium head blight transferred to Chinese Spring wheat. *Botany*, *89*(5), 301–311. https://doi.org/10.1139/b11-017

Moore, G. (2014). Wheat meiosis and the *Ph1* locus. Retrieved January 4, 2015, from https://www.jic.ac.uk/staff/graham-moore/Wheat_meiosis.htm

Mudge, A. M., Dill-Macky, R., Dong, Y., Gardiner, D. M., White, R. G., & Manners, J. M. (2006). A role for the mycotoxin deoxynivalenol in stem colonisation during crown rot disease of wheat caused by *Fusarium graminearum* and *Fusarium pseudograminearum*. *Physiological and Molecular Plant Pathology*, *69*(1–3), 73–85. https://doi.org/10.1016/j.pmpp.2007.01.003

Ohm, H., & Anderson, J. (2007). Utilization and Performance in Wheat of Yellow Dwarf Virus Resistance Transferred From *Thinopyrum Intermedium*. In H. T. Buck, J. E. Nisi, & N. Salomón (Eds.), *Wheat Production in Stressed Environments* (pp. 149–152). Springer Netherlands. https://doi.org/10.1007/1-4020-5497-1_19

Okubara, P. A., & Jones, S. S. (2011). Seedling resistance to *Rhizoctonia* and *Pythium* spp. in wheat chromosome group 4 addition lines from *Thinopyrum* spp. *Canadian Journal of Plant Pathology*, *33*(3), 416–423. https://doi.org/10.1080/07060661.2011.590532

Olivieri, F., Zanetti, M. E., Oliva, C. R., Covarrubias, A. A., & Casalongué, C. A. (2002). Characterization of an Extracellular Serine Protease of *Fusarium eumartii* and its Action on Pathogenesis Related Proteins. *European Journal of Plant Pathology*, *108*(1), 63–72. https://doi.org/10.1023/A:1013920929965

Ouellet, T., Gou, L., Konkin, D., Hattori, J., Tekieh, F., Wolfe, D., … Fedak, G. (2016). Collective effort to develop genomics and genetics tools for the cloning of the FHB-resistance locus from Thinopyrum elongatum chromosome 7EL. In *Proceedings of the 8th Canadian Workshop on Fusarium Head Blight* (p. 14). Ottawa, Canada. Retrieved from https://static1.squarespace.com/static/56be29e022482ec146a7c5b8/t/583f78142e69cf3fe08362cf/1480554518607/8th+CWFHB+Proceedings.pdf

Ouellet, T., Gou, L., Konkin, D., Hattori, J., Tekieh, F., Wolfe, D., … Fedak, G. (2016). Towards Cloning of the Fusarium Head Blight-Resistance Locus from *Thinopyrum elongatum* Chromosome 7EL. Presented at the Plant and Animal Genome XXIV Conference (Poster), San Diego, CA, USA: Plant and Animal Genome. Retrieved from https://pag.confex.com/pag/xxiv/webprogram/Paper18757.html

Parry, D. W., Jenkinson, P., & McLeod, L. (1995). Fusarium ear blight (scab) in small grain cereals - a review. *Plant Pathology*, *44*(2), 207–238. https://doi.org/10.1111/j.1365-3059.1995.tb02773.x

Pekkarinen, A. I., & Jones, B. L. (2002). Trypsin-Like Proteinase Produced by *Fusarium culmorum* Grown on Grain Proteins. *Journal of Agricultural and Food Chemistry*, *50*(13), 3849–3855. https://doi.org/10.1021/jf020027x

Pekkarinen, A. I., & Jones, B. L. (2003). Purification and Identification of Barley (Hordeum vulgare L.) Proteins That Inhibit the Alkaline Serine Proteinases of Fusarium culmorum. *Journal of Agricultural and Food Chemistry*, *51*(6), 1710–1717. https://doi.org/10.1021/jf026035v

Plant Inventory Books. (n.d.). Retrieved December 5, 2016, from https://www.ars.usda.gov/northeast-area/beltsville-md/beltsville-agricultural-research-center/national-germplasm-resources-laboratory/docs/plant-inventory-books/

Poland, J. A., Brown, P. J., Sorrells, M. E., & Jannink, J.-L. (2012). Development of High-Density Genetic Maps for Barley and Wheat Using a Novel Two-Enzyme Genotyping-by-Sequencing Approach. *PLOS ONE*, *7*(2), e32253. https://doi.org/10.1371/journal.pone.0032253

Ponts, N., Pinson-Gadais, L., Boutigny, A.-L., Barreau, C., & Richard-Forget, F. (2011). Cinnamic-Derived Acids Significantly Affect *Fusarium graminearum* Growth and In Vitro Synthesis of Type B Trichothecenes. *Phytopathology*, *101*(8), 929–934. https://doi.org/10.1094/PHYTO-09-10-0230

Ponts, N., Pinson-Gadais, L., Verdal-Bonnin, M.-N., Barreau, C., & Richard-Forget, F. (2006). Accumulation of deoxynivalenol and its 15-acetylated form is significantly modulated by oxidative stress in liquid cultures of *Fusarium graminearum*. *FEMS Microbiology Letters*, *258*(1), 102–107. https://doi.org/10.1111/j.1574-6968.2006.00200.x

Pozniak, C. J., Sharpe, A. G., Poland, J., Thompson, M., Stein, N., Distelfeld, A., … Rogers, J. (2016). IWGSC whole genome shotgun sequencing of Chinese Spring: Towards a Reference Sequence of Wheat. Presented at the Plant and Animal Genome XXIV Conference - International Wheat Genome Sequencing Consortium Workshop, San Diego, CA: Plant and Animal Genome. Retrieved from https://pag.confex.com/pag/xxiv/webprogram/Paper22378.html

PrimerQuest Tool, Integrated DNA Technologies (IDT). (n.d.). Retrieved July 29, 2016, from https://www.idtdna.com/PrimerQuest/Home/Index

Proctor, R. H., Holm, T. M., & McCormick, S. P. (1995). Reduced virulence of *Gibberella zeae* caused by disruption of a trichothecene toxin biosynthetic gene. *The American Phytopathological Society*, *8*, 593–601.

Qi, L., Friebe, B., Zhang, P., & Gill, B. S. (2007). Homoeologous recombination, chromosome engineering and crop improvement. *Chromosome Research: An International Journal on the Molecular, Supramolecular and Evolutionary Aspects of Chromosome Biology*, *15*(1), 3–19. https://doi.org/10.1007/s10577-006-1108-8

Riley, R., & Chapman, V. (1958). Genetic Control of the Cytologically Diploid Behaviour of Hexaploid Wheat. *Nature*, *182*(4637), 713–715. https://doi.org/10.1038/182713a0

Riley, R., & Chapman, V. (1964). The effect of the deficiency of the long arm of chromosome 5B on meiotic pairing in Triticum aestivum. *Wheat Information Service*, pp. 12–15.

Roundy, B. A. (1985). Emergence and Establishment of Basin Wildrye and Tall Wheatgrass in Relation to Moisture and Salinity. *Journal of Range Management*, *38*(2), 126–131. https://doi.org/10.2307/3899254

Schroeder, H. W., & Christensen, J. J. (1963). Factors affecting resistance of Wheat to scab caused by Gibberella zeae (Schw.) Petch. *Phytopathology*, *53*(7, 1), 831–838.

Sears, E. R. (1977). Induced mutant with homoeologous pairing in common wheat. *Canadian Journal of Genetics and Cytology*, *19*, 585–593. https://doi.org/10.1139/g77-063

Seong, K.-Y., Pasquali, M., Zhou, X., Song, J., Hilburn, K., McCormick, S., … Kistler, H. C. (2009). Global gene regulation by *Fusarium* transcription factors *Tri6* and *Tri10* reveals adaptations for toxin biosynthesis. *Molecular Microbiology*, *72*(2), 354–367. https://doi.org/10.1111/j.1365-2958.2009.06649.x

Shaner, G. (2002). Resistance in hexaploid wheat to Fusarium head blight. In *2002 National Fusarium Head Blight Proceedings* (pp. 208–211). Erlanger, Ky.

Shaner, G. (2003). Epidemiology of Fusarium head blight of small grain cereals in North America. In K. J. Leonard & W. R. Bushnell (Eds.), *Fusarium Head Blight of Wheat and Barley* (pp. 84–119). St. Paul, MN: American Phytopathological Society.

Shen, X., Lingrang, K., & Ohm. (2004). Fusarium head blight resistance in hexaploid wheat (*Triticum aestivum*) - *Lophopyrum* genetic lines and tagging of the alien chromatin by PCR markers. *TAG Theoretical and Applied Genetics*, *108*(5), 808–813. https://doi.org/10.1007/s00122-003-1492-9

Shen, X., & Ohm, H. (2007). Molecular mapping of *Thinopyrum*-derived Fusarium head blight resistance in common wheat. *Molecular Breeding*, *20*(2), 131–140. https://doi.org/10.1007/s11032-007-9079-9

Snijders, C. H. A. (1990). Genetic variation for resistance to Fusarium head blight in bread wheat. *Euphytica*, *50*(2), 171–179. https://doi.org/10.1007/BF00023642

Tulpan, D., Leger, S., Konkin, D., & Ouellet, T. (2016). Visualization of orthology-based plant genome zipper seeding using circular diagrams. Presented at the 2016 Annual Science and Business Meeting (Poster), Saskatoon, SK, Canada.

Voigt, C. A., Schäfer, W., & Salomon, S. (2005). A secreted lipase of *Fusarium graminearum* is a virulence factor required for infection of cereals. *The Plant Journal*, *42*(3), 364–375. https://doi.org/10.1111/j.1365-313X.2005.02377.x

Walter, S., Nicholson, P., & Doohan, F. M. (2010). Action and reaction of host and pathogen during Fusarium head blight disease. *New Phytologist*, *185*(1), 54–66. https://doi.org/10.1111/j.1469-8137.2009.03041.x

Wang, J.-R., Wang, L., Gulden, S., Rocheleau, H., Balcerzak, M., Hattori, J., … Ouellet, T. (2010). RNA profiling of fusarium head blight-resistant wheat addition lines containing the *Thinopyrum elongatum* chromosome 7E. *Canadian Journal of Plant Pathology*, *32*(2), 188–214. https://doi.org/10.1080/07060661003740512

Wang, S., Wong, D., Forrest, K., Allen, A., Chao, S., Huang, B. E., … Akhunov, E. (2014). Characterization of polyploid wheat genomic diversity using a high-density 90 000 single nucleotide polymorphism array. *Plant Biotechnology Journal*, *12*(6), 787–796. https://doi.org/10.1111/pbi.12183

Wang, Y., Yang, L., Xu, H., Li, Q., Ma, Z., & Chu, C. (2005). Differential proteomic analysis of proteins in wheat spikes induced by *Fusarium graminearum*. *PROTEOMICS*, *5*(17), 4496–4503. https://doi.org/10.1002/pmic.200401317

Weng, Y. Q., Wu, L. F., Chen, P. D., & Liu, D. J. (1993). Development of alien addition lines of wheat scab resistance from *Roegneria kamoji*. In Z. S. Li & Z. Y. Xin (Eds.), *Proceedings of the 8th international wheat genetics symposium (Beijing, China)* (pp. 365–368). China Agric. Sci. Press, Beijing.

Wheat Seq Repository: Assemblies. (2016, July 4). Retrieved September 13, 2016, from

Williamson, B., Tudzynski, B., Tudzynski, P., & van Kan, J. A. L. (2007). Botrytis cinerea: the cause of grey mould disease. *Molecular Plant Pathology*, *8*(5), 561–580. https://doi.org/10.1111/j.1364-3703.2007.00417.x

World Population Clock: 7.5 Billion People (2016) - Worldometers. (2016). Retrieved December 4, 2016, from http://www.worldometers.info/world-population/

APPENDICES

Appendix I

I.I Stock concentrations and dilutions of the extracted DNA samples

Table App-I.1: Stock concentrations and the dilutions of the extracted genomic DNA samples.

(A)

DNA Sample	Stock Concentration (ng/µl)	Dilution (50 ng/µl)		
		Dilution	Amount of DNA (µl)	Amount of Water (µl)
CS-7EL	478.4	9x	20	160
CS-7ES	311.6	6x	30	150
CS	270.4	5x	40	160
1-72	320.7	6x	30	150
1-73	280.9	5x	40	160
1-74	331.5	6x	30	150
1-86	184.7	3x	50	100
'elongatum'	459.7	9x	20	160

(B)

Family	Pot #	Stock Concentration (ng/µl)	First Dilution (50 ng/µl)			Second Dilution (4×) (12 ng/µl)	
			Dilution	Amount of DNA (µl)	Amount of Water (µl)	Amount of DNA (µl)	Amount of Water (µl)
64-8-2	1	1355.6	27×	10	260	50	150
	2	534.7	10×	20	180	50	150
	3	678.7	13×	20	240	50	150
	4	1119.8	22×	10	210	50	150
	5	283.1	5×	40	160	50	150
	6	507.1	10×	20	180	50	150
	7	1147.8	22×	10	210	50	150
	8	929.6	18×	10	170	50	150
	9	870.7	17×	20	320	50	150
	10	283.5	5×	40	160	50	150
	11	688.2	13×	20	240	50	150
	12	968.7	19×	10	180	50	150
	13	675.5	13×	20	240	50	150
	14	911.3	18×	10	170	50	150
	15	730.0	14×	20	260	50	150
	16	906.4	18×	10	170	50	150
	17	689.9	13×	20	240	50	150

(B)-continue

Family	Pot #	Stock Concentration (ng/µl)	First Dilution (50 ng/µl)			Second Dilution (4×) (12 ng/µl)	
			Dilution	Amount of DNA (µl)	Amount of Water (µl)	Amount of DNA (µl)	Amount of Water (µl)
64-8-2	18	817.8	16×	20	300	50	150
	19	1107.5	22×	10	210	50	150
	20	945.5	18×	10	170	50	150
	BC_1F_3 Plant	72.2	1.5×	100	50	50	150
64-8-17	2	538.6	10×	10	260	50	150
	3	997.6	19×	20	180	50	150
	5	518.6	10×	20	240	50	150
	BC_1F_3 Plant	113.6	2×	100	100	50	150
64-8-27*	1	1001.4	20×	10	190	50	150
	2	1079.9	21×	10	200	50	150
	3	709.8	14×	20	260	50	150
	4	694.3	13×	20	240	50	150
	5	972.0	19×	10	180	50	150
	6	835.0	16×	20	300	50	150
	7	932.8	18×	10	170	50	150
	8	648.4	12×	20	220	50	150
	9	863.8	17×	20	320	50	150
	10	546.2	10×	20	180	50	150
	11	655.0	13×	20	240	50	150
	12	202.4	4×	50	150	50	150
	13	571.7	11×	20	200	50	150
	14	515.5	10×	20	180	50	150
	15	1393.8	27×	10	260	50	150
	16	349.9	6×	30	150	50	150
	17	539.8	10×	20	180	50	150
	18	839.6	16×	20	300	50	150
	19	563.1	11×	20	200	50	150
	20	966.8	19×	10	180	50	150
	BC_1F_3 Plant	20.3	---	---	---	100	100

(C)

Sample	Stock Concentration (ng/µl)	First Dilution (50 ng/µl)			Second Dilution (4×) (12 ng/µl)	
		Amount of Dilution (µl)	Amount of DNA (µl)	Amount of Water (µl)	Amount of DNA (µl)	Amount of Water (µl)
CS-7E(7D)-1	291.1	6x	30	150	50	150
CS-7E(7D)-2	238.7	5x	40	160	50	150
CS-7E(7D)-3	248.0	5x	40	160	50	150
CS-7E(7D)-4	436.8	9x	20	160	50	150
CS-7E(7D)-5	138.2	3x	50	100	50	150

I.II Multi reaction PCR template

Table App-I.2: PCR reaction template for screening the Th. elongatum accessions (11 reactions) and BC_1F_4 progeny (51 reactions).

Reaction Mix	1 Reaction (µl)	11 Reactions (µl)	51 Reactions (µl) 48 R. + 3 Extra
H_2O	5.575 or 2.575	65	132
10× PCR Buffer II (Applied Biosystems)	1	11	51
$MgCl_2$ [25 mM]	1	11	51
dNTPs (ThermoScientific) [10 mM]	0.3	3.3	15.3
AmpliTaq gold® DNA Polymerase (Applied Biosystems) [5 U/ µl]	0.125	1.4	6.4
Forward Primer [10 µM]	0.5	5.5	25.5
Reverse Primer [10 µM]	0.5	5.5	25.5
DNA Sample [50 or 12 ng/µl]	1 or 4	---	---
Total	10	---	---

I.III Information about all of the designed primer pairs

Table App-I.3: The amplicon size (bp), PCR annealing temperature (°C) and number of cycles, forward and reverse sequences of all the designed 7EL- and 7DL-specific primer pairs in the first approach, for markers physically associated with selected 7E-specific markers identified in the second objective. The primer pairs used as markers for the screening of BC_1F_4 progeny are indicated in the last column.

	Primer Pairs	Size (bp)	Anneal. TM (°C)	Cycle	Sequence (5'-3')		Selected Markers
					Forward	Reverse	
1	3488-A1-7E	567	60	35	TGCCAACACATCCTCATAGAAC	GCACTTGCCATGATCCACTAA	
2	**3488_A2_7E**	**411**	**60**	**35**	**GCTACCAAATGAGCCCTA**	**CATCTAGCAAGCAGCCAT**	✓
3	3488-A1-7DL	400	60	35	AGATGCTTGTACATGGTTACTTTCT	CCGTACTCTAGGGCAATTTCAA	
4	**3488_A2_7DL**	**355**	**60**	**35**	**GCCAACACATCCTCACATGAT**	**GGTAATTTCTAAATGGGTACATGGC**	✓
5	3488-B1-7E	275	60	35	CCTCGGGTACCTTGGTTATGT	GAGCCTTCTAGATGCTGCATTG	
6	3488-B2-7E	418	60	35	TGTTTGCTCCCTTGCATTCG	GGAAGACGACAAGGAGATGACT	
7	3488-B3-7E	440	60	35	ACATGCGGCTCAACTGTTT	GGGTAAATGGAAGACGACAAGG	
8	3488-B4-7E	278	60	35	TACCTTGGTTATGTCACCATCTATTC	TCAGCAGTCAGAGCCTTCTA	
9	3488-B1-7DL	390	60	35	GACAGAGCGAGAGAGAGAAAGA	TACTGCGTGCGAAATGAAGAG	
10	3488-B2-7DL	293	60	35	TGGATTTCGCTGGAGTTTGG	CTAGCCGCTTAATTTGGGAGATAA	
11	3488-B3-7DL	305	60	35	GGCTCTGTTGGATTTCGCT	CCGCCTAGCCGCTTAATTT	
12	**154_A1-7E**	**288**	**60**	**35**	**TTTGCGTTAGCAGCATCC**	**GAGCGGAGAGATTTCAATTCAT**	✓
13	154-A2-7E	482	60	35	CTCTAGGGAGAACCACCTACAA	TCGCTCCACCAGAGAGTAAA	
14	154-A3-7E	316	60	35	GCAGGAAACACCATTTACATTTCA	CTACCCAGGTTCCACCTAGAG	
15	154-A4-7E	269	60	35	TTGCCCAAGACGGTAAATGTAT	CCCTCCCAGAGGGAAGTT	
16	**154_E1_7DL**	**507**	**60**	**38**	**TCAACGAGCTAGTCCGATAGAG**	**ATCATTCCAGCCTGTCCTTTG**	✓
17	154-E2-7DL	570	60	35	GGGTCGTGTTCATCACATCAT	GGATTGGGCTACCTTGCTAAA	
18	154-E3-7DL	430	60	35	TCATAGTTTGGGTCGTGTTCATC	CGTTGGGTTCGACATTCTTACT	
19	154-C1-7E	274	60	35	GCTTCATCACAGAAATAAATAACATGCC	CTCATGACTCTTCTGGTCCATCTC	
20	154-C2-7E	314	60	35	CTCTCTCTCTCTCTCGTGTTCTT	CTTGGTCGTCATGGCTCAC	
21	154-C1-7DL	317	60	35	TCAGTCGGGTTAGTTCTAATGAAATC	CCAAATGCCCTCTCGACATAC	
22	154-C2-7DL	479	60	35	TGGACCTGCTAAACAATGGG	CCATGGACACGGATTGGG	
23	154-D1-7E	471	60	35	GTGTTCTTCATTGCAGCATGATATT	GAAGTAGAGTGGTTTGTGGGTTT	
24	**154_D2-7E**	**466**	**60**	**35**	**ACCCTGGGTACCTAAGATTCTC**	**GAGGAGTGTATGTGGGAGTTTATTT**	✓
25	154-D3-7E	310	60	35	TGGCATGTGATTGTCCTATGG	GGTCTATGATTCGGATGTGGTATATT	
26	154-D4-7E	572	60	35	AATTTCCCTGTACCCTCCATATTT	CTCGACCTCCAAGCTTCATTT	
27	154-D1-7DL	348	60	35	CCAACCAGGACTAAAGGGTATTG	CTTGAGGACGAGCAGGAATTAAG	
28	154-D2-7DL	402	60	35	CAGACACCAACCAGGACTAAAG	GCTAGGTAGCATTCCACATCAA	
29	**154_D3_7DL**	**339**	**60**	**35**	**ATAACGCGACCGTGACTATTG**	**TGTTGGGATGCCTGAGTATTG**	✓
30	154-D4-7DL	471	60	35	AGAACAAAGTAGCACACACCTC	GCTGATACGTCTCCTCGTATCTAT	
31	154-B1-7E	333	60	35	TCTAACCTCCTCCGGAATTGT	GAGCACACCTGGTCTCTTTATC	
32	154-B2-7E	261	60	35	CAGATGGACGAAAGCGAACA	GATCGGGACATGAACCACAAT	
33	154-B3-7E	449	60	35	CGAAATGGGTTGGCTTGTTAGA	CCCAACATCGCTTTCCATTACA	
34	154-B4-7E	310	60	35	CCGCCTGTCACAGAAAGAAA	GGTTGACCAGTGAGCAATTGTA	
35	2506-A1-7E	310	60	35	ACGATGATCTCCTCCTCAGC	CCTCTCTTACGTCGGGTTACA	
36	2506-A2-7E	265	60	35	GTGCGAAGATTGACGATGAT	GTGTTACGTGGTTCTCCTACTG	
37	2506-A3-7E	495	60	35	CTTCGCCAAGTTTGTTGCTTAC	TGTTTACCCACCGTATGCTATTT	
38	**2506_A4_7E**	**256**	**60**	**35**	**TCCTCAGCACGCTCACC**	**GGAGCTGTTTACGTGGTGTTAC**	✓
39	**2506_A1_7DL**	**452**	**60**	**35**	**TGGTCTGTGCCAGCATTTAG**	**CGTGTGCAGGAGCTGTTTAT**	✓
40	2506-A2-7DL	533	60	35	ACTTACCATGTTTCGGCAGTAG	GCGTTCCCGCGATATCTATTTA	
41	2506-A3-7DL	295	60	35	CCCTTCGTACTCCCTCTGTTT	CTGCATCATCCCTTCCTCTTTG	
42	2506-A4-7DL	600	60	35	TTTCAACTAGTGAAGCGTAACAC	TACCCATGAGGGATTGACAAC	

Table App-I.4: The amplicon size (bp), PCR annealing temperature (°C) and number of cycles, forward and reverse sequences of the designed 7EL- and 7DL-specific primer pairs in the second approach, for markers presumed to be in the neighborhood of previous 7E-specific markers.
The primer pairs highlighted in orange were designed by K. Joustra. The primer pairs used as markers for the screening of BC_1F_4 progeny are indicated in the last column.

	Primer Pairs	Size (bp)	Anneal. TM. (°C)	Cycle	Sequence (5'-3')		Selected Markers
					Forward	Reverse	
1	2485-A1-7DL	382	60	38	AGGAAGGAAGGAGGGAAAGAA	ATGTGGCCGTAACAGTTTCC	
2	2485-A2-7DL	493	60	38	GTACCTGGAAGGAGAGGAAGAG	GAAGCATGAGCACGAGAAGAG	
3	**2485-A3-7DL**	**580**	**60**	**38**	**GGATCGCAACGGGAATGAA**	**TTCCTTCCACACACTCAACAC**	✓
4	2485-A1-7E	255	60	38	CGCCACCGAGCGTAAGTA	GGCGATGGTCTTGTTGAAATCC	
5	2485-A2-7E	489	60	38	CTCCTCCTCTTCCTCTCCTTC	TCCTGCCCAAGCAAACATAA	
6	2485-A3-7E	463	60	38	CCCAACGCACACTCCTATC	GTGTAGGCGATGGTCTTGTT	
7	2485-A4-7E	578	60	38	TCTTTCCCTCCTTCCTTCCT	CCGTGGTCTCTTTCTACCATAAC	
8	2485-C1-7DL	420	60	38	CGGAACATCACCCTCTTAATACC	GTCGACTTCTTCCACGGTTATAC	
9	2485-C2-7DL	536	60	38	GAAGAAGCCAAGGAGGAGAAG	GCGAGGTATTAAGAGGGTGATG	
10	2485-C3-7DL	518	60	38	GAGTTGCTCCACTCAGTTTCTT	TCGGAGGAGAGAGTATCACTTG	
11	2485-C1-7E	505	60	38	TAGCGTCCCTCCCTATTCATT	GAGTTGCTCCACTCAGTTTCTT	
12	2485-C2-7E	355	60	38	GGACGTGAGCTACAAGAACAA	GAGGCTGCTCCCGTATAATAAC	
13	2485-C3-7E	580	60	38	ACGAGATGTTAAGCTGGTGATG	CCCTTCACTTTCAGACGAGAAA	
14	507-A1-7DL	278	60	38	AAAGTGGCCCTCGCAAAT	GGATTCCTTTGCCACCTGAA	
15	**507-A2-7DL**	**448**	**60**	**38**	**GTAGACAATGTACCCGCATCAG**	**TGCCACCTTGCTTATACTAACG**	✓
16	507-A3-7DL	440	60	38	GTGGCAAAGGAATCCACTCTAT	CTGCATTGCCTAGAGCACAA	
17	507-A1-7E	265	60	38	CATCGCCCAGATGCAGAG	AAAGGCAGAGCAAGAGTGAG	
18	507-A2-7E	316	60	38	AAATTCTAGCCCGCACATCG	AGAGCAAGAGTGAGAGCACTA	
19	507-A3-7E	489	60	38	CAGGGACACATGTCTACAACTAAC	GGATGGGTGCGAATCCTATTAC	
20	507-B1-7DL	387	60	38	GCTGTTCTACCCATCTTCTCTTC	AGTCAGGCACCATCCATCTA	
21	507-B2-7DL	501	60	38	CGTGACCGTGTAGTTGGTTAAA	CAAGCAGAGAGGTGGAGAAAC	
22	507-B3-7DL	466	60	38	GAGTAGGCTGTTCTACCCATCT	GTTGCCGGTTACAAGGAGAAA	
23	507-B1-7E	424	60	38	CCGGGACTAAAGGTGCTAAAG	CAGTCGGTCTCGTTGGTTAAAT	
24	507-B2-7E	325	60	38	GTGTTGTCAACCGGGACTAAA	GTGCAGACTTGGAAACTAGGG	
25	507-B3-7E	349	60	38	TCACCCATCCTCTCACTACTC	TTGATACTCCCTCCGTTCCA	
26	3571-A1-7DL	322	60	38	CAGTTGTTAGGCATCAAGCAATAG	ACTGCTGTATTAAGGATGTGTAGG	
27	**3571-A2-7DL**	**355**	**56**	**38**	**TCAACGAGCATTCAGTTGTTAGG**	**ACCACTAGTCTTCGAGGGAAC**	✓
28	3571-A3-7DL	400	60	38	CACACTGAAGTTGCACAGGTA	GAGGGAACACTGCTGTATTAAGG	
29	3571-A1-7E	268	60	38	TGGAATGGCTGTAGGGAGATAG	AAGGATACAATCGCATCATGTAGTT	
30	3571-A2-7E	254	60	38	GCTGTAGGGAGATAGGTAGACA	CAATCGCATCATGTAGTTTCAAATG	
31	**3571-A3-7E**	**278**	**60**	**37**	**TACCTTGCTGAAGATAGCCAGA**	**GCATCATGTAGTTTCAAATGTTAGTCG**	✓
32	959-A1-7DL	267	60	38	TGAGGGTCTCTCGTTTGTTAATG	AAGAGGTTCCGCTGTCTTTG	
33	959-A2-7DL	556	60	38	GGTAGGTTCCTCGGGTTCTT	TCCGCTGTCTTTGCTCTTTG	
34	**959-A3-7DL**	**273**	**60**	**37**	**ATCGATCATATCCCTCCCATGA**	**GTCTTTGCTCTTTGCCATGAATAC**	✓
35	959-A1-7E	517	60	38	CGGAAGCAACTCTAACCACATAA	GAGATATGAGCTGTCCACCAAAG	
36	**959-A2-7E**	**464**	**56**	**38**	**ATATATCACGCGGAAGCAACTC**	**GCAGGGAGCAAATGGATCTT**	✓
37	959-A3-7E	413	60	38	CCGCAAATAAAGTGTGCATCAA	AAAGCGCAGGGAGCAAAT	
38	1952-A1-7DL	295	60	38	TTGCTAGTTATAGATGGGCTTT	TAACCGTCGCTTGGCTT	
39	1952-A2-7DL	440	60	38	GGAACCCAGTATCCAACCGA	ATATCGGAGATGGCACGTCA	
40	1952-A3-7DL	444	60	38	TGATGGGCCGAAAGTGAAC	CCCTCCTCCCGTAGATAGATTG	
41	1952-A4-7DL	479	60	38	AACCCAGTGGAACCCAGTAT	TGACGCCATGATTGGGATTTAG	
42	1952-A5-7DL	477	60	38	CGAAAGTGAACCCAGTGGAA	ATTGGGATTTAGGAGAGGAGGA	
43	1952-A6-7DL	491	60	38	ATTGGCCTCCCGTCTTCT	ACATGGATAGGCTTCGGAGT	
44	**1952-A1-7E**	**363**	**60**	**35**	**GCGCCTCTTGCTAGTAGTTTAT**	**GTGTTCGGGCTGTAAGTGTAG**	✓
45	1952-A2-7E	389	60	38	ATGGGCTTCGATGCTTAACG	GTAAAGGAGACAGGGCAAAGG	

	Primer Pairs	Size (bp)	Anneal. TM. (°C)	Cycle	Sequence (5'-3')		Selected Markers
					Forward	Reverse	
46	1952-A3-7E	296	60	38	TGGAGAAGGAGCAGAAGGATAA	TGACGCCACGAGGAAGA	
47	2500-A1-7DL	269	60	38	CTAGTTCCTTAGCCTGGCAAATA	GGATACTCCTTCCGTCCGA	
48	2500-A2-7DL	264	60	38	ATTGATCTGTTTGCTGCTAGT	AAACTTGTCCCAAGCTTAGAT	
49	**2500-A3-7DL**	**386**	**60**	**38**	**AGGGCAGATAACCTGCAAAG**	**AGATACATCCATTTGAGGGACAAG**	✓
50	**2500-A1-7E**	**393**	**60**	**38**	**AAGGCTGTGCTACCAATTGAA**	**AGTCCTGAGTAACTGCGAAGA**	✓
51	2500-A2-7E	321	60	38	CCGCAATGGTGACAGATGTAT	CGACCCGAATTAGTTGCCTTAG	
52	2500-A3-7E	291	60	38	GGGTCGGAGGGAGTATAATCTT	AGCGCTTCTTCCTCTCCTT	
53	1383-A1-7DL	389	60	38	GGCAGAAGTTCACCTAGCTATC	GGCCTCATGGATTCGTCATT	
54	**1383-A2-7DL**	**369**	**56**	**38**	**CTCCATCTAAACCATCCACATACA**	**CGATTGTCTCCGTCGGATTT**	✓
55	1383-A1-7E	314	60	38	TTCGTGATTTCGCGGTATGG	GTGGAAACACAGGCGTAATTTG	
56	1383-A2-7E	336	60	38	TTTCGCGGTATGGTTTGGTG	CTAAACCGTCCACACACATCAC	
57	**1383-A3-7E**	**356**	**56**	**38**	**TATGGTTTGGTGTGCTGTGG**	**AGGTACCGTGTAAACCTGATCT**	✓
58	2368-A1-7DL	284	60	38	GATTCCCTTCACCACACCATAC	GCCATGGGATTGCTCCTATT	
59	2368-A2-7DL	392	60	38	CTTGACACAGAGAGCGTCATATAG	AGGCAAAGGATTTCCAGACTC	
60	**2368-A3-7DL**	**343**	**56**	**38**	**CCCATCTCATTGTTCTAAGAAATAGC**	**GATTTCCAGACTCTGTGCCA**	✓
61	2368-A1-7E	351	60	38	GCATTCATTCAGGCGACGA	TTGGCAGCGGTGAGGAG	
62	**2368-A2-7E**	**256**	**60**	**38**	**CGCCCTCGAACCCATCT**	**CTGAATGAATGCCTGCGTCA**	✓
63	2368-A3-7E	351	60	38	TGACGCAGGCATTCATTCAG	GGTGAGGAGGCCATAGAGAAA	
64	**455-A1-7E**	**332**	**60**	**38**	**CAAACAATCCTCTGTTCGCTCTA**	**ACTGAACCTTGTTGTCCAATGA**	✓
65	455-A2-7E	458	60	38	GCTCGCAAACAATCCTCTGT	GGCTTGGAGGTGTAGGATGTA	
66	**577-A1-7E**	**261**	**60**	**38**	**CCATCTTACCAGTTGCCTACAC**	**ATCCATTGTAACGGGCAAGATAA**	✓
67	577-A2-7E	452	60	38	GTATGGAGGACCGCTCATTTG	GTGTAGGCAACTGGTAAGATGG	
68	577-A3-7E	366	60	38	CTCAAGCACTGAAGCAACAAC	CACTGTAGTACTCTTGCGAACAT	
69	1480-A1-7E	275	60	38	TTAGCCTTGTGGGAGCAATAC	CTCTCTCGATTATGCCTGGATTT	
70	1480-A2-7E	481	60	38	ATCCAGGCATAATCGAGAGAGA	GTAAACTAGCAGTAGTCTGATGGC	
71	1480-A3-7E	429	60	38	GGCATAATCGAGAGAGAACAATCT	ACCGGAATTGCGTGGTG	
72	**1480-B1-7E**	**315**	**56**	**38**	**TGGACGGAGGTAGTATGAAACA**	**TGGTTGAATCGGACTGCATTTA**	✓
73	1480-B2-7E	540	60	38	ACAACCAAGGATACATCGTCTTC	TAAGTGAGCCCTGAATTGTGTC	
74	1480-B3-7E	461	60	38	AGTCAGTGTTTGTTCATCCATAGG	TGTCTGCAGCTCCTGAGTTA	
75	1384-A1-7E	561	60	38	ACGGTGGAGAAGTACTGAATCT	TGTCAACAGCCAAGCTAACG	
76	1384-A2-7E	421	60	38	CATGGACCATTCTGCATCGAATA	CTCACCTGTCATAACCTGTCAAC	
77	1384-A3-7E	409	60	38	AGCCGTCCCATGTAGAGAA	AGCAGTTGGCAAGCAGTAG	
78	1384-B1-7E	407	60	38	GCGAACACCTTCCCATCAA	TCCCTCAGCTTCTTCCTCTC	
79	1384-B2-7E	443	60	38	GGGAGGAGGAGAGGAAGAAG	AGCAGCAGACATGACATCAAA	
80	1384-B3-7E	306	60	38	TGCAAACTTCGGTTCAAATTCA	CTGCTCATACGGCGGAAA	
81	542-A1-7DL	378	60	38	CTTGCGGCATTCTAGGAGTT	ATGATGATGGAGGTGAGGGA	
82	**542-A2-7DL**	**538**	**60**	**38**	**GAGAAGATAAGGCGGACTTTCG**	**TTGCAACCACACTGACATTCTA**	✓
83	542-A1-7E	390	60	38	TTCACGTCGAACCCTGAGA	TGCTTCTGCCACTGCTAATG	
84	542-A2-7E	394	60	38	GCTTCTGCTGCTTCACGTC	GCCACTGCTAATGAATGCTAGG	
85	542-A3-7E	309	60	38	CGACGACTACGGGTACTACT	GGACTTGAGAGTTGAGACCTAATG	
86	542-B1-7DL	574	60	38	CTGCATGGGTTATCCAGAAGAA	AGAGTTGGAACTGATTGGACATAG	
87	542-B2-7DL	286	60	38	TCCAGCACTTGTTCTGTTCTAC	GCTTTCAGAGTTGGAACTGATTG	
88	542-B3-7DL	320	60	38	GCAGTTGTATTTCGCGGATCA	CGCTGCTTTCAGAGTTGGAA	
89	542-B1-7E	306	60	38	CGATTTCCTTCCTCACCATACG	AGCTGCAACCAACGATGAA	
90	542-B2-7E	535	60	38	CGTACGCAGCCCTTCTTTATC	ACCGTTCTGATGGAAGAGACTA	
91	542-B3-7E	551	60	38	CCGTCGGATCTCATTCTCATTT	CTGATGGAAGAGACTAGGCAATAC	
92	3201-A1-7E	512	60	38	GGCCTGGAATATCTTTGGACTC	CAGATGCGCGACCCATTTA	
93	**3201-A2-7E**	**256**	**60**	**38**	**CGAGCAGGCCTGGAATATC**	**ACGCGATGCGCTAGAAAG**	✓
94	3201-A3-7E	575	60	38	CCACCCAGCGAACGAATTAT	GGCAGAAATCACCCAGAAGAA	

	Primer Pairs	Size (bp)	Anneal. TM. (°C)	Cycle	Sequence (5'-3')		Selected Markers
					Forward	Reverse	
95	4231-A1-7E	253	60	38	AGACGTACTACTAAGCACTAACTAAC	TTGCTGAGGACTTGCTTATCTC	
96	**4231-A2-7E**	**371**	**56**	**38**	**AAGCACTAACTAACACACTGAGAG**	**AGCGGCCACCTTGTTTAC**	✓
97	4231-A3-7E	542	60	38	CCTTGCCAAAGCTCGATGT	ACAGGGATCTTCATTGGTCTTATTT	
98	6092-A1-7DL	576	60	38	ATGTTGTTGGTGGGCATTCT	TATTCCCTCCGTCCCAAAGT	
99	**6092-A2-7DL**	**584**	**60**	**38**	**TTTCATGGGTGATGGCTGAC**	**CCCAAAGTGACTGTCTCAACTT**	✓
100	6092-A3-7DL	421	60	38	TTTCTGATCGAGGCAGTGAATC	TTTGGGACGGAGGGAGTAT	
101	**2096-A1-7DL**	**315**	**56**	**38**	**ACTAGAGCACACAGCAAATCAA**	**GGTATGTTCTACGAGACTTTGACAG**	✓
102	2096-A2-7DL	393	60	38	GCAGTGGTATGTTCTACGAGAC	CATCTGCCTCATTTCTTTGAACC	
103	2096-A3-7DL	315	60	38	CACACAGCAAATCAATCGTCTG	CTACGAGACTTTGACAGTACAACA	
104	2096-A1-7E	562	60	38	GGGCAAAGGAATAATGGGAGAA	AAATCGTCCCTCAACTCCAATC	
105	2096-A2-7E	438	60	38	CATGAATGGGCCTGCAGATAG	GTTTGGACATTCCAGGAGCTC	
106	**2096-A3-7E**	**505**	**56**	**38**	**TAAGGGCTCCTCTGGTTCAA**	**TCTTGCTTGGTATGTTTCCTCG**	✓
107	**1262_A1_7DL**	**401**	**56**	**38**	**GGCGCTCACACAATAGGATAG**	**TTCTTCGTTGGATCGACCTTG**	✓
108	1262_A2_7DL	494	60	38	CGTGGTCCTTACTCACTCCTAT	GGTTCTCTTCTTCGTTGGATCG	
109	1262_A3_7DL	348	60	38	AGGATAGGAATCTAGGGAGCTTATC	TGAAGAAATCCGCACACCG	
110	1262_A1_7E	277	60	38	CATCTACAGGCTCAACGAAGG	CTATATGTCGCGCGTACTGATT	
111	1262_A2_7E	367	60	38	TTTGCTCACCAGCGCTATATG	TTGATGGGACTGTCAGCTTTG	
112	**1262_A3_7E**	**284**	**56**	**38**	**GATATGCTCTCGGCATATGGTTT**	**AAATCTCGTACTTTGCTCGCTAG**	✓
113	**153_A1_7DL**	**279**	**55**	**38**	**GGGCGGGTATCATCTCTAATTTC**	**CTAATCATTGCTGCCAGTTGTTG**	✓
114	153_A2_7DL	578	60	38	GTCGGCTTTGTTGTCTGAGT	TACTGCATCCAATTCCTGCTG	
115	153_A3_7DL	501	60	38	AAACACGGGTGGACACAAA	CTCTGCAGTCAACTATGCATCA	
116	153_A1_7E	309	60	38	TTGAGGTGTCCGCTTTGATG	CATACACCCTACCAAACACACC	
117	153_A2_7E	482	60	38	AGACCTCTCGAACCATGTATGTA	TTGAGGTGTCCGCTTTGATG	
118	**153_A3_7E**	**268**	**56**	**38**	**CGACATTGCCTTGGTACTACTT**	**CTGTTAGTTGGATCACCTGTCC**	✓

I.IV Guidelines used for homoeology check between *Th. elongatum* 7EL scaffolds and wheat contigs and primer design

a. Wheat contigs generally had smaller sequence lengths than 7EL scaffolds; therefore, in most cases the good homolog wheat contigs were fully covered by 7EL scaffolds. For example, as shown in Figure App-I.1, the 7DL contig was 16,399 bp in length which was completely included the region of homology with the 7EL scaffold that was 42,577 bp in length. However, in some cases where homology occurred at the beginning or end of wheat contigs or 7EL scaffolds, the whole wheat contigs were not covered by 7EL scaffolds. In these situations, markers were designed only in the areas of homology.

b. The identity percentages between wheat contigs and 7EL scaffolds were selected to be around 85 to 95% (Gou et al., 2016). Lower identity percentages suggested that the two sequences might not be homoeologous while higher amounts leading to the existence of highly conserved genes which made the designing procedure challenging. Most of the homolog fragments in Figure App-I.1 have identity percentage higher than 85% and lower than 95%.

c. Locations on 7EL scaffolds or wheat contigs with repeated sequences were not appropriate for designing new 7EL- or 7DL-specific primer pairs.

d. The existence of neighboring genes that were members of the same family and on the 7EL scaffold but not covered in the sequence of the wheat homolog contig made the homology check procedure more complex. In Figure App-I.1, fragments G, I, T, K, P, M, V and E represent an inverted neighboring gene (highlighted in red to demonstrate reverse sequence) while fragments F, H, S, J, O, L, U and D is likely another gene member of the same family. Both genes are seen separately in the 7EL scaffold while duplicate pieces can be seen in the 7DL contig.

e. More often, bigger gaps can be seen between adjacent homolog pieces in 7EL scaffolds comparing to the wheat contigs. These gaps represent introns or intergenic areas which have different sizes between different species' genome. These gaps are suitable regions to design markers specific to 7EL or 7DL unless they contain repeated sequences.

f. Sometimes, the absence of homology in one region was due to the lack of available sequence in one or both databases. Therefore, the regions with no homology needed to be checked on both 7EL scaffolds and 7DL contigs to confirm the presence of sequence. In Figure App-I.1, the big gap (8740 bp) between the "C" and "R" fragments in the 7EL scaffold was due to the absence of that region in the database.

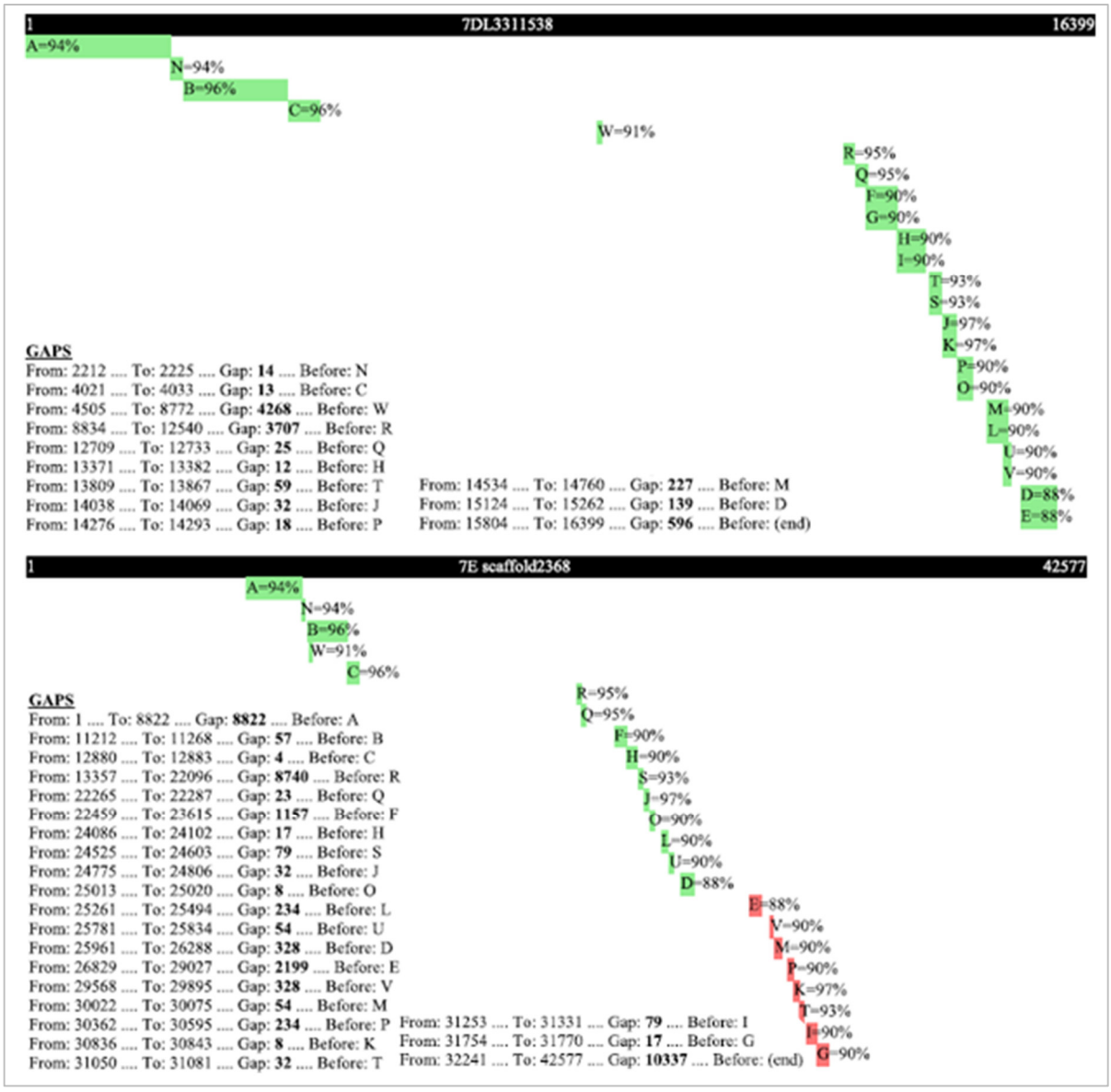

Figure App-I.1: An example of homology check (7DL3311538/7EL Scaffold 2368) as visualized by the homology check software.
Upper panel, position of 7EL homoeologous fragments onto 7DL3311538; lower panel, position of 7DL homoeologous fragments onto 7EL scaffold 2368. The green and red (inverted) bars indicate the size of homoeologous fragments.

I.V Rating of FHB progression in *Th. elongatum* accessions

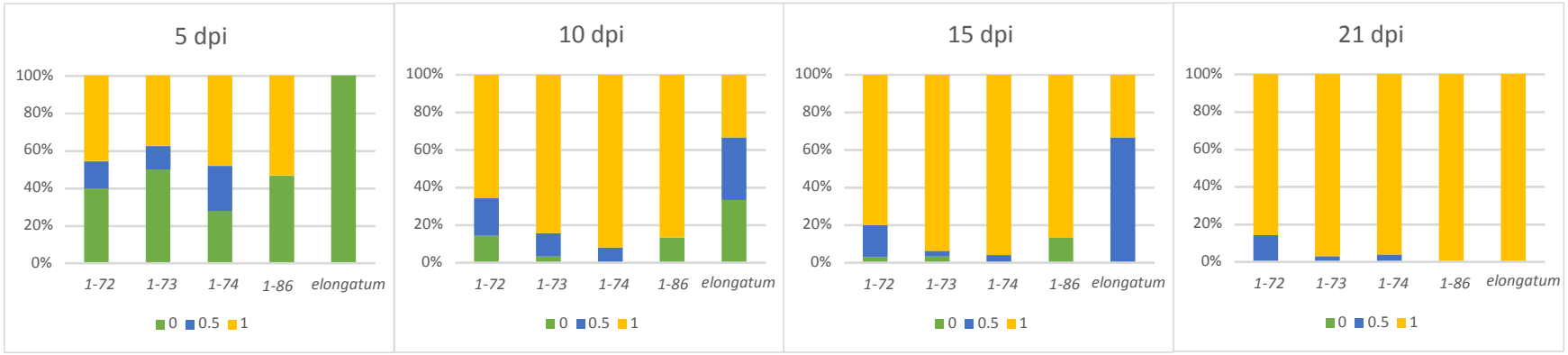

Figure App-I.2: Percentage of FHB infection in non-inoculated florets located within inoculated spikelets, at 5, 10, 15 and 21 DPI. The healthy, partially infected and fully infected florets were rated as 0 (green), 0.5 (blue) and 1 (yellow) respectively.

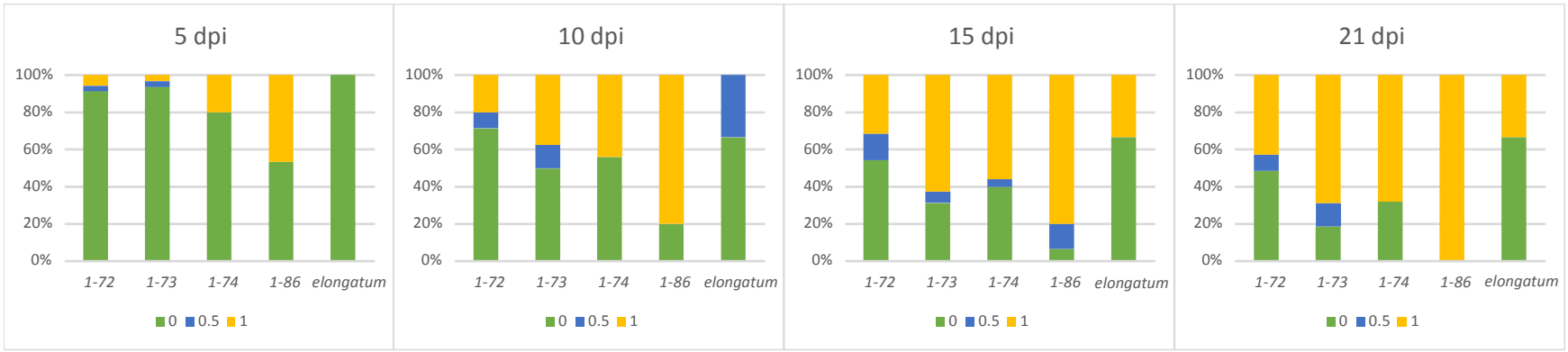

Figure App-I.3: Percentage of bleached inoculated spikelets, at 5, 10, 15 and 21 DPI. The healthy, partially bleached and fully bleached inoculated spikelets were rated as 0 (green), 0.5 (blue) and 1 (yellow) respectively.

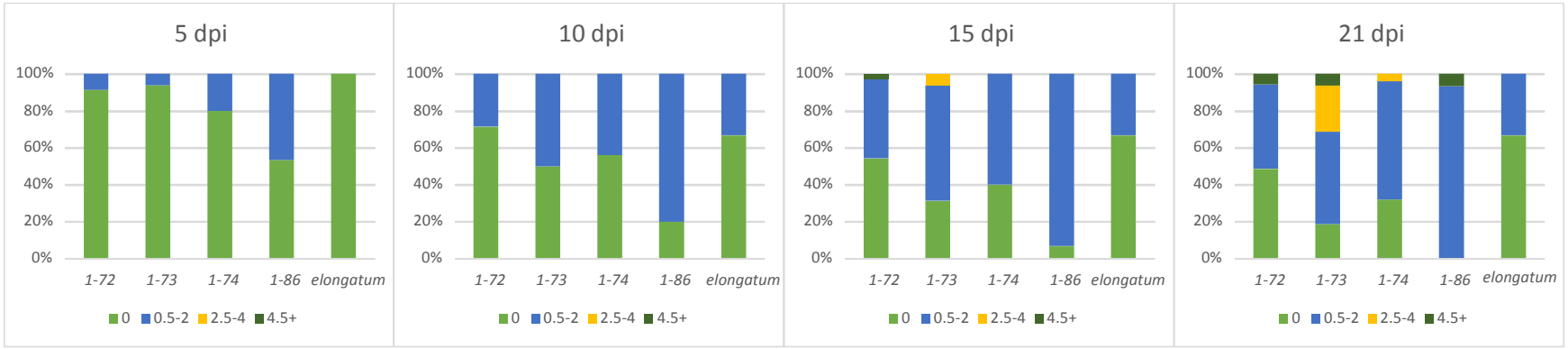

Figure App-I.4: Percentage of spikes in each interval category of bleached spikelets, at 5, 10, 15 and 21 DPI.
Green represents all spikelets were healthy; blue, yellow and dark green represent 0.5-2, 2.5-4 and 4.5+ bleached spikelet(s) respectively per spike.

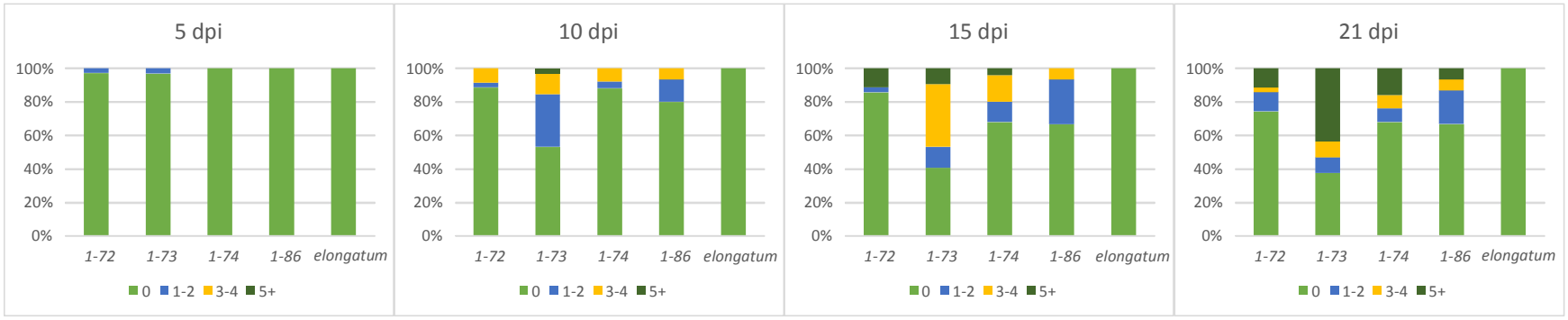

Figure App-I.5: Percentage of spikes in each interval category of infected internodes, at 5, 10, 15 and 21 DPI.
Green represents all internodes were healthy; blue, yellow and dark green represent 1-2, 3-4 and 5+ bleached internode(s) respectively per spike.

I.VI Detailed results collected from "wheat/7EL cross-walking" strategy for designing new markers presumed to be in the neighborhood of selected 7EL-sepecific markers

Table App-I.5: Results that were collected from step one to three of the "wheat/7EL cross-walking" strategy (see Figure 2.9) to design new markers presumed to be in the neighborhood of selected 7E-specific markers (presented in the first column).
The associated 7EL scaffolds and homoeologous 7ABD wheat contigs are presented in the second and third columns. The corresponding SNPs and their associated mapping data for three crosses from Axiom, iSelect and KASP arrays (arrays), as well as a genetic consensus map from the iSelect dataset (S. Wang et al., 2014) are provided. Results from the last 7E-specific markers highlighted in orange were obtained by K. Joustra.

7E-Specifc Markers	7EL Scaffolds	Wheat contigs	SNPs	Assays	AxC		SxR		SxO		Consensus Dataset	
					Chrom.	cM	Chrom.	cM	Chrom.	cM	Chrom.	cM
Lu-287-2	-	7AL3384095	AX-94772883	Axiom	7A	195.0413			7A	827.0829		
			AX-94742461	Axiom	7A	195.0413						
			BS00021261_51	iSelect	7A	327.5					7A	438.54
		7BL6739531	AX-94772883	Axiom	7A	195.0413			7A	827.0829		
			BS00021261_51	iSelect	7A	327.5						
		7DL3315998	-	-	-	-	-	-	-	-	-	-
Lu-387-2	-	-	-	-	-	-	-	-	-	-	-	-
Lu-9736	3488	7AL4556192	AX-94404953	Axiom	7B	256.0821						
			AX-95156591	Axiom	7B	196.708						
			AX-94571964	Axiom	7B	195.9205						
			AX-94463366	Axiom	7B	32.45992	7D	28.57484				
			AX-95206919	Axiom			7D	28.57484				
			Excalibur_rep_c105595_185	iSelect	7A	430.5					7B	547.82
			RAC875_c50676_588	iSelect	7A	430.5					7A	676.55
			Kukri_rep_c69223_241	iSelect	7A	430.5						
			BS00079734_51	iSelect	7D	238.7					7D	460.9
			RAC875_c28750_700	iSelect	7D	232.8	7D	127			7A	676.55
			BS00079734	KASP	7D	117.5	7D	121.0714				
		7BL6641439	AX-94404953	Axiom	7B	256.0821						
			AX-95633065	Axiom	7B	32.45992	7D	28.57484				
			AX-95206919	Axiom			7D	28.57484				
			AX-95024837	Axiom			7D	28.57484	7D	46.71397		
			Excalibur_rep_c105595_185	iSelect	7A	430.5						
			Kukri_rep_c105287_311	iSelect	7D	239.2	7D	127.8			7D	460.9
			BS00021745_51	iSelect	7D	235	7D	127			7D	460.9

7E-Specifc Markers	7EL Scaffolds	Wheat contigs	SNPs	Assays	AxC		SxR		SxO		Consensus Dataset	
					Chrom.	cM	Chrom.	cM	Chrom.	cM	Chrom.	cM
Lu-9736 (cont.)	3488 (cont.)	7DL3371482	AX-94404953	Axiom	7B	256.0821						
			AX-94463366	Axiom	7B	32.45992	7D	28.57484				
			AX-95633065	Axiom	7B	32.45992	7D	28.57484				
			AX-94868225	Axiom					7D	96.17025		
			AX-94770820	Axiom			7D	28.57484				
			AX-95206919	Axiom			7D	28.57484				
			Excalibur_rep_c105595_185	iSelect	7A	430.5						
			RAC875_c50676_588	iSelect	7A	430.5						
			Kukri_rep_c69223_241	iSelect	7A	430.5						
			Kukri_rep_c105287_311	iSelect	7D	239.2	7D	127.8				
			BS00079734_51	iSelect	7D	238.7						
			BS00021745_51	iSelect	7D	235	7D	127				
			RAC875_c28750_700	iSelect	7D	232.8	7D	127				
			BS00079734	KASP	7D	117.5	7D	121.0714				
			BS00021745	KASP	7D	117	7D	121.0714				
Lu-1700	1514	7AL4508970	AX-94994343	Axiom	7B	509.7436						
			AX-94514616	Axiom			7A	312.0154	7A	833.957		
			BS00026622_51	iSelect			7A	220.6			7A	448.64
		7DL3341707	BS00028760_51	iSelect			7D	52				
2506-A4-7E	2506	-	-	-	-	-	-	-	-	-	-	-
Lu-138-1	36	-	-	-	-	-	-	-	-	-	-	-
Lu-387-22	1378	7AL4487156	-	-	-	-	-	-	-	-	-	-
		7AL4554227	IAAV6597								7A	398.8
			Ra_c104959_422								7A	398.8
			wsnp_Ex_c3891_46383475								7A	376.5
		7BL6545191	wsnp_Ex_c33461_41945399								7B	244.3
		7BL6691546	Tdurum_contig54532_206								7B	232.9
Lu-632-2	154	-	-	-	-	-	-	-	-	-	-	-
Lu-1851-2	649	7BL6683213	tplb0035h03_1251								7B	463.6
Lu-5846-1	-	-	-	-	-	-	-	-	-	-	-	-

7E-Specifc Markers	7EL Scaffolds	Wheat contigs	SNPs	Assays	AxC		SxR		SxO		Consensus Dataset	
					Chrom.	cM	Chrom.	cM	Chrom.	cM	Chrom.	cM
Lu-129-21	2321	7AL4525970	BobWhite_c7082_184								7A	398.8
			BobWhite_c7082_196								7B	250.7
			BobWhite_c7082_577								7B	250.7
			Excalibur_c63900_370								7A	398.8
			Excalibur_c63900_433								7A	398.8
			Kukri_c23208_256								7D	285.1
			Kukri_rep_c114803_98								7A	398.8
			RAC875_c7104_929								7B	250.8
			wsnp_Ku_rep_c113718_96236830								7A	398.8
			wsnp_RFL_Contig4018_4483983								7B	251.1
		7BL6567348	Kukri_c10108_115								7B	251.1
			RAC875_c7104_160								7B	251.1
		7BL6658699	BS00105558_51								7B	250.7
			Kukri_c1957_581								7B	251.1
			Kukri_c1957_920								7B	250.8
			Kukri_rep_c109805_195								7B	251.1
			RAC875_rep_c72524_90								7B	250.7
			Tdurum_contig76289_1530								7B	250.7
		7DL3318817	GENE-4924_117								7B	250.7
Lu-3836-1	2361	7AL4484752	Excalibur_c113078_320								7A	521.5
			Kukri_c15912_812								7B	357.1
			Kukri_c15912_860								7B	360
			Kukri_c15912_1189								7B	360
			Kukri_c15912_2330								7B	360
			Ra_c114158_328								7A	435.9
			RAC875_rep_c105769_150								7A	435.9
			wsnp_Ku_c44760_51961180								7A	435.9
		7BL6688094	Excalibur_c113078_320								7A	521.5
			Kukri_c15912_812								7B	357.1
			Kukri_c15912_860								7B	360
			Kukri_c15912_1189								7B	360
			Kukri_c15912_2019								7D	386.7
			Kukri_c15912_2330								7B	360
		7DL3341152	Kukri_c15912_812								7B	357.1
			Kukri_c15912_860								7B	360
			Kukri_c15912_1189								7B	360
			Kukri_c15912_2330								7B	360

Table App-I.6: Results that were collected from step four to six of the "wheat/7ELcross-walking" strategy (see Figure 2.9) to design new markers presumed to be in the neighborhood of selected 7E-specific markers.

Results are regrouped by datasets and their corresponded chromosomes. The wheat contigs associated with the interested 7E-specific markers are considered as original wheat contigs which are presented along their location (cM) in the second column; the neighboring wheat contigs associated with SNPs located in close, intermediate and far distance to the original wheat contigs and their location (cM) are presented in the third column. Both original and neighboring wheat contigs (e.g. 7DL3371482), were always associated with locations (in cM) on the same chromosome (e.g. 7D). The distance category and the "R" number of the associated regions (see Figure 3.15) are presented in the fourth and fifth columns. The 7EL scaffolds homoeologous to the selected neighboring wheat contigs are presented in the last column. Results highlighted in red were obtained by K. Joustra.

Dataset	Original Wheat Contig		Neighboring Wheat contig		Distance	Region	7EL Scaffold | Size
	Name	Location (cM)	Name	Location (cM)			
Axiom SxR	7DL3371482	28.574	7DL3373545	26.987	Close	R10	scaffold4317|size14799
			7DL3391547	26.987	Close	R10	scaffold2485|size40217
			7DL3364819	26.987	Close	R10	scaffold1002|size88947
			7DL3393572	26.987	Close	R10	scaffold404|size140736
			7DL3352272	36.925	Close	R11	scaffold3571|size22569
			7DL3371415	66.038	Far	R11	scaffold774|size101967
			7DL3144868	66.038	Far	R11	scaffold550|size122091
			7DL3328436	66.038	Far	R11	scaffold513|size125801
Axiom (SxO)	7DL3371482	96.17	7DL3321156	85.831	Close	R8	scaffold4918|size10713
			7DL3395966	99.561	Close	R9	scaffold374|size146005
			7DL3315688	101.256	Close	R9	scaffold959|size91212
			7DL3315689	101.256	Close	R9	scaffold959|size91212
			7DL3311341	421.745	Far	R9	scaffold1952|size52695
iSelect (AxC)	7DL3371482	235 - 239.2	7DL3311257	236.8	Close	R20	scaffold2500|size39858
			7DL3387390	234.4	Close	R19	scaffold483|size130024
			7DL3364819	234.4	Close	R19	scaffold1002|size88947
			7DL3351773	233.8	Close	R19	scaffold765|size102405
			7DL3391547	233.8	Close	R19	scaffold2485|size40217
			7DL3368084	215	Intermediate	R18	scaffold5359|size8721
			7DL3320370	215	Far	R18	scaffold1173|size81484
			7DL3391793	113.6	Far	R18	scaffold352|size150052
iSelect (SxR)	7DL3341707	52	7DL3394658	65.8	Close	R21	scaffold1636|size62502
			7DL3341845	65.8	Close	R21	scaffold1383|size72006
	7DL3371482	127-127.8	7DL3341845	65.8	Far	R21	scaffold1383|size72006
			7DL3394658	65.8	Far	R21	scaffold1636|size62502
			7DL3391547	128.6	Close	R22	scaffold2485|size40217
			7DL3393572	128.6	Close	R22	scaffold404|size140736
			7DL3320370	101.8	Intermediate	R21	scaffold1173|size81484
KASP (AxC)	7DL3371482	117-117.5	7DL3311538	28.8	Far	R12	scaffold2368|size42577
			7DL3393572	115.8	Close	R12	scaffold404|size140736
			7DL3320370	96.7	Intermediate	R12	scaffold1173|size81484

Dataset	Original Wheat Contig		Neighboring Wheat contig		Distance	Region	7EL Scaffold | Size
	Name	Location (cM)	Name	Location (cM)			
Axiom (AxC)	7AL3384095	195.0413	7AL4525975	185.604	Close	R1	scaffold4075|size17082
			7AL4557355	185.604	Close	R1	scaffold3881|size18972
			7AL4519433	182.502	Close	R1	scaffold15|size362707
			7AL4373650	182.502	Close	R1	scaffold4741|size11770
			7AL4554941	181.72	Close	R1	scaffold859|size97517
			7AL4489307	181.72	Close	R1	scaffold342|size152732
			7AL2582636	181.72	Close	R1	scaffold3398|size24754
			7AL4447054	174.593	Intermediate	R1	scaffold532|size123933
			7AL4521239	174.593	Intermediate	R1	scaffold2486|size40199
			7AL4556902	172.267	Intermediate	R1	scaffold97|size235690
			7AL4556249	202.137	Close	R2	scaffold10565|size1569
			7AL4536361	202.137	Close	R2	scaffold10565|size1569
			7AL4556250	202.137	Close	R2	scaffold10565|size1569
			7AL4518778	206.024	Close	R2	scaffold474|size131323
			7AL4442603	211.559	Close	R2	scaffold1384|size71993
			7AL4368641	217.855	Intermediate	R2	scaffold4802|size11365
			7AL4534468	220.23	Intermediate	R2	scaffold1994|size51455
			7AL4534469	220.23	Intermediate	R2	scaffold1994|size51455
			7AL4534470	220.23	Intermediate	R2	scaffold1994|size51455
			7AL4492188	227.333	Intermediate	R2	scaffold1601|size63863
			7AL4556232	244.474	Far	R2	scaffold2495|size40000
			7AL4555277	245.268	Far	R2	scaffold3241|size27227
			7AL4438737	245.268	Far	R2	scaffold278|size167393
Axiom (SxR)	7AL4508970	312.015	7AL4520899	307.081	Close	R3	scaffold3770|size20213
			7AL4485213	291.242	Intermediate	R3	scaffold6004|size6474
			7AL4492658	341.26	Far	R4	scaffold836|size99113
			7AL4515454	341.26	Far	R4	scaffold5162|size9573
			7AL2477818	342.848	Far	R4	scaffold153|size205433
Axiom (SxO)	7AL4508970	833.957	7AL4520899	830.5032	Close	R6	scaffold3770|size20213
			7AL4485213	738.2628	Far	R5	scaffold6004|size6474
			7AL4492658	915.252	Far	R7	scaffold836|size99113
			7AL4515454	915.252	Far	R7	scaffold5162|size9573
	7AL3384095	827.0829	7AL4520899	830.5032	Close	R6	scaffold3770|size20213
			7AL4485213	738.2628	Far	R5	scaffold6004|size6474
			7AL4492658	915.252	Far	R7	scaffold836|size99113
			7AL4515454	915.252	Far	R7	scaffold5162|size9573
iSelect (AxC)	7AL4556192	430.5	7AL4385456	423.9	Close	R14	scaffold2500|size39858
			7AL4559670	420.7	Close	R14	scaffold478|size130816
			7AL4441057	420.7	Close	R14	scaffold478|size130816
			7AL4488310	419	Close	R14	scaffold4224|size15659
			7AL4556556	415.4	Close	R14	scaffold476|size131124
			7AL4554209	414.3	Close	R14	scaffold3201|size27826
			7AL4552780	412.3	Close	R14	scaffold4602|size12648
			7AL4550273	433.4	Close	R15	scaffold4231|size15589
			7AL4557311	433.4	Close	R15	scaffold621|size183678

Dataset	Original Wheat Contig		Neighboring Wheat contig		Distance	Region	7EL Scaffold | Size
	Name	Location (cM)	Name	Location (cM)			
iSelect (AxC) - Cont.	7AL4556192 (cont.)	430.5	7AL4476425	433.4	Close	R15	scaffold3905|size18767
			7AL4494080	457	Intermediate	R15	scaffold993|size89424
			7AL4494678	391.5	Intermediate	R14	scaffold704|size107582
			7AL4482836	387	Intermediate	R14	scaffold2670|size36608
			7AL4388478	383.6	Intermediate	R14	scaffold292|size164239
			7AL4437302	367.4	Far	R14	scaffold1134|size82980
			7AL4484752	367.4	Far	R14	scaffold2361|size42702
			7AL4464798	367.4	Far	R14	scaffold455|size133170
			7AL4372558	350.6	Far	R14	scaffold2383|size42281
			7AL4493872	344.9	Far	R14	scaffold2402|size41931
			7AL4474554	344.9	Far	R14	scaffold2278|size44358
			7AL4368641	344.9	Far	R14	scaffold4802|size11365
			7AL4443698	343.4	Far	R14	scaffold374|size146005
			7AL4491854	340.3	Far	R14	scaffold1130|size83105
			7AL4552312	338.3	Far	R14	scaffold2174|size46818
	7AL3384095	327.5	7AL4554615	323.2	Close	R13	scaffold397|size141600
			7AL1206673	323.2	Close	R13	scaffold542|size123240
			7AL4525975	323.2	Close	R13	scaffold4075|size17082
			7AL4555891	318.2	Intermediate	R13	scaffold822|size99486
			7AL4464758	317	Intermediate	R13	scaffold1392|size71567
			7AL4490444	314.4	Far	R13	scaffold1802|size57324
			7AL4548608	314.4	Far	R13	scaffold375|size145583
			7AL4553769	314.4	Far	R13	scaffold1777|size58231
			7AL4489307	314.4	Far	R13	scaffold342|size152732
			7AL4443427	314.4	Far	R13	scaffold1030|size87792
			7AL4440341	312.3	Far	R13	scaffold3040|size82684
			7AL4486335	312.3	Far	R13	scaffold1901|size54252
			7AL4466148	312.3	Far	R13	scaffold1320|size75355
			7AL4557010	312.3	Far	R13	scaffold882|size95988
iSelect (SxR)	7AL4508970	220.6	7AL4520899	217.3	Close	R16	scaffold3770|size20213
			7AL4372558	226.2	Close	R17	scaffold2383|size42281
			7AL4464798	237.8	Intermediate	R17	scaffold455|size133170
			7AL4490444	199.1	Intermediate	R16	scaffold1802|size57324
			7AL4548608	178.9	Far	R16	scaffold375|size145583
			7AL2477818	254.4	Far	R17	scaffold153|size205433
Consensus	7AL4554227	376.5	7AL603955	332.69	Don't Follow	R23	-
		376.5	7AL4493872	363.86	Don't Follow	R23	-
	7AL4525970	398.8	7AL4373898	392.1	Close	R24	scaffold2096
	7BL6691546	232.9 - 251.1	-	-	-	R25	-
	7BL6688094	357.1 - 360	7BL6514240	306.41	Close	R26	scaffold1262
	7BL6683213	463.6	7BL6630673	427.7	Close	R27	scaffold153
	7BL6688094	285.1	-	-	-	R28	-

I.VII Schematic representations using SNPs and mapping information associated with wheat contigs homoeologous to selected 7EL-specific markers

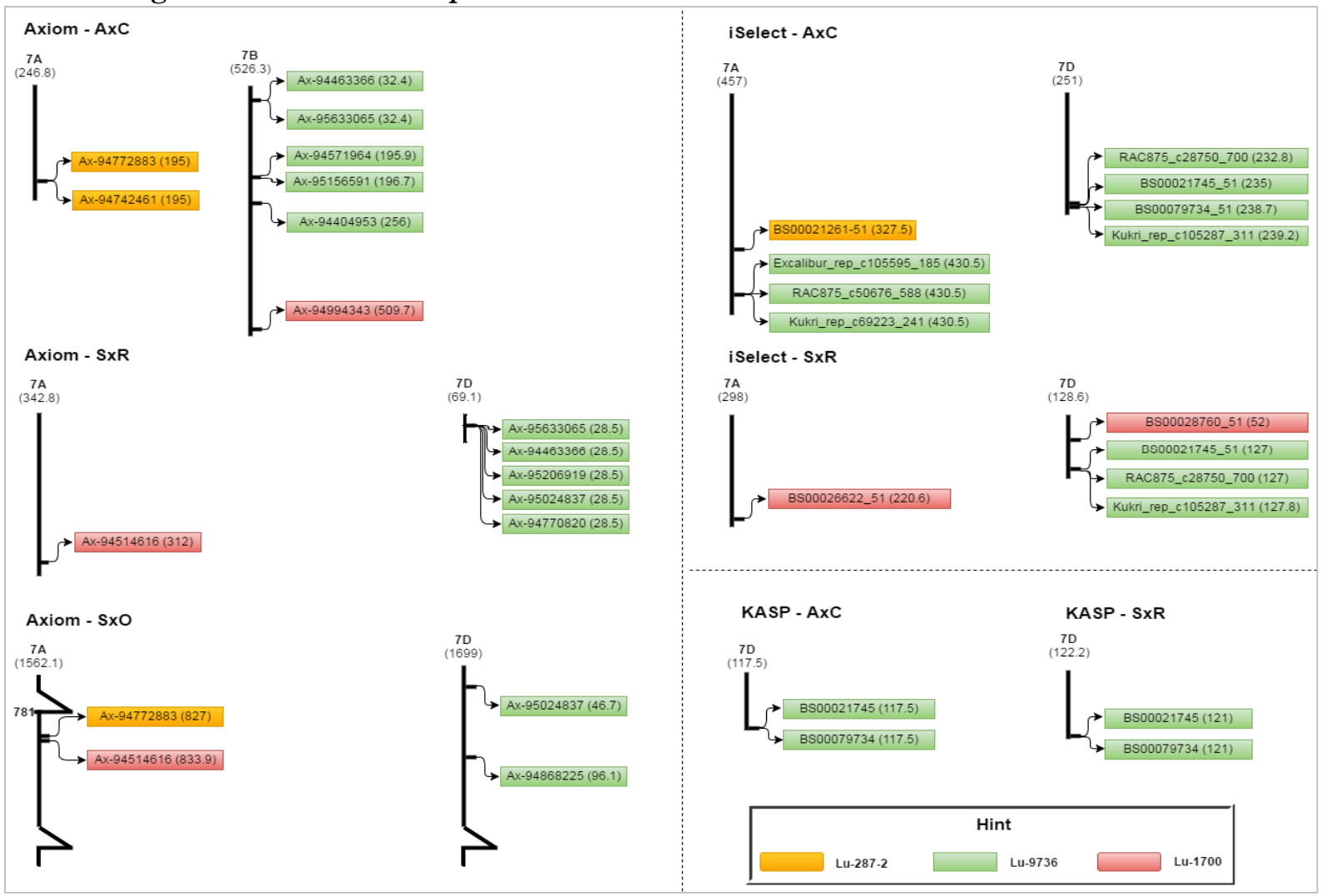

Figure App-I.6: Schematic representations using SNPs and mapping information associated with wheat contigs homoeologous to selected 7EL-specific markers. SNPs positions are shown in brackets after their names, in cM. Mapping data were from publicly available datasets produced with the Axiom, iSelect and KASP assays for populations from the crosses of Avalon x Cadenza (AxC), Savannah x Rialto (SxR) and Synthetic x Opata (SxO).

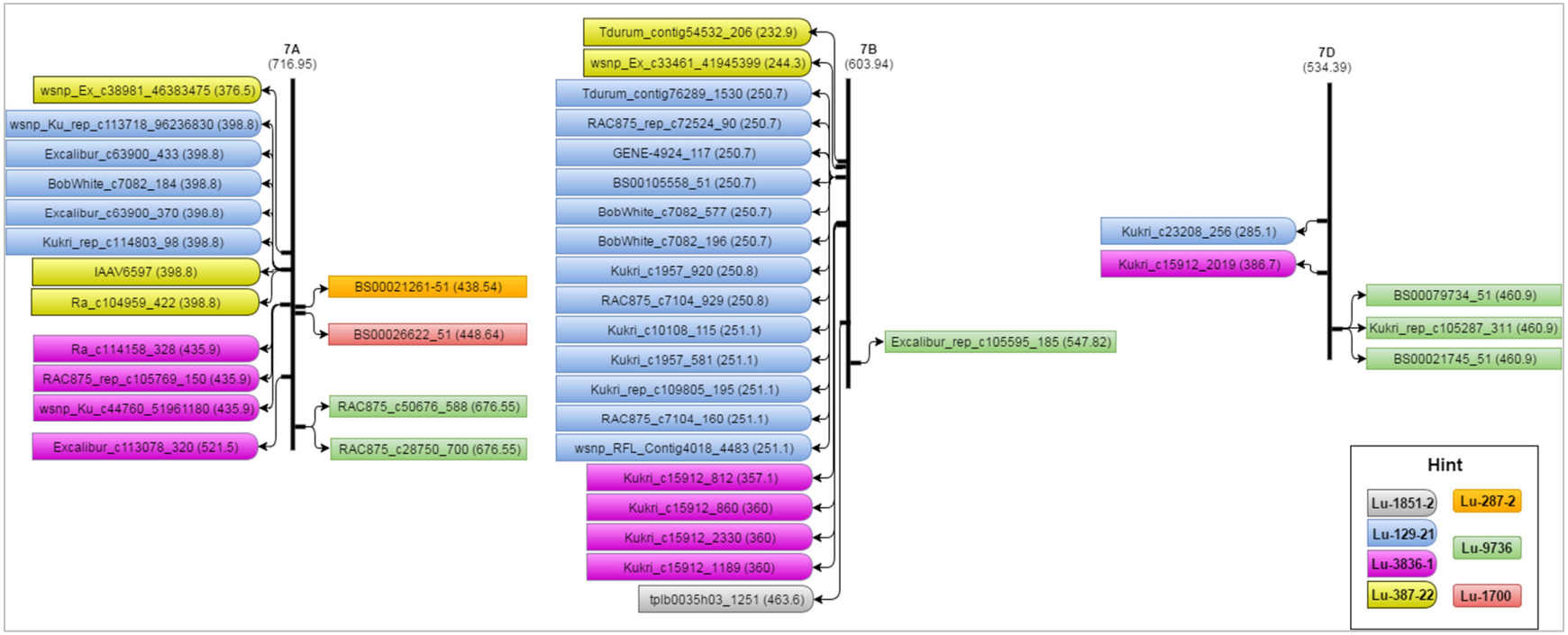

Figure App-I.7: Schematic representations using SNPs and mapping information associated with wheat contigs homoeologous to selected 7EL-specific markers. SNPs positions are shown in brackets after their names, in cM. Mapping data were from a publicly available consensus dataset produced with the iSelect assay (S. Wang et al., 2014). The mapping information for the SNPs shown on the left side of each chromosome was provided by K. Joustra.

I.VIII Bioinformatics data collected towards the proposition of a genetic order for previous 7EL-specific markers

Table App-I. 7: Data collected from step one to three of fourth objective (Figure 2.10).
First column represents the 31 7E-specific markers selected from objective 2, second and third column contains the associated 7EL scaffold and 7ABD wheat contig sequences associated with each marker, fourth column indicates the SNPs associated with the wheat contigs. The SNPs and their associated mapping data for 3 crosses from Axiom, iSelect and KASP arrays (assays), as well as a genetic consensus map from iSelect data are provided in the rest of table. Mapping data were from publicly available datasets produced with Axiom, iSelect and KASP assays for populations from the crosses of Avalon x Cadenza (AxC), Savannah x Rialto (SxR) and Synthetic x Opata (SxO), and also from a consensus dataset produced with the iSelect assay (S. Wang et al., 2014).

7E-specific Marker	7EL Scaffold	Wheat Contig	SNP ID	Axiom, iSelect, KASP Datasets							Concensus Dataset	
				Array	AxC	cM_AxC	SxR	cM_SxR	SxO	cM_SxO	Chr.	cM
Lu-1851-2	**649**	7DL3329321	AX-95070606	Axiom	-	-	-	-	7D	185.4589	-	-
Lu-8964-2 & Lu-625	**6092**	7AL4480027	AX-95213765	Axiom	7B	116.1192	-	-	-	-	-	-
		7AL4480027	AX-94899055	Axiom	7B	116.1192	-	-	-	-	-	-
		7BL6750133	IAAV2580	iSelect	7A	390.4	7A	253.6	-	-	-	-
		7BL6750133	Excalibur_c7338_242	iSelect	-	-	7B	24.3	-	-	7B	427.7
		7BL6750133	Kukri_c16814_103	iSelect	-	-	7B	24.3	-	-	7B	427.7
		7BL6750133	AX-94899055	Axiom	7B	116.1192	-	-	-	-	-	-
		7DL3376588	AX-95004702	Axiom	7B	330.2339	7B	56.94326	7B	321.8197	-	-
		7DL3376588	AX-94383827	Axiom	-	-	7A	342.8482	-	-	-	-
		7DL3376588	BS00003699_51	iSelect	-	-	7A	254.4	-	-	7B	418.37
		7DL3376588	Kukri_c11959_587	iSelect	-	-	7B	24.3	-	-	7B	427.7
		7DL3376588	Kukri_c16814_103	iSelect	-	-	7B	24.3	-	-	-	-
		7DL3376588	AX-95213765	Axiom	7B	116.1192	-	-	-	-	-	-
		7DL3376588	AX-94899055	Axiom	7B	116.1192	-	-	-	-	-	-
Lu-4301-1	**2500**	7AL4541883	Kukri_c64163_128	iSelect	7D	233.3	-	-	-	-	7D	450.87
		7AL4552263	AX-94409791	Axiom	7B	34.0108	-	-	-	-	-	-
		7BL6534954	AX-94409791	Axiom	7B	34.0108	-	-	-	-	-	-
		7DL3311257	Kukri_c9728_1171	iSelect	7A	423.9	-	-	-	-	7A	637.2
		7DL3311257	BS00043018_51	iSelect	7D	251.1	-	-	-	-	7A	635.34
		7DL3311257	BS00022875_51	iSelect	7D	236.8	-	-	-	-	7D	450.87
		7DL3311257	Kukri_c64163_128	iSelect	7D	233.3	-	-	-	-	-	-
		7DL3311257	IAAV5220	iSelect	7D	233.3	-	-	-	-	-	-
		7DL3311257	BS00010677_51	iSelect	7D	233.3	-	-	-	-	7A	624.47
		7DL3311257	AX-94786708	Axiom	7B	149.6555	-	-	-	-	-	-
		7DL3311257	AX-94821207	Axiom	7B	34.0108	-	-	-	-	-	-
		7DL3311257	AX-94409791	Axiom	7B	34.0108	-	-	-	-	-	-
		7DL3311257	AX-94849557	Axiom	7B	34.0108	-	-	-	-	-	-
		7DL3311257	AX-94750097	Axiom	7B	34.0108	-	-	-	-	-	-
Lu-1274-1	**4231**	7AL4550273	AX-94814303	Axiom	-	-	-	-	7A	997.5048	-	-
		7AL4550273	AX-94733648	Axiom	-	-	-	-	7A	995.6858	-	-
		7AL4550273	AX-94428861	Axiom	-	-	-	-	7D	97.86581	7B	547.82
		7AL4550273	BobWhite_c4240_1493	iSelect	7A	433.4	-	-	-	-	7A	670.6
		7AL4550273	Kukri_c11530_92	iSelect	7A	433.4	-	-	-	-	7A	681.58
		7AL4550273	RAC875_c12733_1509	iSelect	7A	433.4	-	-	-	-	7A	670.6
		7AL4550273	Kukri_c11530_60	iSelect	7A	433.4	-	-	-	-	7A	670.6
		7AL4550273	RAC875_c8752_1079	iSelect	7A	433.4	-	-	-	-	7B	508.97
		7AL4550273	Kukri_c11530_168	iSelect	7A	433.4	-	-	-	-	7B	547.82
		7AL4550273	RAC875_c34939_939	iSelect	7B	153.7	-	-	-	-	-	-
		7AL4550273	RAC875_c34939_963	iSelect	7B	153.7	-	-	-	-	7B	547.82
		7AL4550273	AX-94879781	Axiom	7B	217.6399	-	-	-	-	-	-

7E-specific Marker	7EL Scaffold	Wheat Contig	SNP ID	Axiom, iSelect, KASP Datasets							Concensus Dataset	
				Array	AxC	cM_AxC	SxR	cM_SxR	SxO	cM_SxO	Chr.	cM
Lu-1274-1 (cont.)	4231 (cont.)	7BL6699942	AX-94814303	Axiom	-	-	-	-	7A	997.5048	-	-
		7BL6699942	AX-94767893	Axiom	7B	204.9382	-	-	7B	356.2404	-	-
		7BL6699942	BobWhite_c4240_1493	iSelect	7A	433.4	-	-	-	-	-	-
		7BL6699942	RAC875_c12733_1509	iSelect	7A	433.4	-	-	-	-	-	-
		7BL6699942	RAC875_c34939_939	iSelect	7B	153.7	-	-	-	-	-	-
		7BL6699942	BS00040070_51	iSelect	7B	153.7	-	-	-	-	-	-
		7BL6699942	RAC875_c34939_963	iSelect	7B	153.7	-	-	-	-	-	-
		7BL6699942	RFL_Contig2647_624	iSelect	7B	153.7	-	-	-	-	7B	534.63
		7BL6699942	BobWhite_c4240_78	iSelect	7B	153.7	-	-	-	-	7B	547.82
		7BL6699942	AX-94879781	Axiom	7B	217.6399	-	-	-	-	-	-
		7DL3295310	AX-94814303	Axiom	-	-	-	-	7A	997.5048	-	-
		7DL3295310	AX-94928623	Axiom	-	-	-	-	7A	995.6858	-	-
		7DL3295310	AX-94733648	Axiom	-	-	-	-	7A	995.6858	-	-
		7DL3295310	AX-94428861	Axiom	-	-	-	-	7D	97.86581	-	-
		7DL3295310	RAC875_c8752_1079	iSelect	7A	433.4	-	-	-	-	-	-
		7DL3295310	RFL_Contig2814_859	iSelect	7A	433.4	-	-	-	-	7A	670.6
		7DL3295310	BobWhite_c32883_84	iSelect	7A	433.4	-	-	-	-	7A	670.6
		7DL3295310	RAC875_c12733_1509	iSelect	7A	433.4	-	-	-	-	-	-
		7DL3295310	RFL_Contig2814_604	iSelect	7A	433.4	-	-	-	-	7A	670.6
		7DL3295310	RFL_Contig2814_1213	iSelect	7A	433.4	-	-	-	-	7B	547.82
		7DL3295310	BS00004403_51	iSelect	7B	159	-	-	-	-	-	-
		7DL3295310	IACX6478	iSelect	7B	153.7	-	-	-	-	-	-
		7DL3295310	RAC875_c34939_939	iSelect	7B	153.7	-	-	-	-	-	-
		7DL3295310	BobWhite_c4240_78	iSelect	7B	153.7	-	-	-	-	-	-
		7DL3295310	RAC875_c34939_963	iSelect	7B	153.7	-	-	-	-	-	-
		7DL3295310	AX-94879781	Axiom	7B	217.6399	-	-	-	-	-	-
		7DL3295310	AX-95012310	Axiom	7B	203.3755	-	-	-	-	-	-
		7DL3295310	AX-95025537	Axiom	7B	203.3755	-	-	-	-	-	-
		7DL3295310	AX-94551053	Axiom	7B	203.3755	-	-	-	-	-	-
Lu-336	133	7AL4536781	AX-94927789	Axiom	7B	203.3755	-	-	7B	356.2404	-	-
		7AL4539427	AX-94927789	Axiom	7B	203.3755	-	-	7B	356.2404	-	-
		7AL4539427	BS00061593_51	iSelect	7A	430.5	-	-	-	-	7A	663.85
		7AL4539427	AX-94441635	Axiom	7B	4.153718	-	-	-	-	-	-
		7BL6672306	AX-94425840	Axiom	7B	36.35503	-	-	-	-	-	-
		7BL6672580	AX-94441635	Axiom	7B	4.153718	-	-	-	-	-	-
		7DL1397928	AX-94425840	Axiom	7B	36.35503	-	-	-	-	-	-
		7DL3366096	BS00061593_51	iSelect	7A	430.5	-	-	-	-	-	-
		7DL3366096	AX-94441635	Axiom	7B	4.153718	-	-	-	-	-	-
Lu-495	102	7DL3392782	AX-94716438	Axiom	7B	95.13802	-	-	7B	536.3152	-	-
Lu-270-1	286	7AL4558446	AX-95179928	Axiom	7B	144.9538	-	-	7A	955.767	-	-
		7AL4558446	RAC875_rep_c83934_91	iSelect	7A	419	-	-	-	-	7A	625.38
Lu-480-1	4317	7AL4455953	BS00010967_51	iSelect	-	-	7D	128.6	-	-	-	-
		7AL4455953	AX-94662063	Axiom	7B	34.0108	7D	23.81134	-	-	-	-
		7AL4455953	RFL_Contig5480_408	iSelect	7B	145.1	-	-	-	-	7B	508.33
		7AL4455953	AX-94736858	Axiom	7B	34.0108	-	-	-	-	-	-
		7BL6739810	BS00010967_51	iSelect	-	-	7D	128.6	-	-	-	-
		7BL6739810	BS00087197_51	iSelect	7B	149	-	-	-	-	7B	508.33
		7BL6739810	RFL_Contig5480_408	iSelect	7B	145.1	-	-	-	-	-	-
		7DL3373545	BS00010967_51	iSelect	-	-	7D	128.6	-	-	-	-
		7DL3373545	AX-94384437	Axiom	-	-	7D	26.98701	-	-	-	-
		7DL3373545	AX-94662063	Axiom	7B	34.0108	7D	23.81134	-	-	-	-
		7DL3373545	RFL_Contig5480_408	iSelect	7B	145.1	-	-	-	-	-	-
		7DL3373545	AX-94736858	Axiom	7B	34.0108	-	-	-	-	-	-
Lu-3757-1	-	7DL3366438	BS00021979_51	iSelect	7D	233.3	7D	128.6	-	-	-	-
		7DL3366438	BS00022511	KASP	7D	115.8	7D	122.2481	-	-	-	-
		7DL3366438	AX-94834911	Axiom	-	-	7D	23.81134	-	-	-	-
		7DL3366438	AX-94731902	Axiom	-	-	7D	23.81134	-	-	-	-
		7DL3366438	RAC875_rep_c72959_187	iSelect	7B	139.2	-	-	-	-	7B	501.16

7E-specific Marker	7EL Scaffold	Wheat Contig	SNP ID	Axiom, iSelect, KASP Datasets							Concensus Dataset	
				Array	AxC	cM_AxC	SxR	cM_SxR	SxO	cM_SxO	Chr.	cM
Lu-3757-1 (cont.)	-	7DL3366438	AX-94765678	Axiom	7B	165.5146	-	-	-	-	-	-
		7DL3366438	AX-94741948	Axiom	7B	159.1887	-	-	-	-	-	-
		7DL3366438	AX-94451126	Axiom	7B	34.0108	-	-	-	-	-	-
		7AL4512345	AX-94691842	Axiom	-	-	-	-	7B	351.0357	-	-
		7AL4512345	Excalibur_c6788_200	iSelect	7D	233.8	7D	128.6	-	-	7B	511.19
		7AL4512345	Ku_c16600_805	iSelect	7D	233.3	7D	128.6	-	-	7A	644.81
		7AL4512345	BS00012122	KASP	7D	117	7D	122.2481	-	-	-	-
		7AL4512345	BS00022511	KASP	7D	115.8	7D	122.2481	-	-	-	-
		7AL4512345	AX-94704171	Axiom	-	-	7D	26.98701	-	-	-	-
		7AL4512345	AX-94661850	Axiom	-	-	7D	26.98701	-	-	-	-
		7AL4512345	AX-94565706	Axiom	-	-	7D	26.98701	-	-	-	-
		7AL4512345	AX-94718470	Axiom	7B	34.0108	7D	23.81134	-	-	-	-
		7AL4512345	AX-94834911	Axiom	-	-	7D	23.81134	-	-	-	-
		7AL4512345	Ku_c15539_433	iSelect	7B	139.2	-	-	-	-	7B	501.16
		7AL4512345	Kukri_c18148_1177	iSelect	7B	138.7	-	-	-	-	7B	510.25
		7AL4512345	AX-94650444	Axiom	7B	159.1887	-	-	-	-	-	-
		7AL4512345	AX-95137812	Axiom	7B	34.0108	-	-	-	-	-	-
		7AL4512345	AX-95185400	Axiom	7B	24.33905	-	-	-	-	-	-
		7AL4512345	AX-94434390	Axiom	7B	6.737276	-	-	-	-	-	-
		7AL4557610	BS00022511	KASP	7D	115.8	7D	122.2481	-	-	-	-
		7AL4557610	AX-94834911	Axiom	-	-	7D	23.81134	-	-	-	-
		7AL4557610	Ku_c15539_433	iSelect	7B	139.2	-	-	-	-	-	-
		7AL4557610	AX-94741948	Axiom	7B	159.1887	-	-	-	-	-	-
		7AL4557610	AX-94650444	Axiom	7B	159.1887	-	-	-	-	-	-
		7BL6751881	RAC875_rep_c72959_187	iSelect	7B	139.2	-	-	-	-	-	-
		7BL6751881	Excalibur_rep_c69840_85	iSelect	7B	139.2	-	-	-	-	7B	501.16
		7BL6751881	Ku_c15539_433	iSelect	7B	139.2	-	-	-	-	-	-
		7BL6751881	AX-94650444	Axiom	7B	159.1887	-	-	-	-	-	-
Lu-3836-1	2361	7AL4484752	AX-94937740	Axiom	7B	450.4179	-	-	-	-	-	-
		7AL4484752	AX-95105594	Axiom	-	-	-	-	7A	892.6364	-	-
		7AL4484752	AX-95252631	Axiom	7A	246.8752	-	-	7A	892.6364	-	-
		7AL4484752	Excalibur_c113078_320	iSelect	7A	365.9	-	-	-	-	7A	521.5
		7AL4484752	Kukri_c15912_812	iSelect	7B	34.3	-	-	-	-	7B	357.1
		7AL4484752	Kukri_c15912_860	iSelect	7B	34.3	-	-	-	-	7B	360
		7AL4484752	Kukri_c15912_1189	iSelect	7B	33.8	-	-	-	-	7B	360
		7AL4484752	Kukri_c15912_2330	iSelect	7B	34.3	-	-	-	-	7B	360
		7AL4484752	Ra_c114158_328	-	-	-	-	-	-	-	7A	435.9
		7AL4484752	RAC875_rep_c105769_150	-	-	-	-	-	-	-	7A	435.9
		7AL4484752	wsnp_Ku_c44760_51961180	-	-	-	-	-	-	-	7A	435.9
		7BL6688094	AX-94564853	Axiom	7B	450.4179	-	-	-	-	-	-
		7BL6688094	AX-94937740	Axiom	7B	450.4179	-	-	-	-	-	-
		7BL6688094	AX-95105594	Axiom	-	-	-	-	7A	892.6364	-	-
		7BL6688094	AX-95252631	Axiom	7A	246.8752	-	-	7A	892.6364	-	-
		7BL6688094	Excalibur_c113078_320	iSelect	7A	365.9	-	-	-	-	7A	521.5
		7BL6688094	Kukri_c15912_812	iSelect	7B	34.3	-	-	-	-	7B	357.1
		7BL6688094	Kukri_c15912_860	iSelect	7B	34.3	-	-	-	-	7B	360
		7BL6688094	Kukri_c15912_1189	iSelect	7B	33.8	-	-	-	-	7B	360
		7BL6688094	Kukri_c15912_2019	-	-	-	-	-	-	-	7D	386.7
		7BL6688094	Kukri_c15912_2330	iSelect	7B	34.3	-	-	-	-	7B	360
		7DL3341152	AX-94937740	Axiom	7B	450.4179	-	-	-	-	-	-
		7DL3341152	AX-95105594	Axiom	-	-	-	-	7A	892.6364	-	-
		7DL3341152	Kukri_c15912_812	iSelect	7B	34.3	-	-	-	-	7B	357.1
		7DL3341152	Kukri_c15912_860	iSelect	7B	34.3	-	-	-	-	7B	360
		7DL3341152	Kukri_c15912_1189	iSelect	7B	33.8	-	-	-	-	7B	360
		7DL3341152	Kukri_c15912_2330	iSelect	7B	34.3	-	-	-	-	7B	360

7E-specific Marker	7EL Scaffold	Wheat Contig	SNP ID	Axiom, iSelect, KASP Datasets							Concensus Dataset	
				Array	AxC	cM_AxC	SxR	cM_SxR	SxO	cM_SxO	Chr.	cM
Lu-5875	2847	7AL4462127	AX-94701970	Axiom	7B	270.028	-	-	7B	351.0357	-	-
		7BL6749384	AX-94701970	Axiom	7B	270.028	-	-	7B	351.0357	-	-
		7DL3352074	AX-95222073	Axiom	7B	34.0108	7D	26.98701	-	-	-	-
		7DL3352074	AX-94934185	Axiom	-	-	7D	23.81134	-	-	-	-
Lu-367	1246	7DL3372171	AX-94890317	Axiom	-	-	7B	77.626	-	-	-	-
Lu-1974	280	7DL3356480	D_GB5Y7FA02GG15C_348	-	-	-	-	-	-	-	7D	300.22
Lu-114-21	1114	7BL6694713	AX-94803195	Axiom	-	-	-	-	7B	553.4309	-	-
		7DL3368915	AX-94803195	Axiom	-	-	-	-	7B	553.4309	-	-
Lu-485	3466	7DL3359838	Tdurum_contig26215_339	-	-	-	-	-	-	-	7A	398.79
		7AL4534411	Tdurum_contig26215_425	-	-	-	-	-	-	-	7D	301.64
Lu-193-2	85	7DL3363709	D_contig15144_136	-	-	-	-	-	-	-	7D	302.13
		7DL3363709	D_GBF1XID01A409A_114	-	-	-	-	-	-	-	7D	302.13
Lu-843-1	110	-	-	-	-	-	-	-	-	-	-	-
Lu-4301-1	2500	-	-	-	-	-	-	-	-	-	-	-
Lu-295	441	-	-	-	-	-	-	-	-	-	-	-
Lu-1654	36	-	-	-	-	-	-	-	-	-	-	-
Lu-1225302	2339	-	-	-	-	-	-	-	-	-	-	-
p7es-68	2058	7BL6638991	AX-94478315	Axiom	7B	36.35503	-	-	7D	99.56138	-	-
		7BL6681356	AX-94540691	Axiom	7B	32.45992	-	-	-	-	-	-
p7es-21	1164	-	-	-	-	-	-	-	-	-	7B	287.58
				-	-	-	-	-	-	-	7A	435.86
p7es-45	907	7BL6715533	AX-95078974	Axiom	7B	289.1992	-	-	-	-	-	-
p7es-49	1497	7BL6698178	AX-94537587	Axiom	7B	427.7339	-	-	7B	132.0238	-	-
		7BL6732560	Ra_c21094_506	iSelect	7B	54.4	-	-	-	-	7B	383.16
p7es-48	730	-	-	-	-	-	-	-	-	-	-	-
p7es-56	2298	-	-	-	-	-	-	-	-	-	-	-
p7es-1	2625	-	-	-	-	-	-	-	-	-	-	-
p7es-16	1244	-	-	-	-	-	-	-	-	-	-	-
p7es-59	1241	-	-	-	-	-	-	-	-	-	-	-

I.IX Schematic representations relating previously used 7EL-specific markers to the novel designed ones

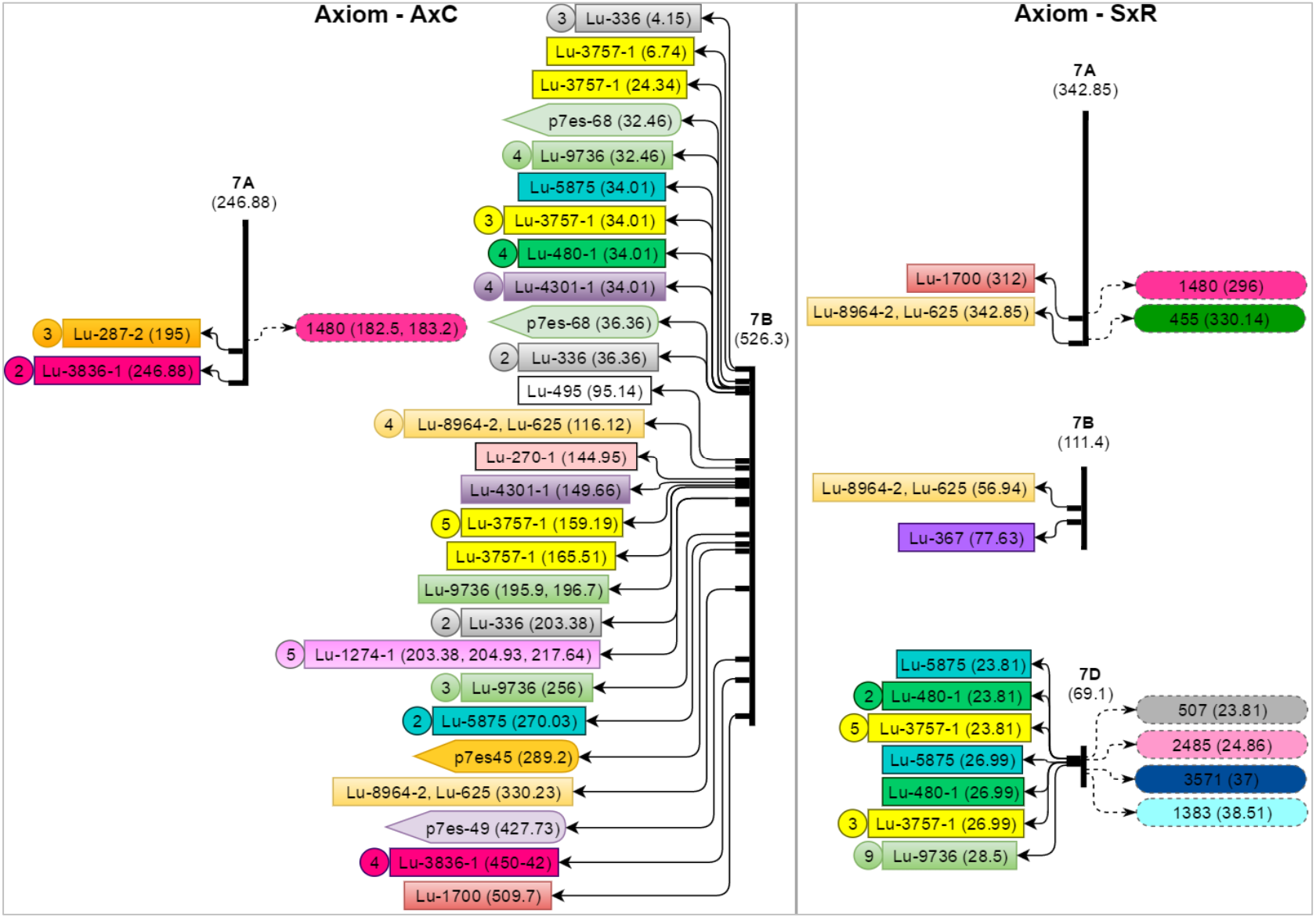

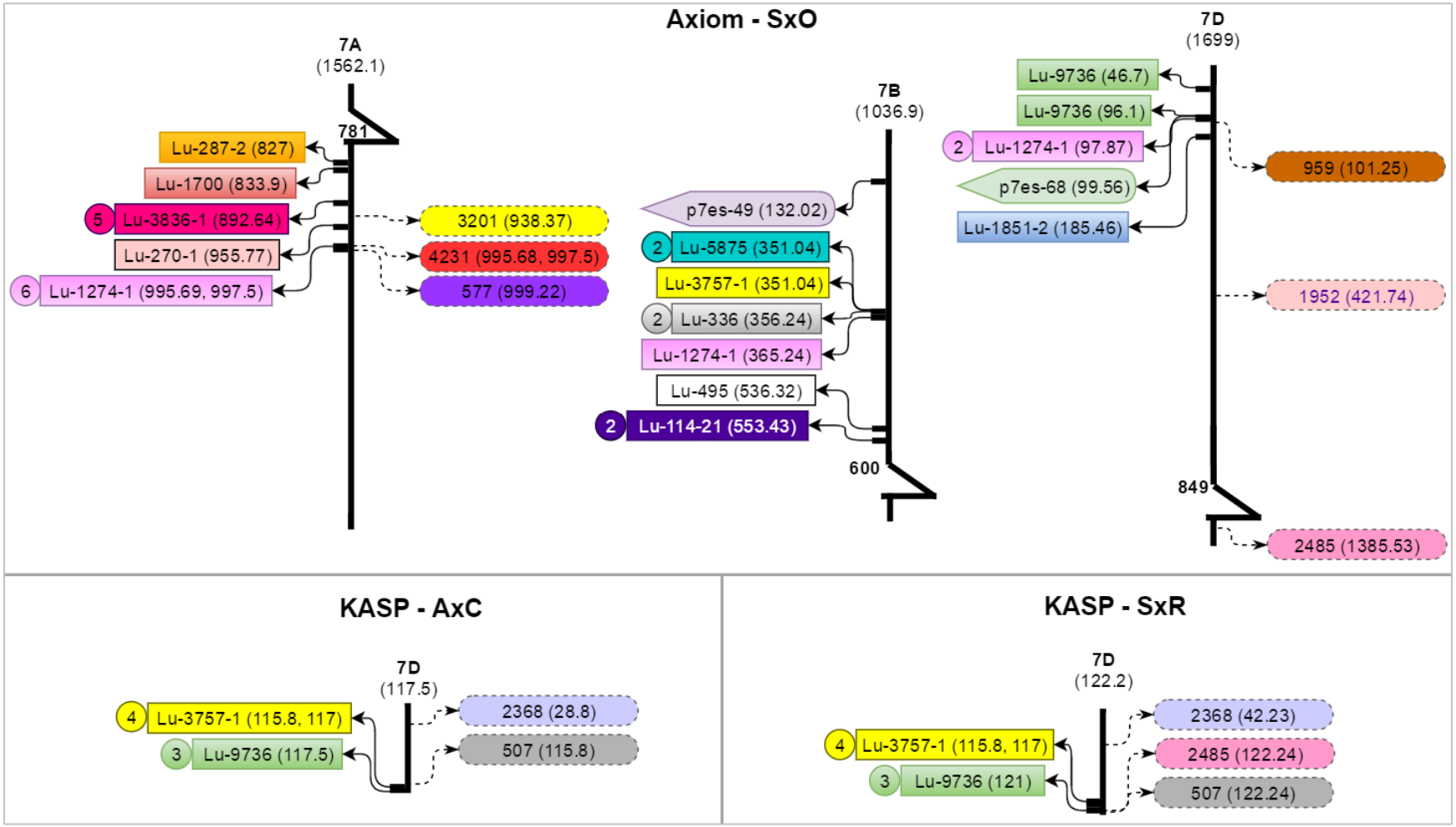
Axiom - SxO
7A
(1562.1)
781
Lu-287-2 (827)
Lu-1700 (833.9)
5 Lu-3836-1 (892.64)
Lu-270-1 (955.77)
6 Lu-1274-1 (995.69, 997.5)
3201 (938.37)
4231 (995.68, 997.5)
577 (999.22)
7B
(1036.9)
p7es-49 (132.02)
2 Lu-5875 (351.04)
Lu-3757-1 (351.04)
2 Lu-336 (356.24)
Lu-1274-1 (365.24)
Lu-495 (536.32)
2 Lu-114-21 (553.43)
600
7D
(1699)
Lu-9736 (46.7)
Lu-9736 (96.1)
2 Lu-1274-1 (97.87)
p7es-68 (99.56)
Lu-1851-2 (185.46)
959 (101.25)
1952 (421.74)
849
2485 (1385.53)
KASP - AxC
7D
(117.5)
4 Lu-3757-1 (115.8, 117)
3 Lu-9736 (117.5)
2368 (28.8)
507 (115.8)
KASP - SxR
7D
(122.2)
4 Lu-3757-1 (115.8, 117)
3 Lu-9736 (121)
2368 (42.23)
2485 (122.24)
507 (122.24)

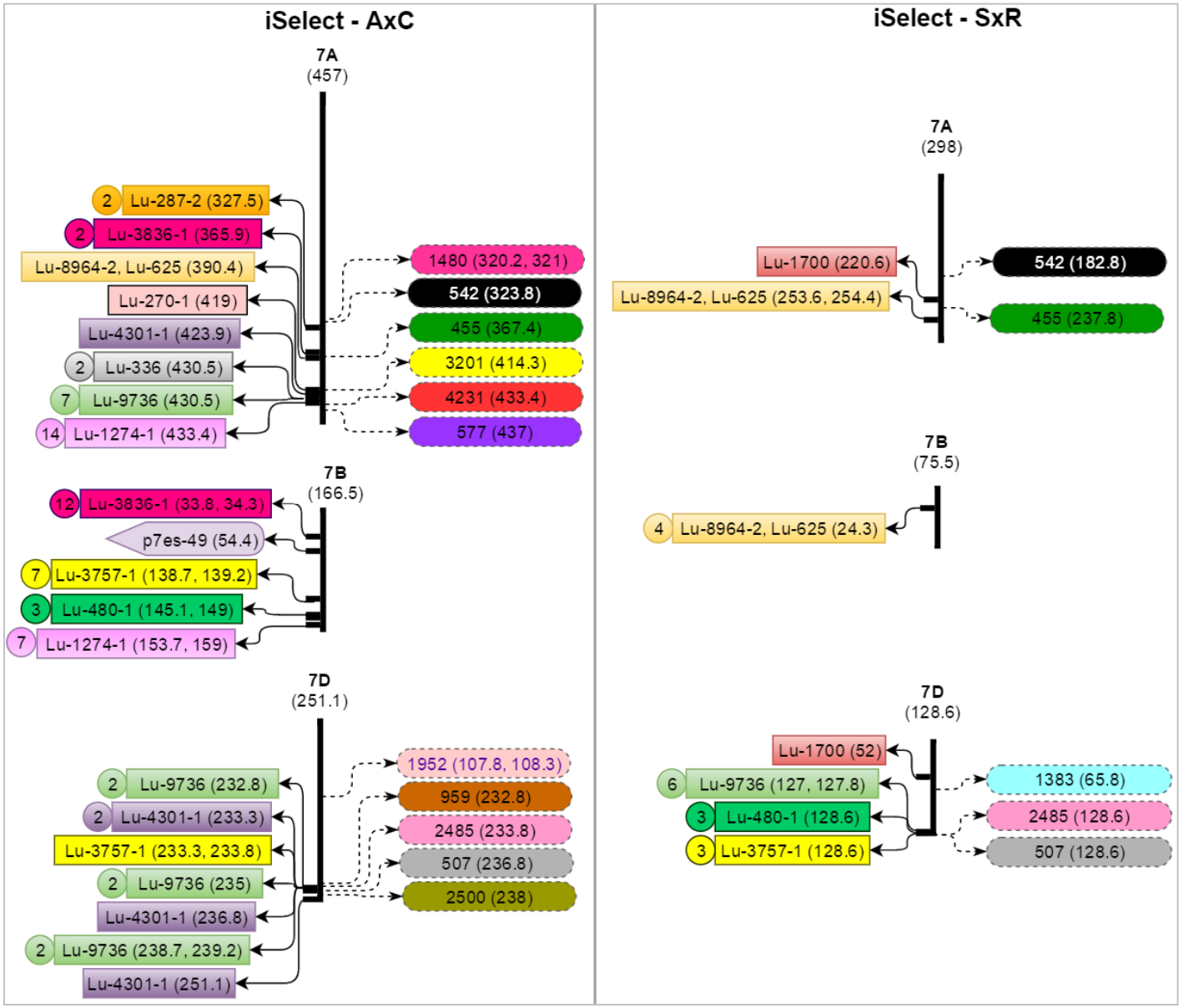
iSelect - AxC
7A
(457)
2 Lu-287-2 (327.5)
2 Lu-3836-1 (365.9)
Lu-8964-2, Lu-625 (390.4)
Lu-270-1 (419)
Lu-4301-1 (423.9)
2 Lu-336 (430.5)
7 Lu-9736 (430.5)
14 Lu-1274-1 (433.4)
1480 (320.2, 321)
542 (323.8)
455 (367.4)
3201 (414.3)
4231 (433.4)
577 (437)
7B
(166.5)
12 Lu-3836-1 (33.8, 34.3)
p7es-49 (54.4)
7 Lu-3757-1 (138.7, 139.2)
3 Lu-480-1 (145.1, 149)
7 Lu-1274-1 (153.7, 159)
7D
(251.1)
2 Lu-9736 (232.8)
2 Lu-4301-1 (233.3)
Lu-3757-1 (233.3, 233.8)
2 Lu-9736 (235)
Lu-4301-1 (236.8)
2 Lu-9736 (238.7, 239.2)
Lu-4301-1 (251.1)
1952 (107.8, 108.3)
959 (232.8)
2485 (233.8)
507 (236.8)
2500 (238)
iSelect - SxR
7A
(298)
Lu-1700 (220.6)
Lu-8964-2, Lu-625 (253.6, 254.4)
542 (182.8)
455 (237.8)
7B
(75.5)
4 Lu-8964-2, Lu-625 (24.3)
7D
(128.6)
Lu-1700 (52)
6 Lu-9736 (127, 127.8)
3 Lu-480-1 (128.6)
3 Lu-3757-1 (128.6)
1383 (65.8)
2485 (128.6)
507 (128.6)

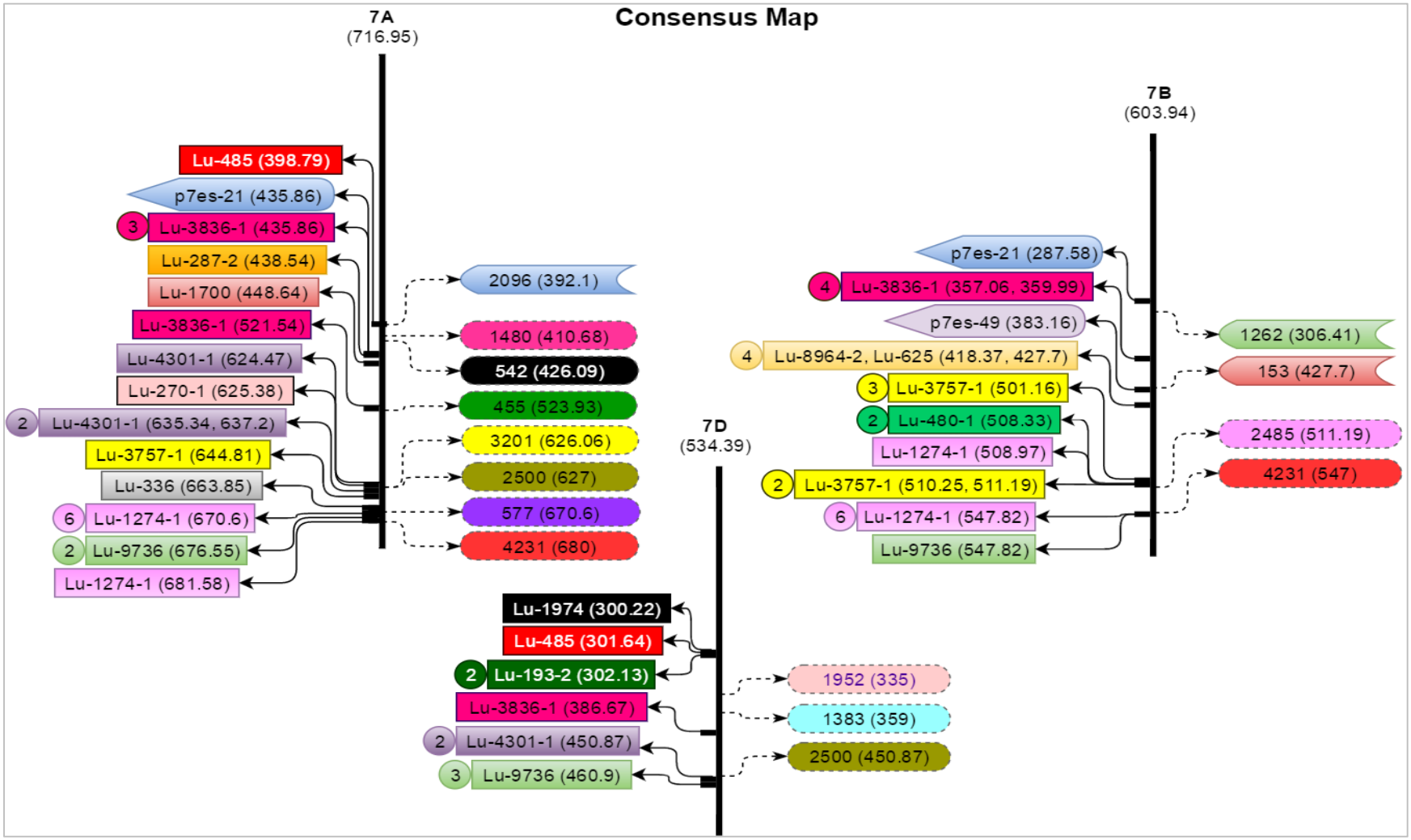

Figure App-I. 8: Schematic representations showing the position of previously used 7EL-specific markers, based on information for associated SNPs, in relation with the novel 7EL-specific markers.

Markers located on the right side of each chromosome schema were designed in the third objective, while the previously used markers are represented on the left side. Only the first part of the marker name (associated 7E scaffold) is displayed for markers that were designed in this project. Numbers in bracket represent the genetic position, in cM. Numbers located in a circle beside the marker boxes represent the number of SNPs associated with that specific position. See Figure App-I. 9, hint box, for more information on the groups of markers.

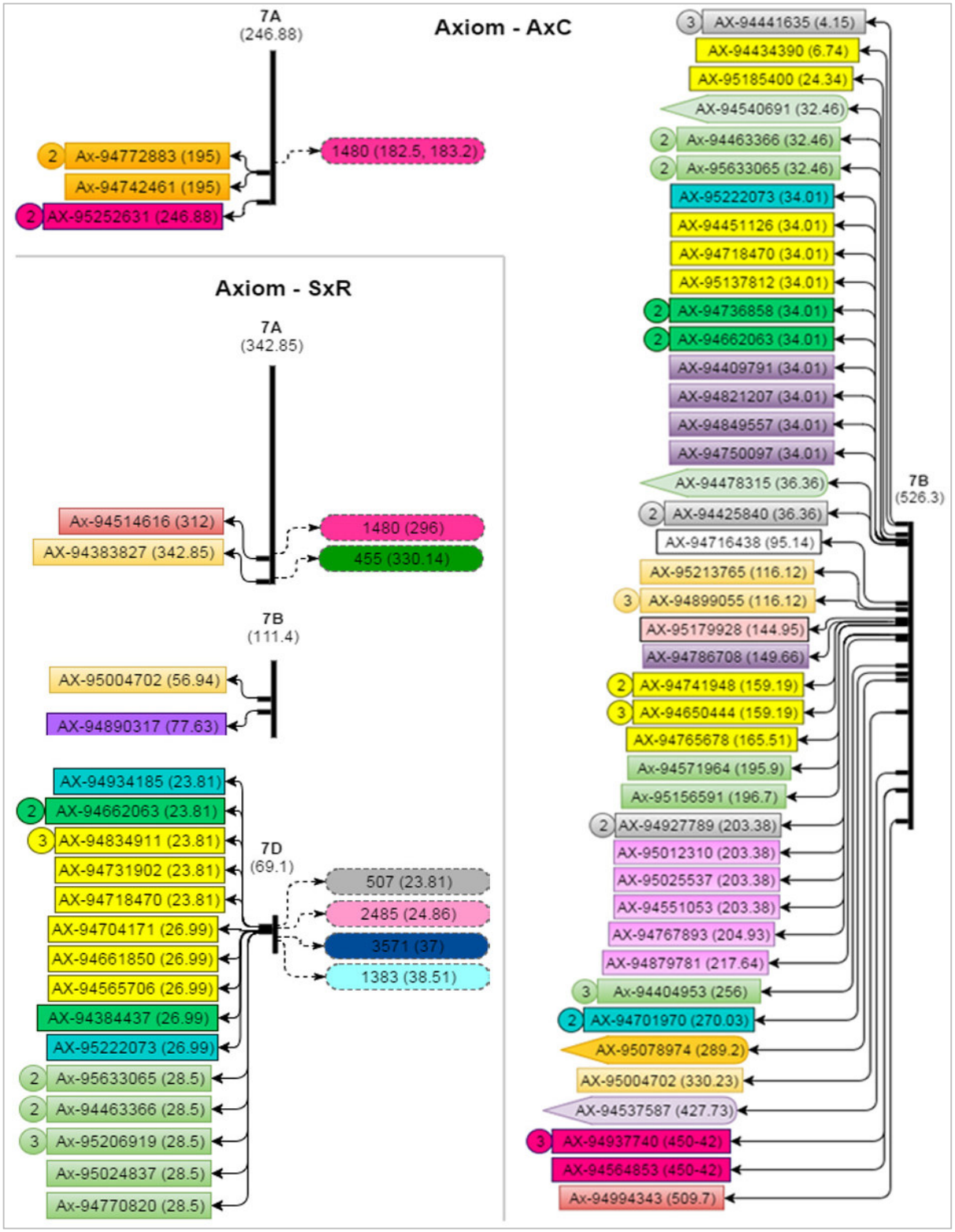
Axiom - AxC
7A
(246.88)
2 Ax-94772883 (195)
Ax-94742461 (195)
2 AX-95252631 (246.88)
1480 (182.5, 183.2)
Axiom - SxR
7A
(342.85)
Ax-94514616 (312)
AX-94383827 (342.85)
1480 (296)
455 (330.14)
7B
(111.4)
AX-95004702 (56.94)
AX-94890317 (77.63)
AX-94934185 (23.81)
2 AX-94662063 (23.81)
3 AX-94834911 (23.81)
AX-94731902 (23.81)
AX-94718470 (23.81)
AX-94704171 (26.99)
AX-94661850 (26.99)
AX-94565706 (26.99)
AX-94384437 (26.99)
AX-95222073 (26.99)
2 Ax-95633065 (28.5)
2 Ax-94463366 (28.5)
3 Ax-95206919 (28.5)
Ax-95024837 (28.5)
Ax-94770820 (28.5)
7D
(69.1)
507 (23.81)
2485 (24.86)
3571 (37)
1383 (38.51)
3 AX-94441635 (4.15)
AX-94434390 (6.74)
AX-95185400 (24.34)
AX-94540691 (32.46)
2 Ax-94463366 (32.46)
2 Ax-95633065 (32.46)
AX-95222073 (34.01)
AX-94451126 (34.01)
AX-94718470 (34.01)
AX-95137812 (34.01)
2 AX-94736858 (34.01)
2 AX-94662063 (34.01)
AX-94409791 (34.01)
AX-94821207 (34.01)
AX-94849557 (34.01)
AX-94750097 (34.01)
AX-94478315 (36.36)
2 AX-94425840 (36.36)
AX-94716438 (95.14)
AX-95213765 (116.12)
3 AX-94899055 (116.12)
AX-95179928 (144.95)
AX-94786708 (149.66)
2 AX-94741948 (159.19)
3 AX-94650444 (159.19)
AX-94765678 (165.51)
Ax-94571964 (195.9)
Ax-95156591 (196.7)
2 AX-94927789 (203.38)
AX-95012310 (203.38)
AX-95025537 (203.38)
AX-94551053 (203.38)
AX-94767893 (204.93)
AX-94879781 (217.64)
3 Ax-94404953 (256)
2 AX-94701970 (270.03)
AX-95078974 (289.2)
AX-95004702 (330.23)
AX-94537587 (427.73)
3 AX-94937740 (450-42)
AX-94564853 (450-42)
Ax-94994343 (509.7)
7B
(526.3)

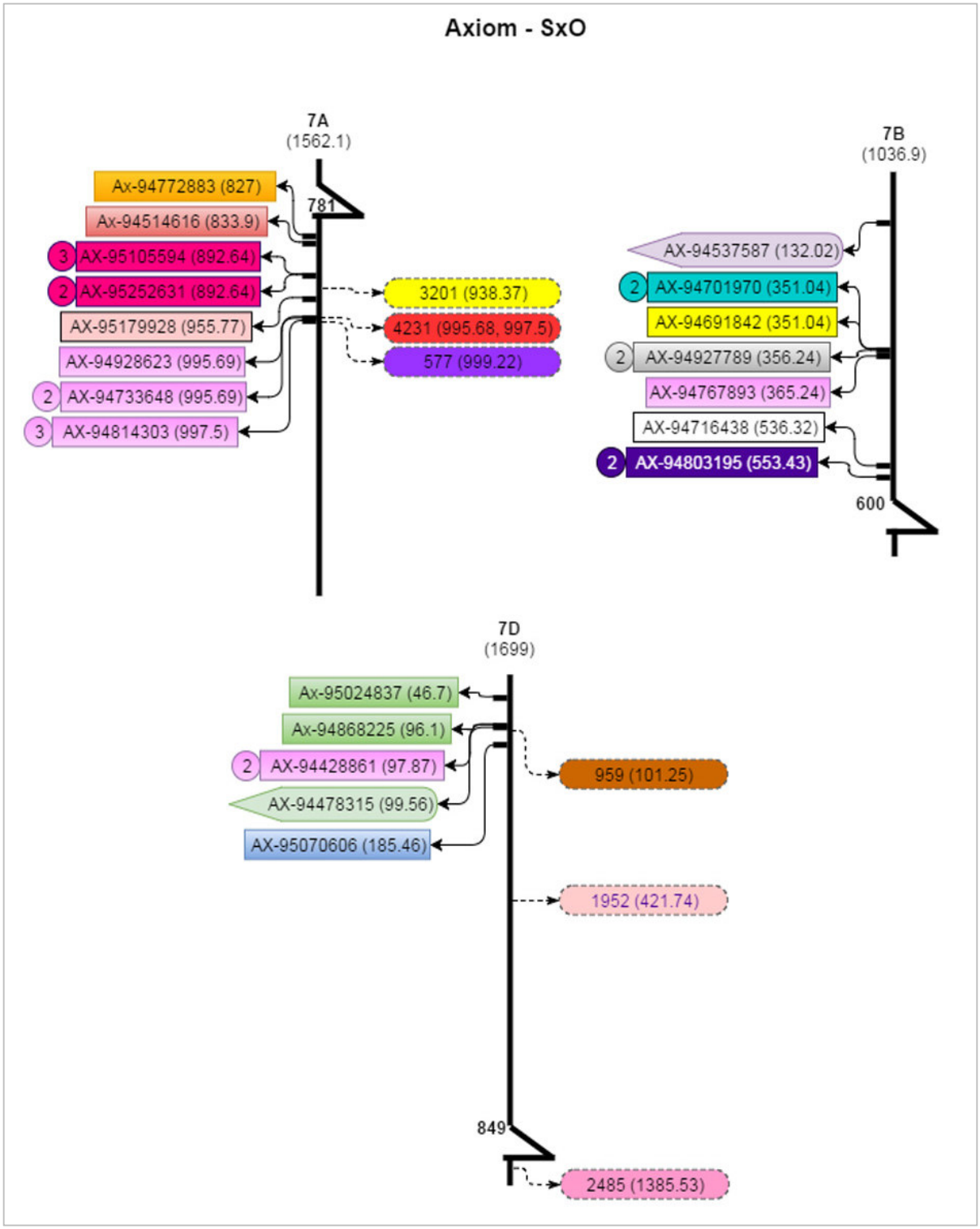
Axiom - SxO
7A
(1562.1)
Ax-94772883 (827)
Ax-94514616 (833.9)
781
3 AX-95105594 (892.64)
2 AX-95252631 (892.64)
AX-95179928 (955.77)
AX-94928623 (995.69)
2 AX-94733648 (995.69)
3 AX-94814303 (997.5)
3201 (938.37)
4231 (995.68, 997.5)
577 (999.22)
7B
(1036.9)
AX-94537587 (132.02)
2 AX-94701970 (351.04)
AX-94691842 (351.04)
2 AX-94927789 (356.24)
AX-94767893 (365.24)
AX-94716438 (536.32)
2 AX-94803195 (553.43)
600
7D
(1699)
Ax-95024837 (46.7)
Ax-94868225 (96.1)
2 AX-94428861 (97.87)
AX-94478315 (99.56)
AX-95070606 (185.46)
959 (101.25)
1952 (421.74)
849
2485 (1385.53)

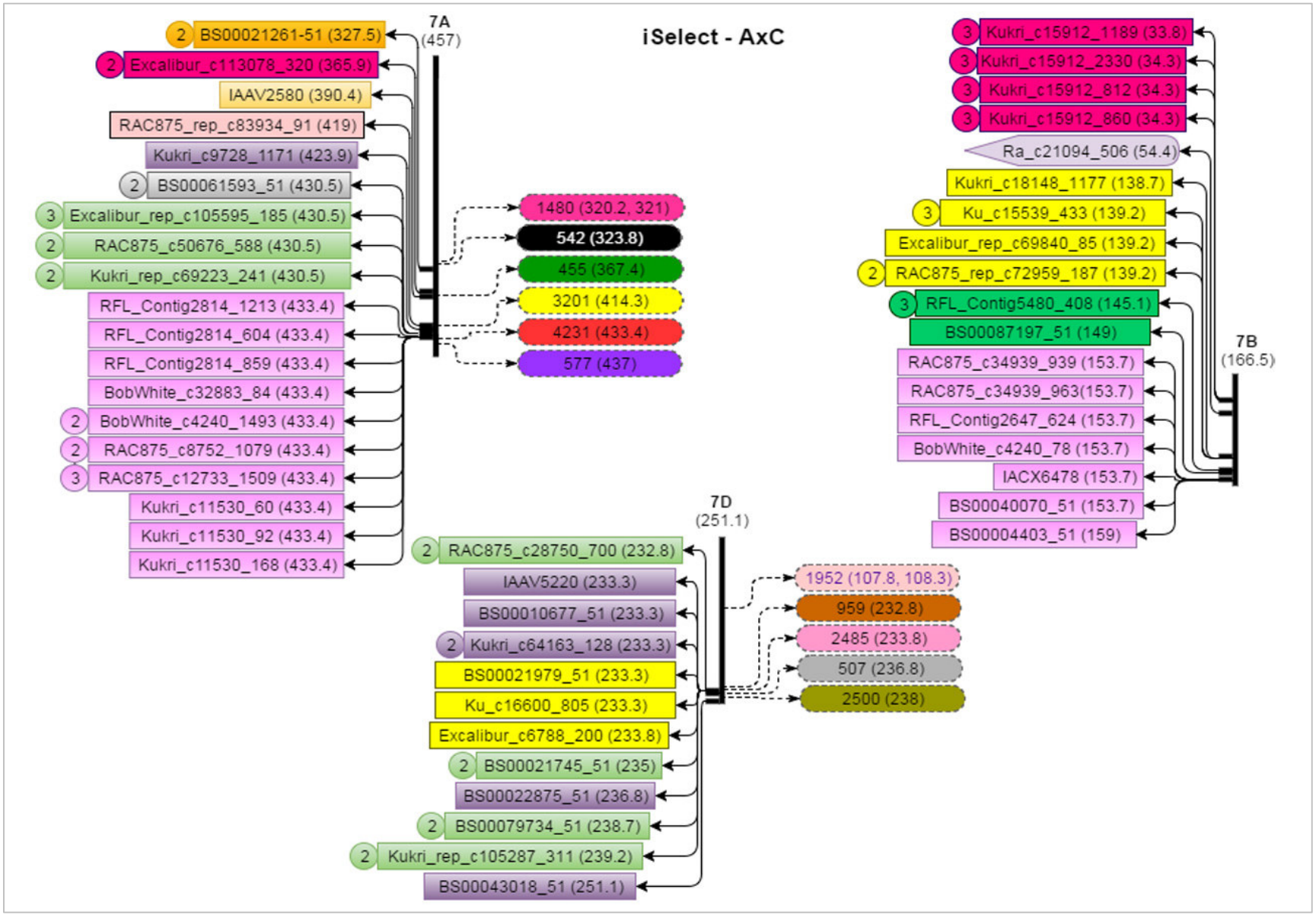
iSelect - AxC
7A
(457)
2 BS00021261-51 (327.5)
2 Excalibur_c113078_320 (365.9)
IAAV2580 (390.4)
RAC875_rep_c83934_91 (419)
Kukri_c9728_1171 (423.9)
2 BS00061593_51 (430.5)
3 Excalibur_rep_c105595_185 (430.5)
2 RAC875_c50676_588 (430.5)
2 Kukri_rep_c69223_241 (430.5)
RFL_Contig2814_1213 (433.4)
RFL_Contig2814_604 (433.4)
RFL_Contig2814_859 (433.4)
BobWhite_c32883_84 (433.4)
2 BobWhite_c4240_1493 (433.4)
2 RAC875_c8752_1079 (433.4)
3 RAC875_c12733_1509 (433.4)
Kukri_c11530_60 (433.4)
Kukri_c11530_92 (433.4)
Kukri_c11530_168 (433.4)
1480 (320.2, 321)
542 (323.8)
455 (367.4)
3201 (414.3)
4231 (433.4)
577 (437)
3 Kukri_c15912_1189 (33.8)
3 Kukri_c15912_2330 (34.3)
3 Kukri_c15912_812 (34.3)
3 Kukri_c15912_860 (34.3)
Ra_c21094_506 (54.4)
Kukri_c18148_1177 (138.7)
3 Ku_c15539_433 (139.2)
Excalibur_rep_c69840_85 (139.2)
2 RAC875_rep_c72959_187 (139.2)
3 RFL_Contig5480_408 (145.1)
BS00087197_51 (149)
RAC875_c34939_939 (153.7)
RAC875_c34939_963(153.7)
RFL_Contig2647_624 (153.7)
BobWhite_c4240_78 (153.7)
IACX6478 (153.7)
BS00040070_51 (153.7)
BS00004403_51 (159)
7B
(166.5)
7D
(251.1)
2 RAC875_c28750_700 (232.8)
IAAV5220 (233.3)
BS00010677_51 (233.3)
2 Kukri_c64163_128 (233.3)
BS00021979_51 (233.3)
Ku_c16600_805 (233.3)
Excalibur_c6788_200 (233.8)
2 BS00021745_51 (235)
BS00022875_51 (236.8)
2 BS00079734_51 (238.7)
2 Kukri_rep_c105287_311 (239.2)
BS00043018_51 (251.1)
1952 (107.8, 108.3)
959 (232.8)
2485 (233.8)
507 (236.8)
2500 (238)

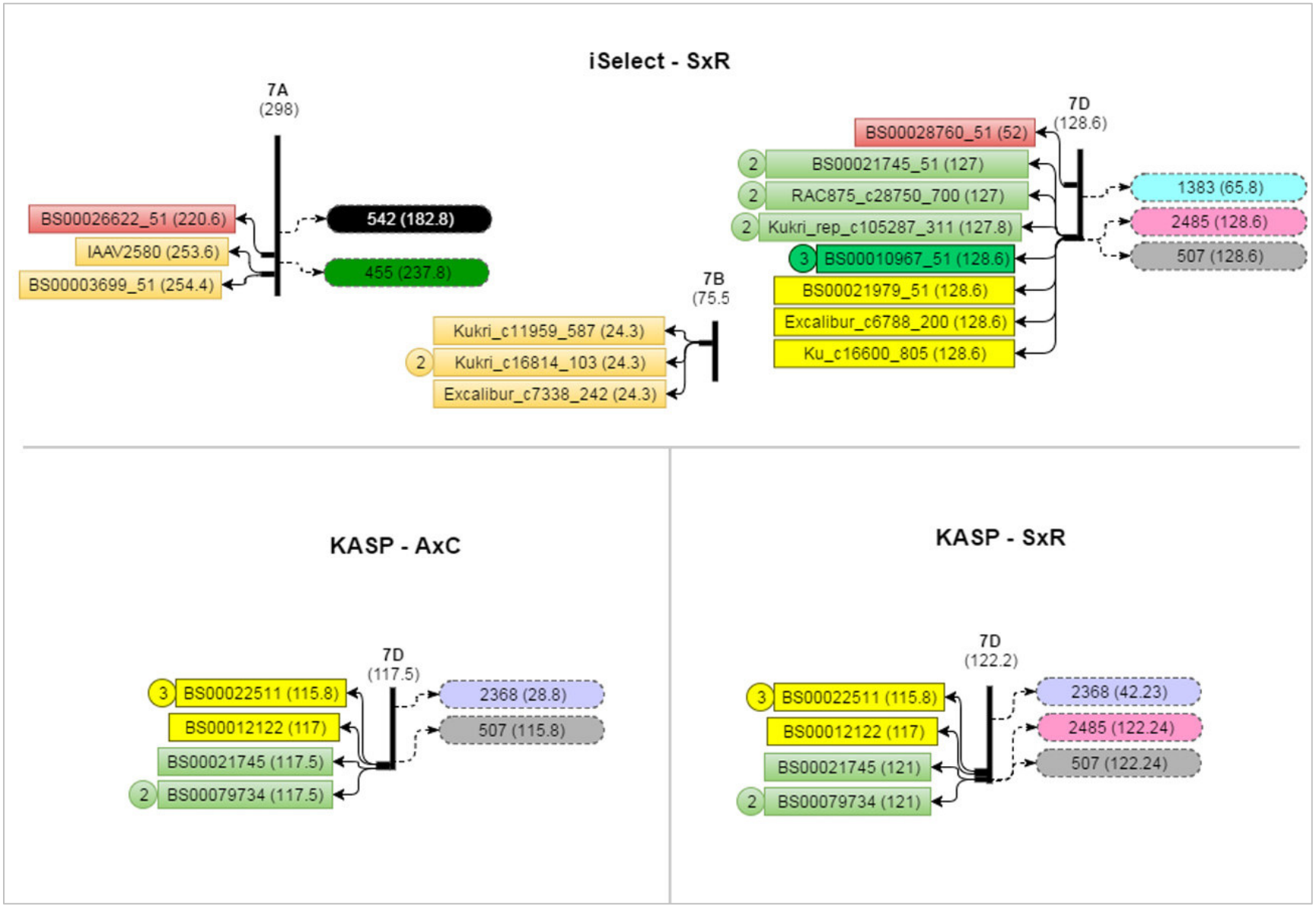
iSelect - SxR
7A
(298)
BS00026622_51 (220.6)
IAAV2580 (253.6)
BS00003699_51 (254.4)
542 (182.8)
455 (237.8)
7B
(75.5
Kukri_c11959_587 (24.3)
2
Kukri_c16814_103 (24.3)
Excalibur_c7338_242 (24.3)
7D
(128.6)
BS00028760_51 (52)
2
BS00021745_51 (127)
2
RAC875_c28750_700 (127)
2
Kukri_rep_c105287_311 (127.8)
3
BS00010967_51 (128.6)
BS00021979_51 (128.6)
Excalibur_c6788_200 (128.6)
Ku_c16600_805 (128.6)
1383 (65.8)
2485 (128.6)
507 (128.6)
KASP - AxC
7D
(117.5)
3
BS00022511 (115.8)
BS00012122 (117)
BS00021745 (117.5)
2
BS00079734 (117.5)
2368 (28.8)
507 (115.8)
KASP - SxR
7D
(122.2)
3
BS00022511 (115.8)
BS00012122 (117)
BS00021745 (121)
2
BS00079734 (121)
2368 (42.23)
2485 (122.24)
507 (122.24)

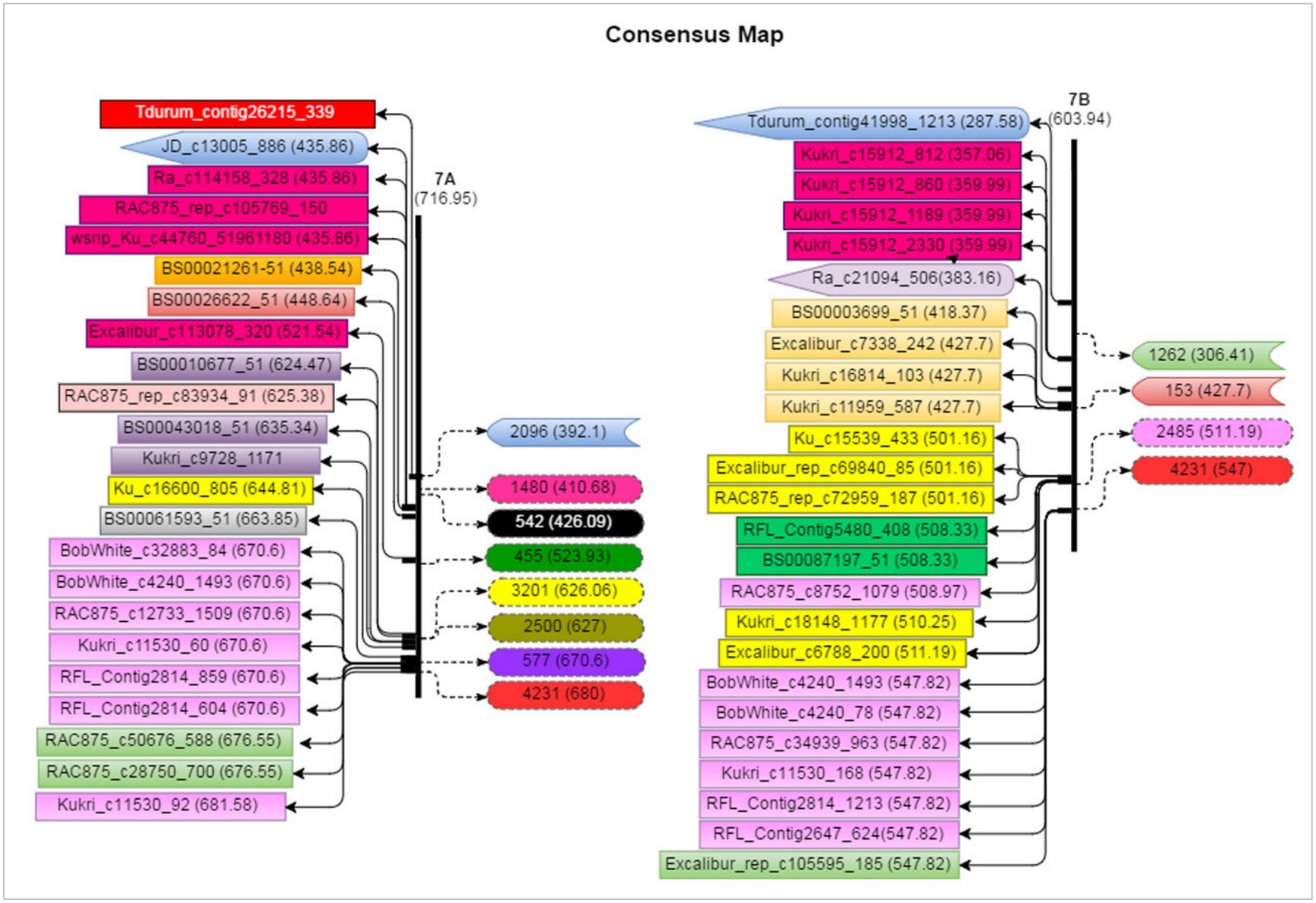
Consensus Map
Tdurum_contig26215_339
JD_c13005_886 (435.86)
Ra_c114158_328 (435.86)
RAC875_rep_c105769_150
wsnp_Ku_c44760_51961180 (435.86)
BS00021261-51 (438.54)
BS00026622_51 (448.64)
Excalibur_c113078_320 (521.54)
BS00010677_51 (624.47)
RAC875_rep_c83934_91 (625.38)
BS00043018_51 (635.34)
Kukri_c9728_1171
Ku_c16600_805 (644.81)
BS00061593_51 (663.85)
BobWhite_c32883_84 (670.6)
BobWhite_c4240_1493 (670.6)
RAC875_c12733_1509 (670.6)
Kukri_c11530_60 (670.6)
RFL_Contig2814_859 (670.6)
RFL_Contig2814_604 (670.6)
RAC875_c50676_588 (676.55)
RAC875_c28750_700 (676.55)
Kukri_c11530_92 (681.58)
7A
(716.95)
2096 (392.1)
1480 (410.68)
542 (426.09)
455 (523.93)
3201 (626.06)
2500 (627)
577 (670.6)
4231 (680)
7B
(603.94)
Tdurum_contig41998_1213 (287.58)
Kukri_c15912_812 (357.06)
Kukri_c15912_860 (359.99)
Kukri_c15912_1189 (359.99)
Kukri_c15912_2330 (359.99)
Ra_c21094_506(383.16)
BS00003699_51 (418.37)
Excalibur_c7338_242 (427.7)
Kukri_c16814_103 (427.7)
Kukri_c11959_587 (427.7)
Ku_c15539_433 (501.16)
Excalibur_rep_c69840_85 (501.16)
RAC875_rep_c72959_187 (501.16)
RFL_Contig5480_408 (508.33)
BS00087197_51 (508.33)
RAC875_c8752_1079 (508.97)
Kukri_c18148_1177 (510.25)
Excalibur_c6788_200 (511.19)
BobWhite_c4240_1493 (547.82)
BobWhite_c4240_78 (547.82)
RAC875_c34939_963 (547.82)
Kukri_c11530_168 (547.82)
RFL_Contig2814_1213 (547.82)
RFL_Contig2647_624(547.82)
Excalibur_rep_c105595_185 (547.82)
1262 (306.41)
153 (427.7)
2485 (511.19)
4231 (547)

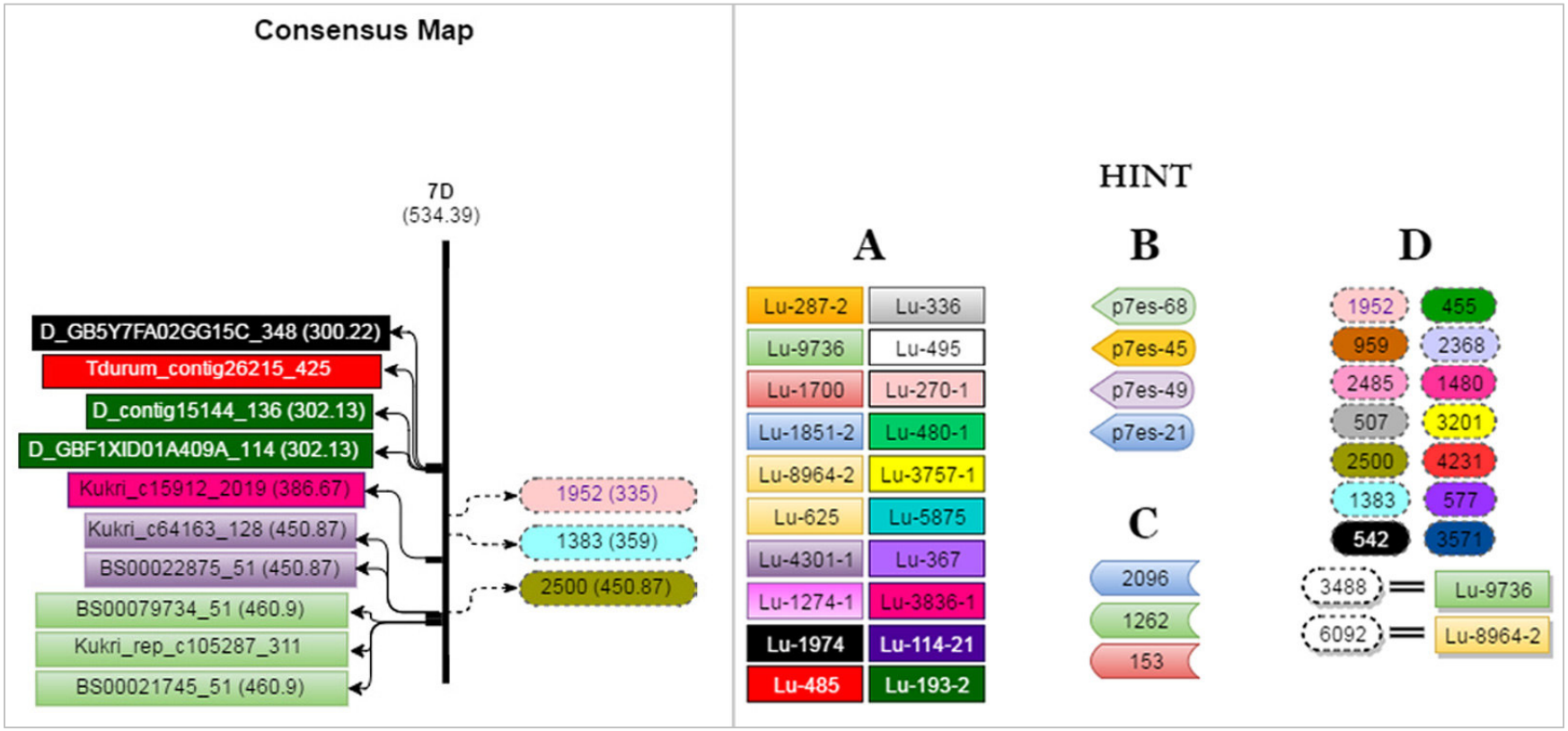

Figure App-I. 9: Schematic representations showing the position of SNPs associated with previously used 7EL-specific markers in relation to the novel 7EL-specific markers.

Markers located on the right side of each chromosome schema were designed in the third objective; while the SNPs associated with previously used markers are represented on the left side. Only the first part of the marker name (associated 7E scaffold) is displayed for markers that were designed in this project. Numbers in bracket represent the genetic position, in cM. Numbers located in circle beside SNPs represent the number of times that the same SNP were found for the specific marker from the different associated wheat contigs from different genomes (A, B, or D); hint groups: A. 7EL-specific expressed gene markers (Gou et al., 2016), B. 7E chromosome-specific markers (Chen et al., 2013); C. markers designed by K. Joustra; D. markers designed in objective three of this project.

Appendix II

Please refer to the attached electronic file named “Tekieh_Farideh_2016_Thesis_Data”.